# REPORT

## of the

# SECOND PILOTED AIRCRAFT FLIGHT CONTROL SYSTEM

## Symposium

### 2, 3, 4 and 5 June 1952

AIRBORNE EQUIPMENT DIVISION
BUREAU OF AERONAUTICS
DEPARTMENT OF THE NAVY
Washington, D. C.

BUAER REPORT AE-61-5-III

# FOREWORD

For four days beginning on 2 June 1952, representatives
of the aircraft industry and the military services met
in Washington, D. C. to present and hear papers on the
design and utilization of piloted aircraft flight control
systems. The eight papers reproduced in this report were
presented at that meeting.

The Navy's appreciation is extended to the authors of
these papers and to the various organizations they
represent.

Comments or questions concerning this report should be
forwarded to the Chief, Bureau of Aeronautics,
Attention AE, Washington 25, D. C.

L. M. GRANT
Rear Admiral, USN
Assistant Chief for
Research and Development

ii

# CONTENTS

# CENTERING CHARACTERISTICS OF POWER BOOSTED AIRCRAFT CONTROL SYSTEMS

by

## C. H. COOKE
## I. E. KASS

of

The Glenn L. Martin Co.
Baltimore, Maryland

# CENTERING CHARACTERISTICS OF POWER BOOSTED
## AIRCRAFT CONTROL SYSTEMS

Within 15 basically different aircraft, the Glenn L. Martin Company has designed and put into service 30 different powered surface control systems of which 15 were power operated. The remaining 15 power boosted surface control systems have presented an unusual combination of requirements for sensitivity, stability, and centering. To meet such requirements while maintaining a simple, reliable mechanism, devoid of functionally complicated accessories, the designer must provide the optimum system arrangement and go to a high degree of refinement in designing the elements.

The design considerations in a power boosted aircraft controls system are as follows:

1. To provide optimum sensitivity and the correct amount of power at all combinations of speed and load.

2. To prevent any form of instability such as chatter or hunt within the mechanism in spite of the sensitivity and low break-away friction.

3. To obtain a high degree of system reversibility so that the mechanism will accurately center or return to the trimmed position, and so that a good force gradient will be felt by the pilot at very low aerodynamic moments.

These considerations are closely interrelated by many system parameters which generally are determined by one consideration and have a direct effect on the other two. Consideration #1 determines system rate gain, circuit power, and valve characteristics, each of which has a direct effect upon stability (consideration #2). Stability also concerns the friction or damping throughout the system, the point of application of the actuator, and the method of obtaining proportional feel, each of which vitally affects the centering characteristics (consideration #3).

There are definite performance requirements which must be met for sensitivity, stability, and centering to make any system satisfactory in service. The ability of the designer to meet these requirements depends upon his understanding the effect of each system parameter upon the requirements. For example, to make a judicious decision regarding the magnitude and distribution of friction, the designer must determine the maximum permissible friction pattern from his established centering requirements, next determine by analysis or test the minimum friction pattern required to maintain stability, and then he can establish the quality control limits of friction within each element of the system.

Centering characteristics as referred to herein may be defined as the relationship between force, position, and rate of motion of a control system in the vicinity of the trimmed neutral position. The critical points ordinarily considered are as follows:

1. Break-away friction - defined as the force (as measured at control lever) required to begin surface motion from neutral.

2. Centering force - defined as the feel force vs. control position when returning to neutral.

3. Centering error - defined as the positional error or distance from neutral at which control stalls when being returned toward neutral by aerodynamic forces.

4. Centering speed - defined as the velocity vs. position of control lever when being returned toward neutral (from various starting positions) by aerodynamic forces.

When a power boosted surface control system is used in an airplane the aerodynamic hinge moments on the surface are approximately directly proportional to surface deflection and thus taper down to zero hinge moment in the trimmed neutral position. A fraction of these hinge moments must react in reverse through the control system to produce feel force at the pilot's control lever and to return or center the mechanism (when displaced), to the neutral position. Therefore, the degree of reversibility of the mechanism determines the centering characteristics.

Figure 1 illustrates the basic elements and the significant external forces acting upon a power boosted control system. The basic arrangement consists of a direct manual drive from pilot to surface with a boost package inserted at one point in the mechanism. The boost package contains the differential linkage, actuator, actuator disconnect, control valve, and hydraulic accessories.

When analyzing centering characteristics, the designer is specifically concerned with six related variables:

1. Control force or pilot effort    $(F_C)$

2. Control surface force    $(F_S)$

3. Control valve force    $(F_V)$

4. Actuator force    $(F_A)$

5. Surface position    $\delta$

6. Surface rate and direction of motion.

The magnitude of acceleration forces throughout the mechanism has been negligible in centering studies to date, which greatly simplifies the analysis by elimination of acceleration as a variable.

4



FIG. I

PROPORTIONAL BOOST CONTROL
SYSTEM

$F_p$, WHEEL FORCE

CONTROL LINKAGE

$F_c$, CONTROL LOAD

$F_s$, SURFACE LOADS
$F_A$, ACTUATOR LOAD

$F_s$, LOAD @ SURF.

DRIVEN
LINKAGE

2.5

.207

$F_v$, VALVE
FORCE

2.273

ACTUATOR

VALVE

ACTUATOR DISCONNECT

BOOST PACKAGE

Since pilot effort and surface force may become independent variables in a centering problem, it is desirable to express each other variable as a function of these two. One solid link in the boost package serves as a follow-up loop and also measures the error signal. The four forces acting upon this link are the first four variables mentioned above. Taking summation of moments on this link about the piston rod bearing and solving for $F_V$ indicates that valve forces are a direct function of control force and surface force only as determined by the geometry of the control mechanism at neutral and as expressed by

Equation (1): $F_V = .09025 \, F_S - 1.181 \, F_C$

Taking summation of moments about the valve rod bearing which eliminates $F_V$ and solving for $F_A$ indicates that actuator forces are also a direct geometrical function of control force and surface force only as expressed by

Equation (2): $F_A = .09 \, F_S - 2.18 \, F_C$

To aid visualization of this problem, a graphical method has been employed. (See Fig. 2.) The independent variables are control forces plotted as ordinates, and surface forces plotted as abscissa on rectangular coordinates. By substitution of various constant values for $F_V$ in the second equation at the top of Fig. 2, valve forces in pounds are plotted as a family of parallel lines with scales along the sides of the chart. By substitution of various constant values of $F_A$ in the first equation, actuator forces in pounds are plotted as a family of parallel lines with a scale along the top of the chart.

Since surface position is approximately a linear function of surface load, it also may be measured along the abscissa by using a scale factor (K) which is determined from the air speed in a given problem, $K = C \, v^2$.

If any two variables are known, a system condition is established as a point on this chart. A value for each other variable can then be obtained from the chart.

Surface rate and direction of motion may be determined by applying the valve load, obtained from Figure 2, to the characteristics of the valve.

To proceed further with the analysis, reliable data must be obtained concerning the operating friction and loads for each element of the system. Figure 3 is a plot of laboratory test data obtained from a typical balanced piston boost cylinder. During frequent intermittent duty, the stall and starting friction piston force in pounds, indicated by the lower solid line on Fig. 3, can be expressed as:

$F_A = 12 + .0144 \, x$ internal pressure (psi)

FIG. 2
BOOST (85%) SYSTEM LOAD CHART
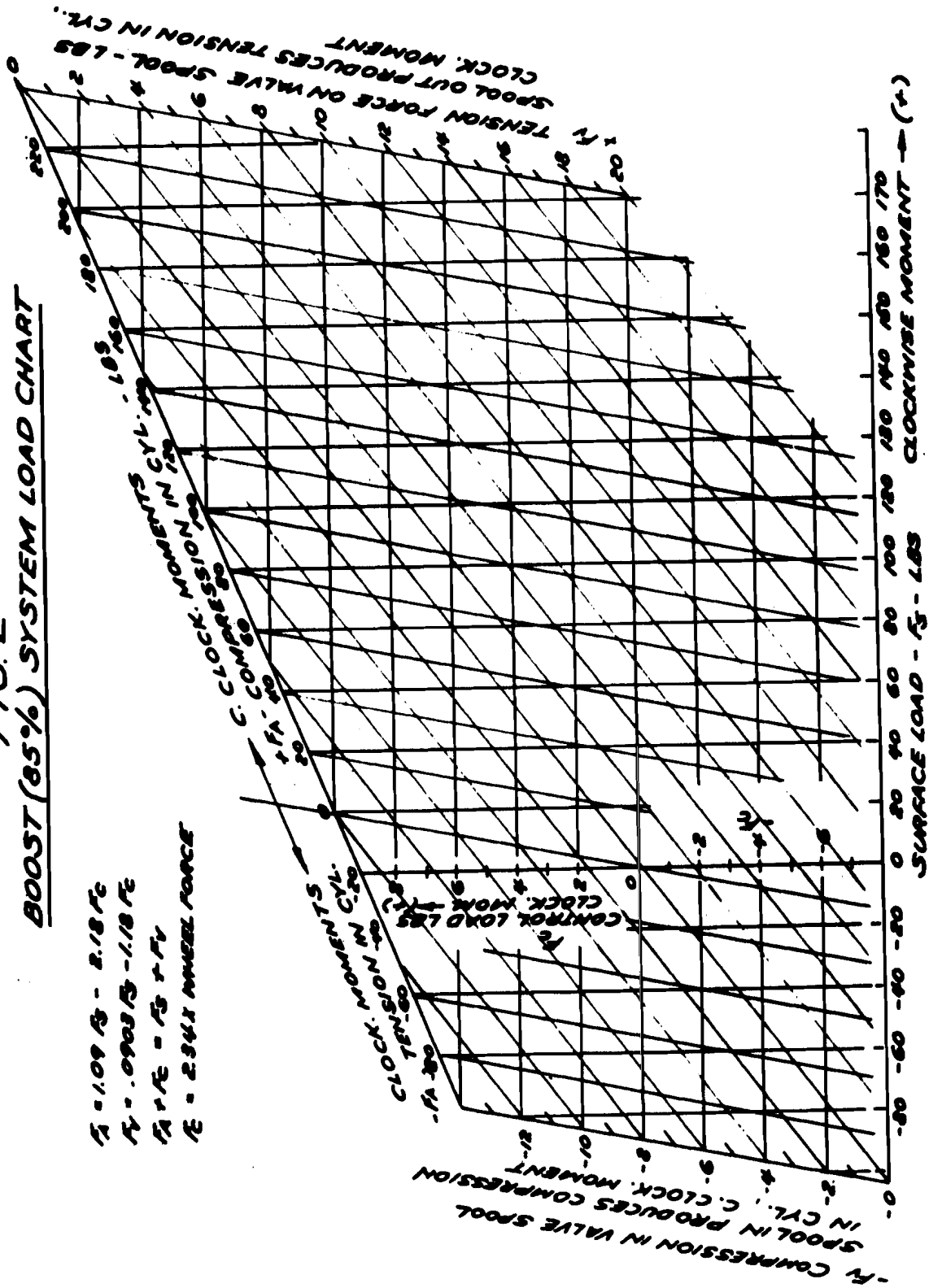
FIG. 3
CYLINDER FRICTION VS PRESSURE
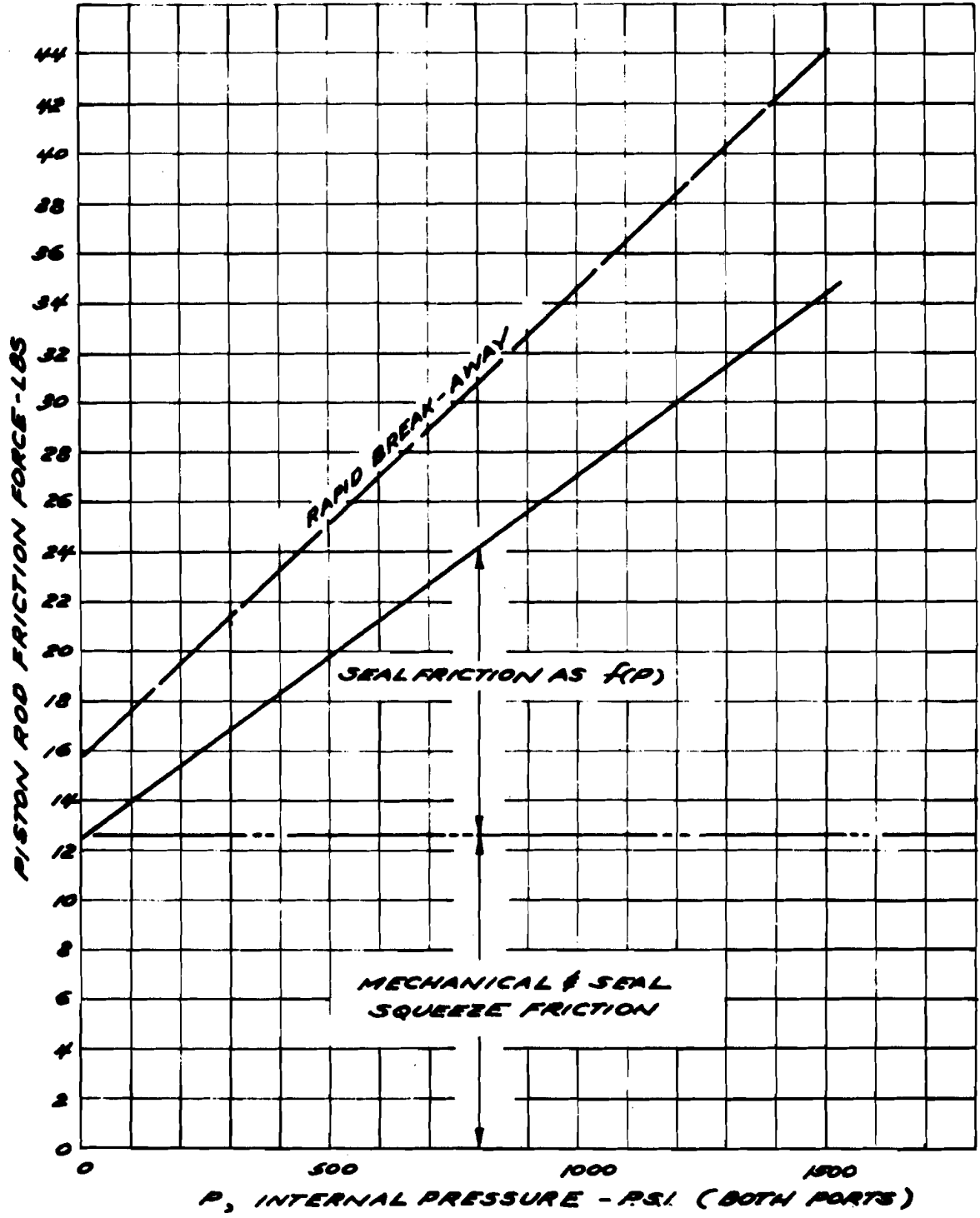
An abrupt change in speed from a creep to rapid motion which takes place at a higher force in pounds, indicated by the broken line on Fig. 3, can be expressed as:

$$F_A = 16 + .019 \text{ x internal pressure (psi)}$$

Figure 4 is a plot of laboratory data of operating loads in a spring loaded slide valve reflecting the spring preload and rate, (broken line) ± approximately 2 lb. constant friction, ± dynamic forces of flow.

In Figure 5 the critical values of cylinder and valve loads are all plotted upon a chart using Figure 2 as a background. A low amplitude cycle of surface deflection is illustrated. The inner loop is the path of system conditions measured at the differential linkage in the boost package. Point (1) at the origin indicates a condition of perfect equilibrium at neutral. Assuming a slowly applied control force, proceed vertically to point (2) where cylinder friction is exceeded. The cylinder will yield allowing the surface to deflect. Proceed along the 12 lb. cylinder friction line until at point (3) the valve preload is exceeded. The valve will direct pressure to the cylinder causing it to change from a retarding to an assisting force as the valve cracking line is followed until the control force is no longer increased. The system will continue to move, proceeding horizontally to point (4) where the valve readjusts toward neutral and the system stalls at point (4) in a surface deflected position.

With a slow decrease of control force, the valve spring will readjust toward a valve neutral position. The cylinder pressure starts to reduce proceeding along (or slightly above) the valve close line to point (5) where cylinder load has reduced to the 12 lb. stall friction. Continued reduction of control load proceeds down cylinder friction line to point (6) where control force at the boost package has reduced to forward control friction and no longer reduces. The mechanism will stall at point (6) indicating centering error. Application of a negative control force will drag the mechanism to neutral proceeding down to point (7).

Starting at point (4), if the control force were rapidly released, proceed down vertically to point (8) where the valve reverses and assists centering to point (9) where the valve closes. Aerodynamic forces must then drive the mechanism along the 2 lb. forward control friction line at a rate determined by hydraulic by-pass provisions to point (6) where the mechanism stalls as before. The outer loop, points (10) through (18), is the path of control forces measured at pilot. This curve is constructed simply by adding or subtracting (depending upon direction of motion) 2 lbs. forward control friction to each previously determined point.

Figure 5 illustrates how the valve centering spring blankets out any valve action in the low load region where centering characteristics are determined. Thus, no hydraulic pressure is contributed to assit break-away from neutral or to assist dragging the mechanism back to the neutral position.

## FIG. 4

### HYDRAULIC VALVE WITH CENTERING SPRING, LOAD CURVES

FIG. 5
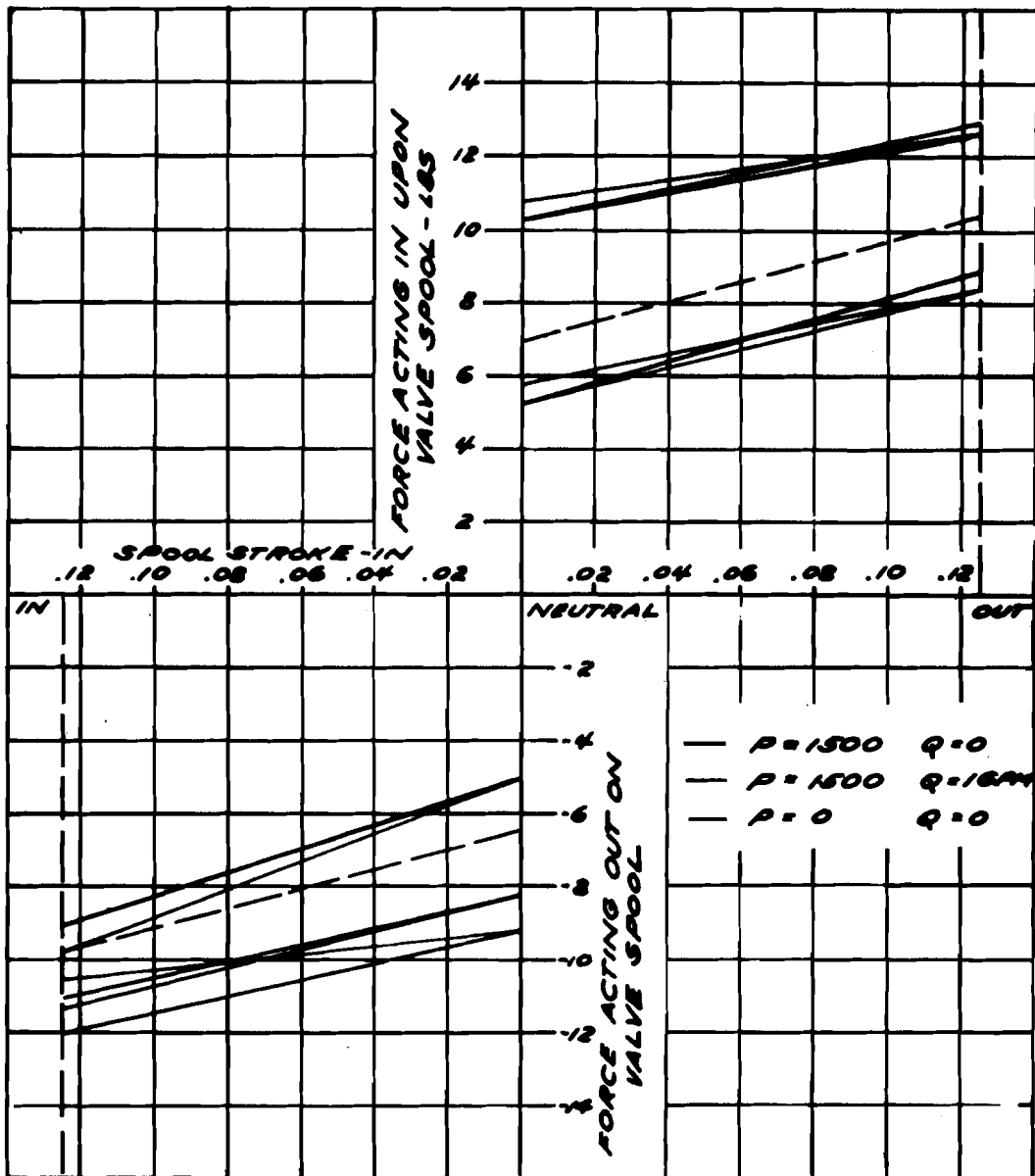
BOOST SYSTEM CENTERING CHARACTERISTICS
WITH VALVE SPRING
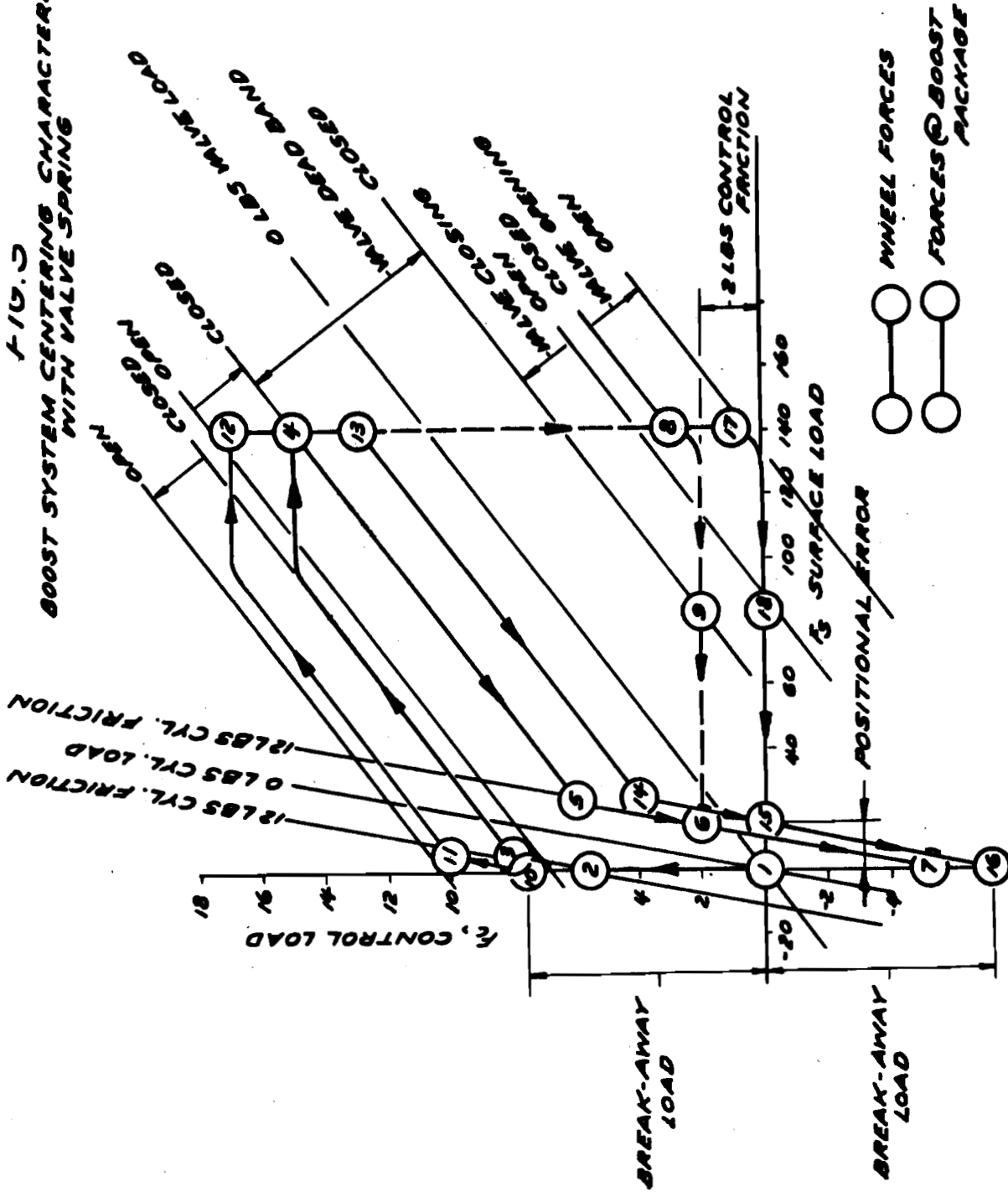
The centering characteristics except centering speed are determined, in this case, from the friction of the system elements. Break-away force indicated by points (10) and (16), is simply a combination of cylinder and control friction. The centering positional error at point (6) is the intersection of the 12 lb. cylinder friction line and the 2 lb. control friction line.

Figure 6 illustrates a surface deflection cycle in a boost system employing a balanced slide valve with no centering spring. The operating load of this valve consists of 2.5 lbs. constant friction as indicated by low slope diagonal line of Fig. 6. Starting again from point (1), equilibrium in neutral, a slowly applied control force proceeds vertically to (2) where valve friction first is overcome. The valve will direct pressure to the cylinder proceeding along the 2.5 lb. valve action line until control force is no longer increased. The system will continue to move, proceeding horizontally to point (3) where the valve readjusts toward neutral and the system stalls at point (3). With a slow decrease in control force, the valve will immediately readjust and assist (as demanded) the return of surface to neutral proceeding along valve action line until the control force reduces to 2 lb. forward control friction (0 force at pilot). The system will continue across the 2 lb. line to point (2) where a reverse valve load will bring the valve to neutral and stall the mechanism. The outer loop points (4), (5), (6) and (1) are again the path of control forces at the pilot and was constructed by adding or subtracting forward control friction from the previously determined points.

Starting at point (3), if the control load is rapidly released, the valve load will exceed 2.5 lb., thus fully opening the valve and centering the mechanism at full flow rate. The values of valve friction and forward controls friction selected result in zero positional error. However, the analysis was simplified thus far by neglecting friction in the driven linkage.

Figure 7 illustrates a surface deflection cycle similar to Figure 6 with the valve friction increased to 3.3 lb., a control friction of 2 lb., and with a driven linkage friction of 10 lb. introduced. The break-away force is 4.6 lb. With this system condition the centering stall point (4) occurs at -10 lb. surface load measured at the boost package. Diamond shaped points (9), (10) and (11) are surface loads as measured at the surface. These points are offset horizontally by ± 10 lb., which is the driven linkage friction from the corresponding system condition points. Point (11) indicates that the actual surface load is zero at the mechanism stall point and thus zero centering positional error is achieved. This is accomplished, as illustrated in the upper left corner of Figure 7, by establishing optimum valve friction from the intersection point of the controls friction and driven linkage friction.

This trick of power operation to a perfectly centered position is dependent upon certain qualifications:

1. No centering spring within control valve.

FIG. 6

BOOST SYSTEM CENTERING CHARACTERISTICS
NO VALVE SPRING (DRIVEN LINKAGE
FRICTION NEGLECTED)

FIG. 7

BOOST SYSTEM CENTERING CHARACTERISTICS
NO VALVE SPRING (INCLUD'G ALL DETAILS)
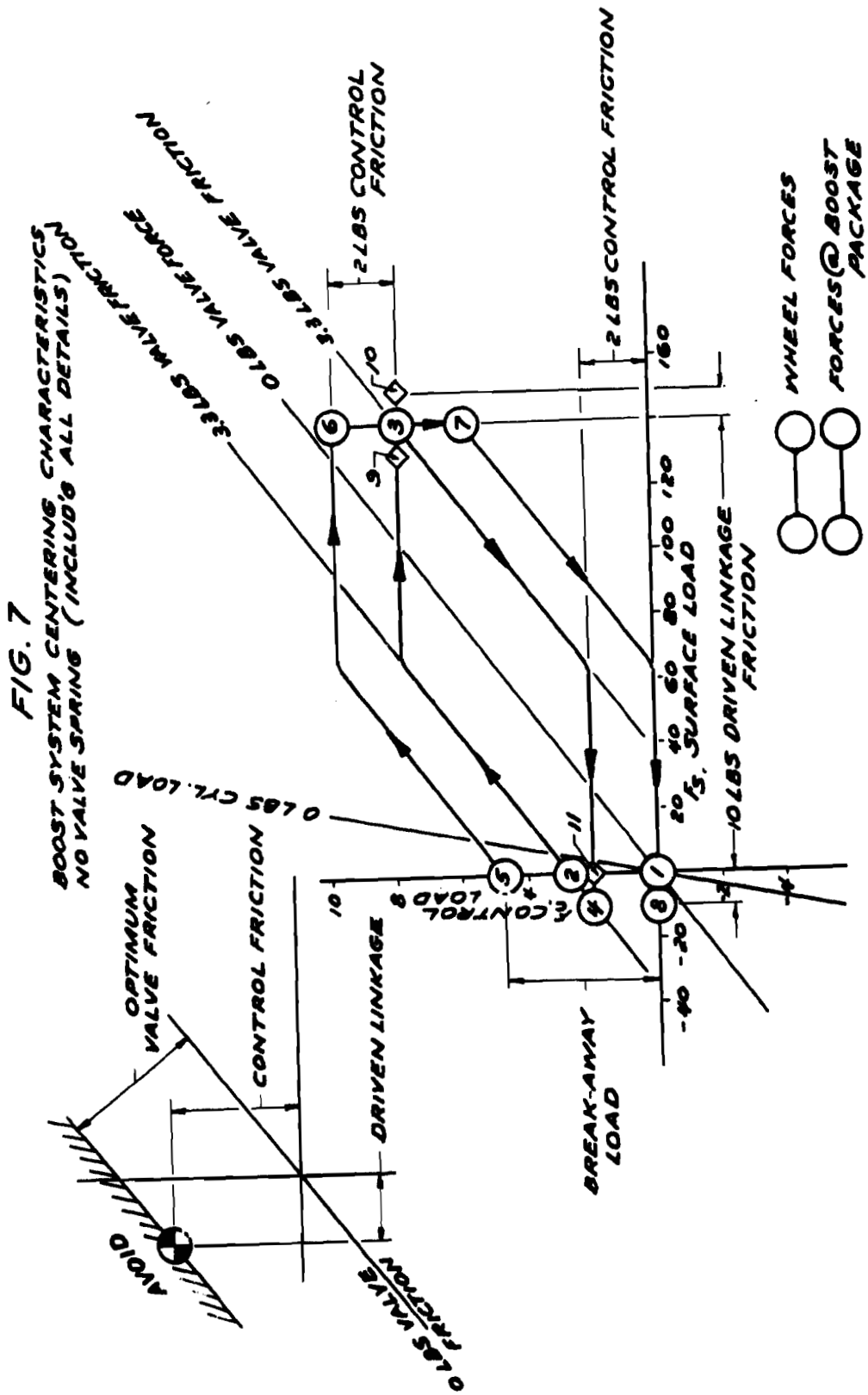
2. A closed center or pressurized type valve must be used to assure perfect centering position under all operating conditions. The valve must cross neutral at the beginning of the centering motion, starting at point (3), and eventually requires a reverse motion and negative valve load to be driven to valve neutral at the stall point of the mechanism. Advantage can be taken on the negative or retarding control friction and driven linkage friction to center the valve at the optimum point.

3. The friction tolerances and adjustments of the system elements must be controlled within the following limits:

   a. In Fig. 7 the valve friction line must not fall outside the intersection point of control and driven linkage friction constants. Failure to meet this self-stalling requirement would result in the system overshooting neutral when centering, and a tendency to hunt or to continue in motion, once started.

   b. The summation of control friction and valve friction must be within the acceptable break-away force limits.

   c. Minimum friction of each element must be in accordance with the friction pattern of the system required to maintain dynamic stability.

From the analysis of a boost mechanism employing a control valve centering spring, it was observed that centering positional error and break-away force were directly effected by actuating cylinder stall friction. In mechanisms with no valve centering spring (see Fig. 6 and 7), the centering characteristics are not effected by cylinder friction. In this case, valve action supplied cylinder pressure to boost out cylinder friction and provides whatever external actuator load is demanded, regardless of internal efficiency.

This analysis has been applied to two current production model airplanes and in both cases has resulted in system changes which have considerably improved the centering characteristics of the controls. During the program, flight test observations were made on an open-center hydraulic boost system, alternately with and without a valve centering spring; and on a closed-center system, alternately with and without a centering spring.

In addition, the above analysis has been confirmed and, to some extent, developed by recent laboratory tests which yielded absolute and comparative data concerning centering characteristics of these four hydraulic boost configurations using the same basic control mechanism. A production boost package was mocked-up with a representative control and driven linkage and with loading provisions for each. During the test, both open and closed center valves were used each with and without a centering spring. The test procedure included the following:

1. Calibration of components, for example, see Fig. 3 and 4.

2. Measurement of break-away force and stall points.

3. Measurement of operating speeds with various combinations of control and surface loads, and with various directions of load change.

Figure 8 is a direct plot of some test results. Surface velocity is plotted along the ordinate against surface force along the abscissa. For each test point the surface force was reduced to a stabilized value. The family of curves in the lower right corner (solid black) describes the centering speed characteristics of a closed-center hydraulic system with a valve centering spring as in Figure 4. The three different curves in this family represent constant control force values of 0, 3 lb. and 6.5 lb., from left to right. These control forces, which are measured at the boost package and are applied in a direction opposing centering motion, represent control linkage frictional drag plus pilot feel. The shape of these curves clearly indicates where valve action takes place. The low curves extending from stall points to 50 lbs. surface load indicate the valve is in neutral and the cylinder motion is highly restricted by the hydraulic by-pass provisions which can be tolerated without excessive dumping of power under load. The steep lines indicate the valve metering range up to approximately 40 degrees/second surface angular velocity. The low slope lines at the top of this family indicate that the orifice characteristics of the fully open valve sharply limit the maximum speed of the mechanism.

When the valve centering spring is removed from this same closed-center system, the centering speed curves will be shifted over to the lower left corner as indicated by the broken lines. The same valve action takes place but at lower surface forces. The centering stall points, where these curves intersect the abscissa or zero speed line, all fall in the low surface load region and extend through zero to a negative surface load. A 2 lb. resisting control force will stall the mechanism at zero surface load which is the trimmed neutral. The slope by which these curves rise indicates snappy centering speeds by positive hydraulic pressure right down to the stall point. The leveling off at the top of these curves near 40 degrees/second surface speed again indicates the point where full flow capacity of the valve limits the speed of the mechanism.

The family of three curves extending to the top of Figure 8 describes the speed characteristics of an open-center control valve containing a centering spring. The stall point for each curve coincides with the stall point on the corresponding curve for a closed-center valve with spring (solid black). The valve is in neutral in the lower portions of these curves, and the valve begins contributing pressure above the break. The steep slope of these curves starting at the abscissa indicates good centering speed as a result of unrestricted by-pass between cylinder lines which is an inherent characteristic of open-center valves.

16



FIG. 8
CONTROL LINKAGE LOAD VS
CONTROL QUADRANT & SURFACE
ANGULAR VELOCITY
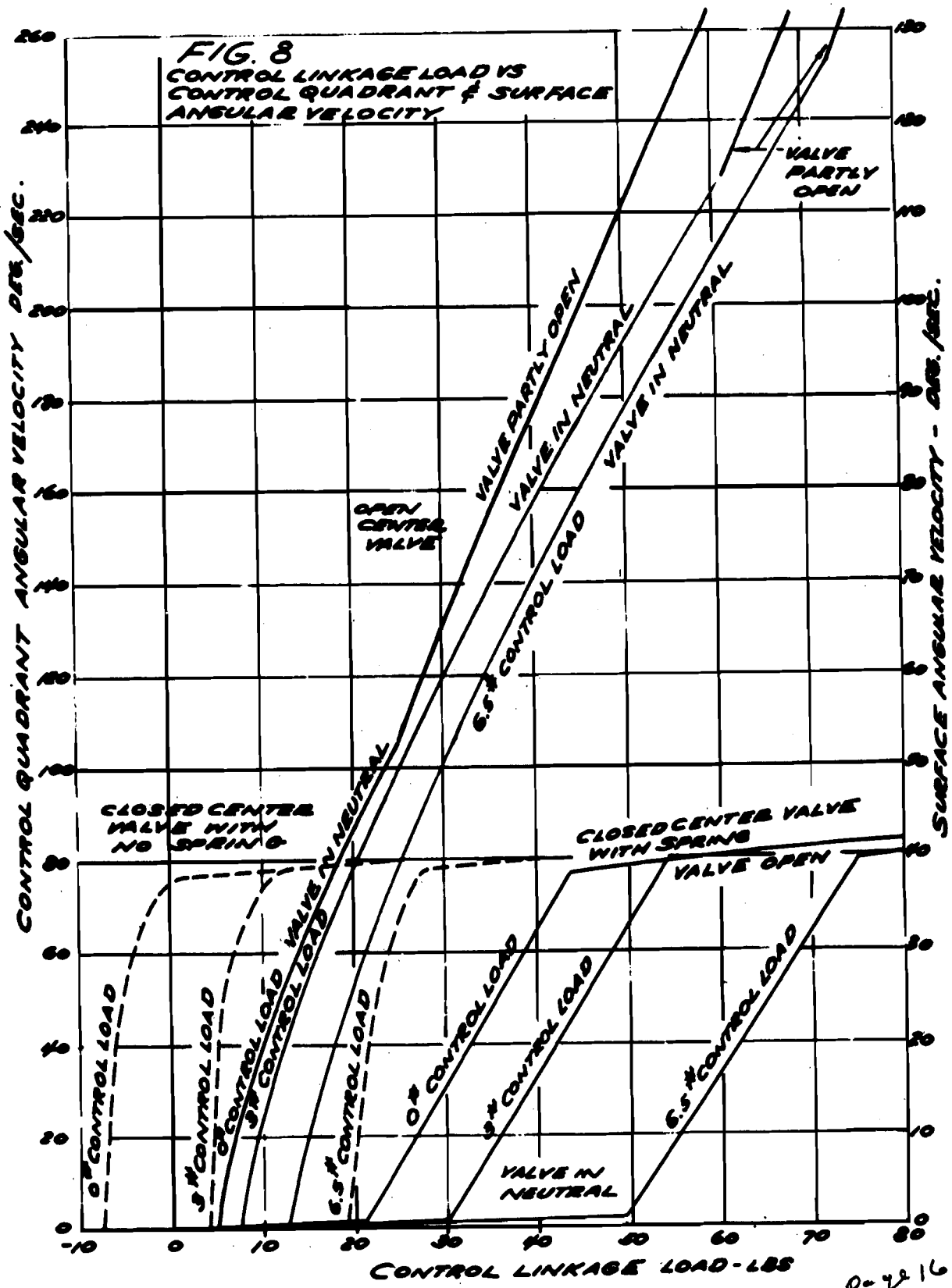
When the centering spring is removed from this open-center valve, the
speed characteristics cannot be represented by a line. Rapid release of
control force results in centering speeds located at the broken line for a
closed-center valve without spring (and this includes stall point location).
Slow release of control force results in centering speeds located at the line
for open-center valve with spring.


## CONCLUSIONS


In the past, centering characteristics of many power boosted surface
control systems have been evaluated only by pilot estimation late in the
flight test program of the airplane. Prior to this point in the life of
the project, many compromises have been made to facilitate manufacture and
to meet other performance requirements, such as power and stability, with
no analysis of their adverse effect upon centering characteristics. At
this point in the life of the project, nothing but minor detail changes can
be made to improve performance without excessive penalties of cost and delay.

This paper proposes that centering characteristics be considered a
basic design problem to be analyzed early in the engineering phase of each
project and to be persued by test and by quality control throughout the
entire project life. To illustrate how this can be accomplished, centering
characteristics have been defined in simple engineering terms, a technique
of analysis has been presented, a test procedure has been outlined, and
application of the analysis and test to four different system variations has
been illustrated.

# HELICOPTER POWERED CONTROL SYSTEM PROBLEMS

by

## WALTER GERSTENBERGER

of

Sikorsky Aircraft Division
United Aircraft Corporation
Bridgeport, Connecticut

# HELICOPTER POWERED CONTROL SYSTEM
## PROBLEMS

## INTRODUCTION

Since the audience comprises mostly "fixed wing" engineers, it is felt that some introductory remarks about the operation of the helicopter, as related to power controls, might be in order. The type of control for maintaining a pitch and roll attitude has gradually boiled down to a single type. It is a method of tilting the rotor thrust vector by tilting the tip path plane of the rotor. It is a reasonable assumption, for a control discussion, that the rotor thrust remains essentially perpendicular to the tip path plane. Hence to go either forward or sidewards, it is merely necessary to tilt the thrust vector in the desired direction. Although a rotor may be mounted on a Gimbal joint and rotated by brute force in the desired direction, the more practical way of accomplishing this is to hinge the blades at their roots so that they may feather and flap; then applying an oscillating change in blade angle at exactly one times rotative speed, which will excite a one times rotative speed flapping of the blades. An observer on the ground would see a constant tilt of the tip path plane rather than the one times rotative speed flapping relative to the rotating drive shaft of the rotor. This type of control is desirable, because the low inertia of the blades about their feathering axis and the smaller moments of the blades about the feathering axis result in smaller control forces necessary to be overcome by the pilot through his control stick. The feathering is accomplished by a simple swash plate on a transfer bearing directly under the rotor hub. Vertical control is obtained by up and down motion of the swash plate as contrasted to the tilt required for azimuth control, and an increase in the thrust vector results from an increase in the blade angle of all the blades.

Before describing in more detail some of the problems of the azimuth control system, a few introductory remarks will be made concerning the directional control. The type of directional control of the helicopter depends largely on its basic configuration, that is, whether the helicopter is a single rotor helicopter or a multi-rotor helicopter. The single rotor helicopter is more analogous to the present day airplane except that the tail surface is instead a small rotor to counteract the aerodynamic torque acting on the main rotor and to provide for directional control above or below the thrust required to oppose the torque. The tail rotor thrust is varied by changing the blade angle of the tail rotor. In multi-rotor helicopters directional control can be varied by controlling the torque distribution between two counter rotating rotors or by tilting two rotors, so that the horizontal projections of the thrust vectors form a couple to oppose the sum of the torques applied to each individual rotor. The foregoing statements apply to mechanically driven rotors. If the rotor is jet driven at the tip of the blade there is no torque compensation required, but some means of directional control must be available either in the form of a tail surface operating in the slip stream of the rotor, a variable, horizontal jet thrust at the tail, an auxiliary rotor or a combination of these devices.

Returning to the discussion of the azimuth control where the tip path plane is tilted by means of the tilt of the swash plate, we can appreciate the problems resulting from the following considerations. The friction resulting from the feathering bearings, which are required to support a centrifugal force of approximately 15,000 lbs. is appreciable. The need for a fine balance is necessary between the aerodynamic thrust on each blade and the centrifugal force component projected along the line of thrust which prevents the rotor from "coning" too much. Also, the variety of vibratory and gust disturbances transmitted into the control system from the aerodynamic surfaces which support the full weight of the helicopter and which move as a complicated piece of machinery might be disconcerting. On top of this a helicopter is inherently unstable in hovering having an unstable mode with a period of the order of magnitude of 10 seconds or more. While the pilot can cope with this unstable oscillation because of the long period, it is desirable that he make frequent corrections without undue effort. The problem was not insurmountable on helicopters of the 5,000 lbs. gross weight category, but did limit the size of the helicopter unless suitable power controls were developed. Various aerodynamic and gyroscopic devices have been incorporated on helicopters. Three of particular interest are the Bell stabilizer bar, the Hiller control rotor and the Kaman blade tab. The Bell stabilizing bar is a large rate gyro rotating at rotor speed (its undamped natural frequency is hence one times rotor speed) with viscous damping, which can be adjusted to optimize the stabilization obtainable with a rate gyro alone. The Hiller control rotor is a similar device which uses the blades of the control rotor to obtain aerodynamic damping. Another feature of this control rotor is that the feathering produces flapping on the small control rotor which introduces feathering on the large rotor. In short, there is an extra stage of an aerodynamic servo in the control loop. The Kaman rotor, the tab is located on the blade near the tip. A preloaded cable control regulates the angle of the tab which introduces a twisting moment on the blade, which in turn twists the very flexible blade to the desired angle without the use of feathering bearings. Each of these devices solve the problem in part, but have certain disadvantages as well. Power requirements for aerodynamic actuated torques should be considered, and tests run at Sikorsky Aircraft with tab controlled rotors with feathering bearings indicated that the additional drag, due to this type of aerodynamic servo, resulted in power loss from 5 to 10% of total power absorbed by the rotor.

The use of hydraulic power appeared to be the most economical method of improving the control of the helicopter. In 1949 a hydraulic power control for the three inputs of the swash plate was installed on the S-51 model helicopter (gross weight 5500 lbs.) The power control had infinite boost ratio, that is no feedback from the output to the input, operated at a pressure of 800 to 1,000 psi obtained from a constant displacement pump and unloading valve charging an accumulator. The average power requirement for this system was practically nil, being less than a quarter horsepower. Although the original purpose of the control was to prove that the helicopter could be flown with this type of control in order to pave the way for the

addition of stabilizing devices through the ontrol, the characteristics of
the helicopter were improved so much that the control was incorporated in
production aircraft immediately. A similar one was incorporated in the S-55
model (gross weight 6800 lbs.) which was in the design stage at the time.
This is the current 10 place helicopter in production under military
designations of H-19, HO4S, and HRS.

## SERVICE EXPERIENCE OF POWERED SURFACE CONTROL SYSTEMS

During the early stages of production with the S-55 model, trouble was
experienced with the breaking of lines at the base of tube flares. With
each failure that the manufacturer could examine, the fault lay in the
stress raiser produced by flaring the tube. The use of a proper type of
flaring tube eliminated this problem. In view of the fact that only one
tube segment failed, and this failure occurred on only a small percentage
of the ships delivered, the manufacturer concluded that the cause of the
failure must have been a combination of high vibration in this particular
locality plus an imperfect flare. Although the entire hydraulic system
including the reservoir was contained on the gear box, flexible lines were
used to and from the pump to minimize failures caused by this combination of
excessive vibration and imperfect flares. Since the running temperature of
the system was not excessive and the adverse cooling characteristic of the
flexible hose could be tolerated, and since extra line pressure drops could
also be tolerated, it is felt that a more reliable system was obtained by
the judicious use of flexible hose.

The S-55 type helicopter was tested in the climatic hanger at Eglin
Field and under actual service conditions in Alaska and at Watertown, New
York. The spherical accumulator functioned well at -65°. The probable
reasons for this fact is a combination of the following facts. The gear
box required preheat before starting and no pressure could be generated
until the gear box was in operation, since the hydraulic pump is rotor driven.
During operation the accumulator still receives some heat from the gear box.
Service tests at Watertown, New York during weather conditions close to the
freezing point indicated that if the helicopter was left standing over night
during pouring rain and then flown the next day at below freezing temperatures
there was a possibility of ice forming in the proximity of the valve. This
would result in a sticking tendency on the input side of the control system
and perhaps necessitate the shutting off of the pressure to allow the pressure
operated by-pass valves in the cylinders to open, so that the pilot could
procede in manual flight. Manual flying in this helicopter is still possible
but at high speed, the lateral stick forces are close to the specification
limits for an untrimmed condition (20 lbs.) Although the forces can't be
trimmed out they can be reduced in a fairly short time by descreasing the
speed of the helicopter. However, these forces have been considered objection-
able and an emergency power control unit, entirely independent on the primary
power control, was developed only for the lateral control system. The
system uses the engine oil at a pressure of approximately 80 psi and is
attached to the lateral control system at all times, and normally works in
a by-pass condition. Upon failure of the primary hydraulic system, a spring

loaded by-pass valve closes, and freedom for the valve of the emergency system
to operate is introduced simultaneously, so that the emergency system, which
was previously idling in the control system, assumes its burden before any
of the control forces are allowed to reach the pilot's stick.  There is
an automatic check by the pilot at every start, because the engine must.
be started before the rotor, and during the interum between engine starting
and rotor clutch engagement the emergency system is the only power control
which can function at that time.  It is true that engine oil is not a
very good fluid for a hydraulic system, especially from the standpoint of
high viscousity at low temperature, but with lagging on the lines and with
a large by-pass located directly in the actuating cylinder, satisfactory
cold weather operation can be obtained.  The utilization of the existing
engine oil system makes the emergency system a convenience which is feasible
from an economic standpoint and weight standpoint, since only an extra
actuator plus connecting lines are required.  There still remains the
undesirable condition of having a cylinder with "O" rings with their inherent
friction connected directly in the control system during normal operation,
and efforts are being made to reduce this friction, although the force in
the stick is approximately 1 pound.

Problems encountered on the previously mentioned helicopters are a
good background for solving the bigger problems of much larger helicopters
now on the design boards.  It is apparent that larger helicopters will have
to depend on power controls for safe operation.  In order to obtain maximum
reliability, the type of power control for an assault type helicopter in
the design stage at the present time consists of two entirely independent
power control systems located in different portions of the helicopter, both
of which should be in operation at all times, and either of which can do
the full job of controlling the helicopter.  One system will have a rotor
driven pump and the other system will have an engine driven pump.  With this.
arrangement the pilot is the input to the first stage, the output of the
first stage is the input to the second stage and the output of the second
stage controls the wobble plate.  The time constants of the servos are
considered high enough so that the additional lag of this tandem configuration
will not be noticeable and the stability of the combined system should be
satisfactory in view of the fact that each power control is of the infinite
boost variety.

## ARTIFICIAL FEEL DEVICES

The use of these irreversible power controls brings up the question of
artificial feel devices.  This problem was not so acute when the power
control was first introduced, because the pilot was liberated from several
kinds of undesirable feel in the control stick.  However, as he became more
accustomed to flying with the power control, the need for extra improvements
was considered.  Helicopters, before the introduction of powered controls, had
trimmable bungees to counteract steady forces in the control system, so that
it was not mandatory for the pilot to hold the control stick at all times.
This automatically provided a spring force gradient in the control stick.

The desirability of the spring force gradient was partially off-set by
the need for trimming this force after changing to a new flight condition.
This configuration may not be important in fixed wing aircraft, but the
helicopter is more apt to be operating over a variety of flight conditions
and there will be more of a tendency for the pilot to forego the trim
changes and cope with the bungee force in the trimmed position. This does
not mean he will not complain about the difficulty of flying in these
conditions. In fact, complaints of a trimmable bungee on the rudder pedals
of the S-55 type helicopter has resulted in the development of a power
control for the tail rudder even though it was not considered necessary
after the initial flignt tests of tne helicopter. After flight testing
the first rudder servo with no feel it was evident that the rudder pedals
were entirely too light and they would still be too light even after 10
or 50 hours of flying with them. A pneumatic cylinder was attached to the
pedal control with a bleed across the piston so that temporary centering
could be obtained, but after a time the pedal force was independent of
pedal position. It must be remembered that there is an appreciable
difference in pedal position between climb and descent because of differences
in rotor torque for these conditions, which have to be compensated for by
the tail rotor. The rate feel of the pneumatic cylinder invokes no objections
but the temporary position feel did. As a result, the type of feel device
proposed for this control was one which consisted of centering springs across
the valve of the power control so that a given rate of servo travel would be
produced by a given force from the pilot.

## THE OVERALL FLIGHT CONTROL SYSTEM

The artificial feel device should be integrated in the overall control
system to aid the pilot in flying the aircraft. It supplements the pilot's
vision and should not transmit any confusing signals. In fact it is believed
that the feel requirements for any aircraft may vary considerably depending
upon what is required to fly that aircraft most proficiently. In the case
of a helicopter, assuming that good flying qualities at high speed have been
obtained with properly designed aerodynamic surfaces, hovering stability
should be approved. At the present time it is a question whether helicopters
will become big enough to afford tne added weight of a suitable auto-pilot,
or whether a sufficiently light weight auto-pilot can be developed to install
in the present helicopters. Sikorsky Aircraft is engaged in a program to
attempt the latter. As flight tests have not been made on the initial proposal
it is difficult to say whether the auto-pilot will be successful, but it is of
the differential input type so that the pilot may fly with the stabilizing
effect of the auto-pilot always present. The system is integrated with the
existing hydraulic power control units, which makes it possible to keep weight
at a minimum. Several types of feel are being considered including a type
where the actual gyro signals convey, by means of a force, what the auto-pilot
considers a proper way to fly a helicopter. There is certainly many problems
connected with such a device which pending flight tests will reveal and lead
to hoped-for solutions.

# FLIGHT RESEARCH ON FORCE WHEEL CONTROL

by DUNSTAN GRAHAM, Lt., USAF
RICHARD C. LATHROP, Capt., USAF
of
Wright Air Development Center
Wright-Patterson Air Force Base, Ohio

In order to accomplish precision flying, static and dynamic stability of the airplane's flight path is required. The provision of this stability need not interfere with the pilot's control of the flight path. Force transducers connected to the pilot's cockpit controls can be used to bias the references of the stabilizing system. This results in easy control by the pilot of flight which is artificially stabilized and coordinated.

The practical success of such a scheme was demonstrated on the All Weather Branch's Force Wheel B-17. Experiments were made in the "steers like a car", natural handling qualities, and nonlinear force gradient configurations.

All Weather Branch's future research plans comprise experiments with the C-45 (described in another paper), and the application of force wheel control to other airframe automatic control combination in an attempt to meet specific operational requirements.

FLIGHT RESEARCH ON FORCE WHEEL CONTROL

The military or economic value of an airplane depends on its ability to traverse a controllable flight path. It is often necessary or desirable that the flight path or certain sections of it be traversed with great precision. Considerations of enroute and terminal area navigation, landing approach and landing, interception and pursuit, formation flying, and bombing runs, illustrates the point.

Fundamentally, the airplane in flight is a velocity vector in space. It has a direction in which it is going and a speed with which it is going there. The time integral of this velocity vector is the flight path. (If instantaneous velocities are multiplied by little bits of time to get little bits of distance travelled, in the direction of the velocity vector, and these are strung end to end, the result is the airplane's flight path.) When the velocity vector is steady the flight path is "straight", and when the vector is changing the participle "maneuvering" describes the flight path. The ease with which a pilot may fly steadily is a function of how well the airplane resists changes in its velocity vector, i.e., its flight path stability; and the ease with which a pilot maneuvers is a function of the means available to him to alter the magnitude and direction of the velocity vector, i.e., control.

Flight path stability and control has several faces. The first of these to show itself was static stability with respect to the relative wind. Leonardo da Vinci convinced himself that the center of gravity of a flying machine should be ahead of the center of wind resistance. His "great bird" of 1506 was designed with a longitudinal static margin of more than fifty percent chord. Almost without exception, since the Wright brothers 1902 glider, successful aircraft have had both longitudinal and directional static stability with respect to the relative wind.

The Wright brothers devoted considerable attention to what they called "balancing." The 1902 glider was their first machine which incorporated a fin and rudder. Together with their previous development of the elevator for longitudinal control, wing warping for roll control, and finally a power plant, it made flying possible. But "balancing" is just what the first flights were, and flying has remained to a large extent a balancing act.

The shadowy face of flight path stability and control has been attitude stability. Attitude stability cannot be inherent in an airframe. By manipulation of the controls a skillful pilot can provide attitude stabilization with respect to a natural or artificial horizon and a direction indication. This is, however, a feat. Fortunately, an automatic pilot can be built to do the same thing more rapidly and

precisely. The first demonstration of automatic pilot control of airplane attitude was made by Lawrence Sperry in 1913. Note that this "inboard" stabilization, by the pilot or automatic pilot, depends on control. It is contrasted with "outboard" stabilization (such as is provided by fixed aerodynamic surfaces) which interferes with control.

The incompatibility of outboard stabilization with control has fostered the opinion that stability is achieved only by sacrificing control. That this is not necessarily the case may be illustrated by considering the example of a simple positioning servomechanism (Figure 1). The first design is deficient in dynamic stability. The output shaft reproduces the angle of the input shaft only after a weakly damped transient has died out. The designer has at least two alternatives. He may add mechanical damping to the output shaft, "outboard". This wastes control power and opposes rapid and accurate control of the output shaft. (Such a system has a steady state error when subjected to a velocity input.) On the other hand the designer may, and usually does, choose to employ the derivative of error signal to stabilize the system. "Inboard" stabilization, accomplished at the signal level, does not waste control power, and does not result in a steady state velocity error. In this case stability does not interfere with control. If anything, control of the output shaft has been enhanced and refined by additional stability.

The concept, illustrated by this simple example of simultaneous stability and control, can be carried over into the airplane handling qualities field. Note, however, that both the stability and the control shown here depend upon feedback.

Flight path stability, composed of attitude stability superimposed on relative wind stability, is commonly achieved by the feedback mechanisms known as automatic pilots. These may be equipped with pedestal controllers which provide a means of introducing control at the signal level. Feedback for control purposes is through the human pilot's visual references and his kinesthetic sense for small finger and wrist movements.

We postulate that a superior form of feedback to the human pilot is force. There is considerable logic and some experimental evidence to substantiate this contention.

Assuming that the feel of the controls is important to flight path control and that compliance with the handling qualities specifications insures adequate feel characteristics, but possible only marginal flight path stability characteristics, it is logical to retain the familiar cockpit controls and their feel and add flight path stability. This is the equivalent of saying that it is logical

# STABILIZATION OF A POSITIONING SERVO
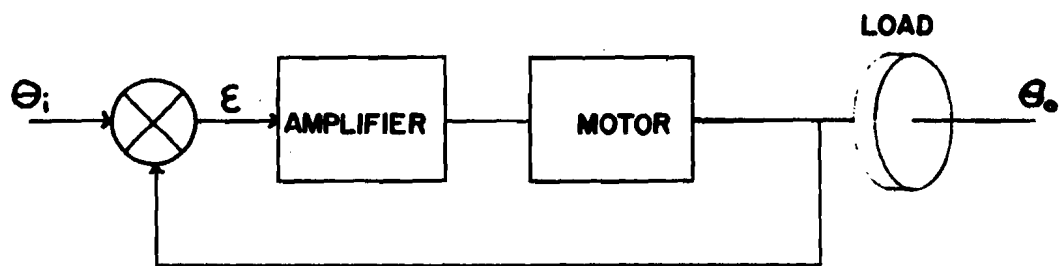


POSITIONING SERVO DEFICIENT IN STABILITY
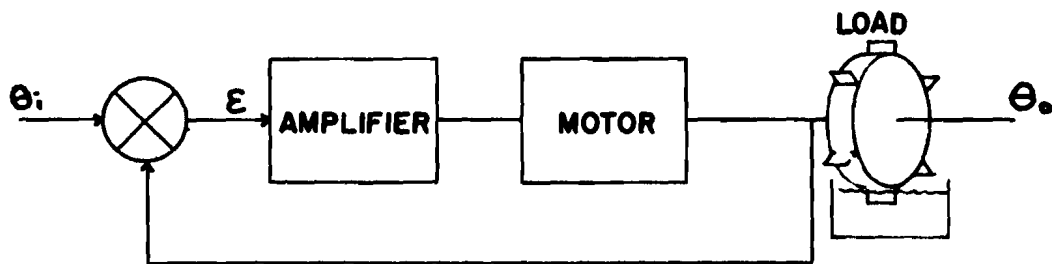


"OUTBOARD" STABILIZATION
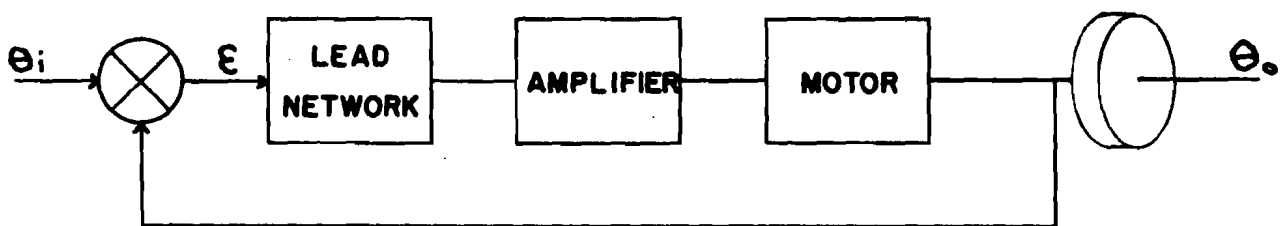


"INBOARD" STABILIZATION

FIGURE 1

to have the cockpit controls command a control system in such a way
that the forces applied at the controls produce predictable and psy-
chologically "correct" airplane responses while the automatic control
system artificially stabilizes and coordinates the flight. It may,
however, be possible or even desirable to take certain liberties with
the normal or natural responses to control forces applied at the
cockpit controls.

In general, the natural responses are as follows:

Elevator force commands a proportional normal acceleration ("g") or a
proportional change from the trim airspeed.

Aileron force commands a proportional wing tip helix angle (roll rate
at a given airspeed).

Rudder force commands a proportional sideslip.

One can't add oranges and apples, however, and the scheme in which force
is measured directly and is used to command an artificial stability
system to produce natural responses requires that the primary referen-
ces for the stabilizing system be the flight variables which it is
desired to command.

No such system yet exists, but in the fall of 1950, at the behest
of the late Major Patrick L. Kelly, the All Weather Flying Division
undertook to sponsor the development of such a stabilizing system at
the Cornell Aeronautical Laboratory. This system has been described
in another paper.

At the same time a small group under the energetic leadership
of Major Kelly began to construct a jury artificial stability system
with force commands, using components which were readily available.
Flight using automatic stability and force control was first achieved
by All Weather Flying Division on 5 March 1951. Throughout the summer
and fall of that year the automatic stability and force control system
was tested in several configurations. It is the story of those ex-
periments that is the principal subject of this paper. No records of
tests results were ever made. We cut and we tried and cut and tried
again. Our goal was an airplane that had the features of the system—
to show that it could be made to work and that pilots did like it.
Its operational success was to have been measured later. All Weather
Flying Section's research on force control was unfortunately cut short
on 7 November 1951 when the test airplane crashed.

To start with there was an airplane with an automatic pilot
installed. The force control sub-system will probably find its prin-
cipal usefulness in aircraft in which space and weight are at a prem-
ium and the pilot must be relied on to do as much as he can. The

method of control envisioned is most compatible with an automatic
pilot whose primary references would be a roll rate gyro, pitch rate
gyro, or normal accelerometer, and a sideslip meter or lateral accel-
erometer. The initial installation, however, was made in an available
aircraft--a B-17 bomber which had a USAF Type E-4 electric automatic
pilot and its associated approach coupler installed.

The E-4 automatic pilot is designed in such a way that an ILAS
localizer signal orders a bank angle. The rudder is nominally moved
so as to coordinate turns. The ILAS glide path signal orders a pitch
angle.

The force sensors were the same instruments that are normally
used by the Flight Test Division for stability and control flight
testing. At first only the wheel was installed. A force wheel is
made with two spokes, each with a grip on the end. Near the hub the
spokes are narrowed to thin sections. A force applied at the grip
is analogous to the force applied at the free end of a cantilever
beam and produces tension on one side of the narrowed section and
compression on the other. The resulting strains are measured by
bonded wire strain gages. The forces applied at the right and left
hand grips are added algebraically by arranging the strain gages in
a four arm bridge. Theoretically, at least, this obviates the
necessity for temperature compensation and gives zero output if the
handles are twisted. The bridges are excited with 26v. 400 cycles
and the output is amplified. In the original application, the output
is used to drive a null balance servo system whose output shaft posi-
tion is measured. In our application, however, the amplified voltage
was used as an input to the automatic pilot. The instruments show
excellent repeatability, linearity, and accuracy. The wheel instrument
gave the project its nickname.

Pedal instruments, installed later, have three means and four
gages apiece--again two gages are in tension and two in compression
on each pedal. The two pedals are connected electrically so that
the net output is proportional to the algebraic sum of the forces
applied to both pedals.

From an interconnection point of view the very simplest experi-
ment that could be performed was to take the signals from the wheel
and apply them through the approach coupler to the automatic pilot.
This resulted in a system in which elevator force commanded pitch
angle. When you wanted to go down you pushed and kept pushing. If
the force was relaxed the airplane returned to level flight. When
you wanted to turn right you applied right aileron--and kept applying
it. In this respect the airplane steered like an automobile, in
which wheel force commands a lateral acceleration (rate of turn at

constant speed). While this system worked and the pilots experienced no difficulty in flying it, they were unanimous in condemming it. Unfortunately no one flew it who had had no experience in an airplane. This might have shown how natural a method of control it is.

The control position feedback was unnaturally related to the force feedback. The wheel--rigidly connected to the ailerons--followed them in establishing a bank. As every pilot knows, the normal sequence of events is something like this:

1. The wheel is rotated into the turn.

2. It is held in a deflected position.

3. Then it is returned toward neutral.

4. Finally it is slightly rotated out of the turn and held there to counteract the overbanking tendency.

With this first system the automatic pilot did all this while the pilot maintained a <u>constant</u> aileron force. It's almost impossible to believe, but nevertheless true: not only way control smooth and easy, but nobody objected to this peculiar position feedback. The objections were concerned with the <u>magnitude</u> of the forces required to maintain the aircraft in a steady turn. These objections might have been overcome by using washout or nonlinear gradients or both. Brief experiments were conducted with a strong centering characteristic and a low stick force gradient for moderate displacements. This "steers like a car" means of control, with or without nonlinear gradients, however, did not meet with approval and was quickly abandoned.

The next configuration which was tried was designed as a first step toward making the aircraft control characteristics correspond to those of a conventional aircraft. Specifically, the roll control channel was altered in such a way that whenever an aileron force greater than three pounds was applied, the vertical gyro roll signal and vertical gyro roll erection were removed, and, by means of a ratchet relay, remained disconnected until a button on the control wheel was depressed.

The rudder channel was modified as follows: the directional gyro signal was completely removed and a lateral accelerometer was substituted as a yaw reference device. This configuration resulted in a control characteristic in which wheel force in roll commanded an aileron displacement (and therefore rate of roll at a given airspeed)

and rudder force commanded lateral acceleration (and therefore side-slip angle, approximately). The action of the lateral accelerometer was such as to maintain negligible sideslip in the absence of a rudder force signal, so that coordinated turns were made using the wheel alone. This simplified the control of the aircraft in normal maneuvers. Pilots frequently use little or no rudder in normal maneuvers, particularly in multi-engine or high-speed aircraft. The rudder pedal force pickups, however, allowed the pilot to intentionally sideslip the aircraft if he so desired. (Intentional sideslip is used in making cross wind landings, for example.)

No modifications were made in the elevator control channel; the control characteristic in which wheel force commanded pitch angle was retained.

The sequence of events in making a turn with this system was something like this:

1.  The pilot applied a rolling force to the wheel. For very small wheel forces--much smaller than those ordinarily used in rolling into a turn--wheel force commanded aircraft bank angle. When the wheel force reached a value of about 3 pounds, the vertical gyro roll signal was smoothly but rapidly disconnected from the automatic pilot, and roll erection in the vertical gyro was disabled. At this point, wheel force commanded aileron displacement, and the force wheel system acted merely as a control boost.

2.  To maintain a constant turn, the pilot relaxed the wheel force when the proper bank angle had been reached. Coordination was supplied automatically. Minor corrections to bank angle had to be made in the usual manner, since no artificial stability signals were provided.

3.  To return to straight and level flight the pilot had two choices. He could push the button on the wheel and relax wheel force, in which case the vertical gyro roll signal and roll erection would be reengaged, and the aircraft would automatically return to level, stabilized flight. Alternatively, the pilot could return to level flight in the conventional manner, and then reengage the vertical gyro stabilization by depressing the button, if he so desired.

Several flights were made with this system, and preliminary results indicated that it was a very workable and natural system of aircraft control. Some of the pilots were gratifyingly enthusiastic about the improved flight path stability and the ease of flight path
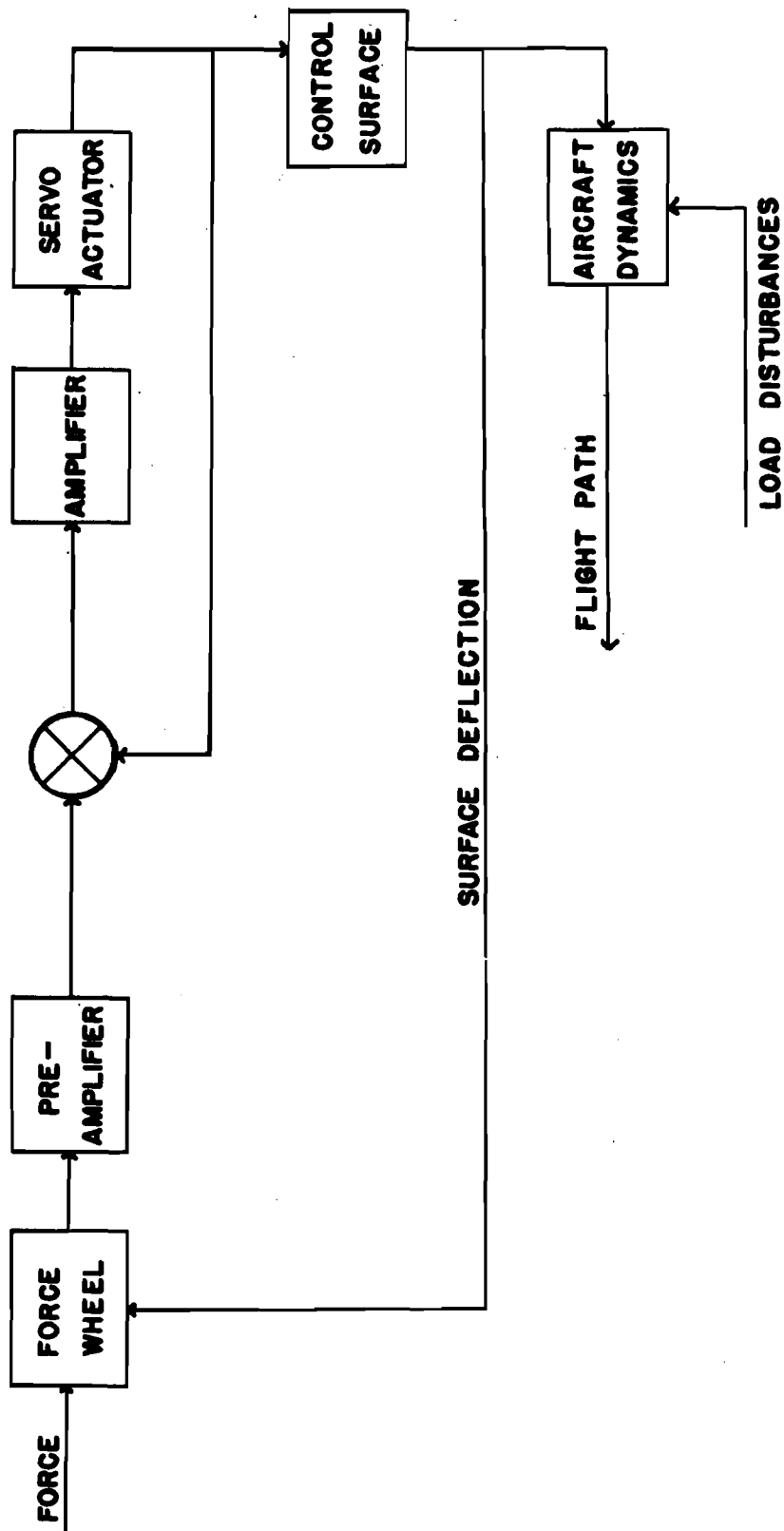
ELEMENTARY FORCE WHEEL CONTROL SYSTEM

WITHOUT ARTIFICIAL STABILITY

FIGURE 2
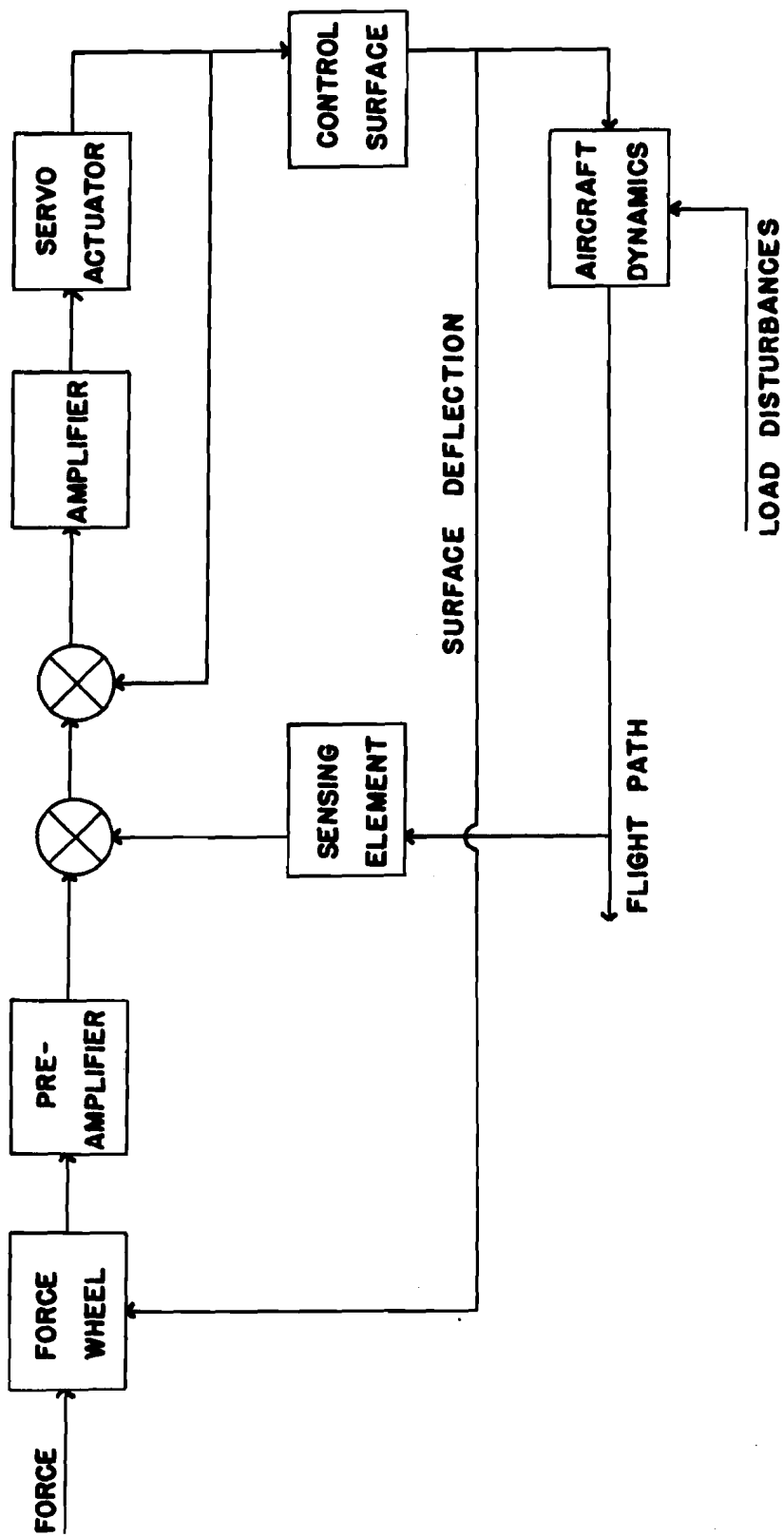
FORCE WHEEL CONTROL SYSTEM
WITH ARTIFICIAL STABILITY

FIGURE 3

34
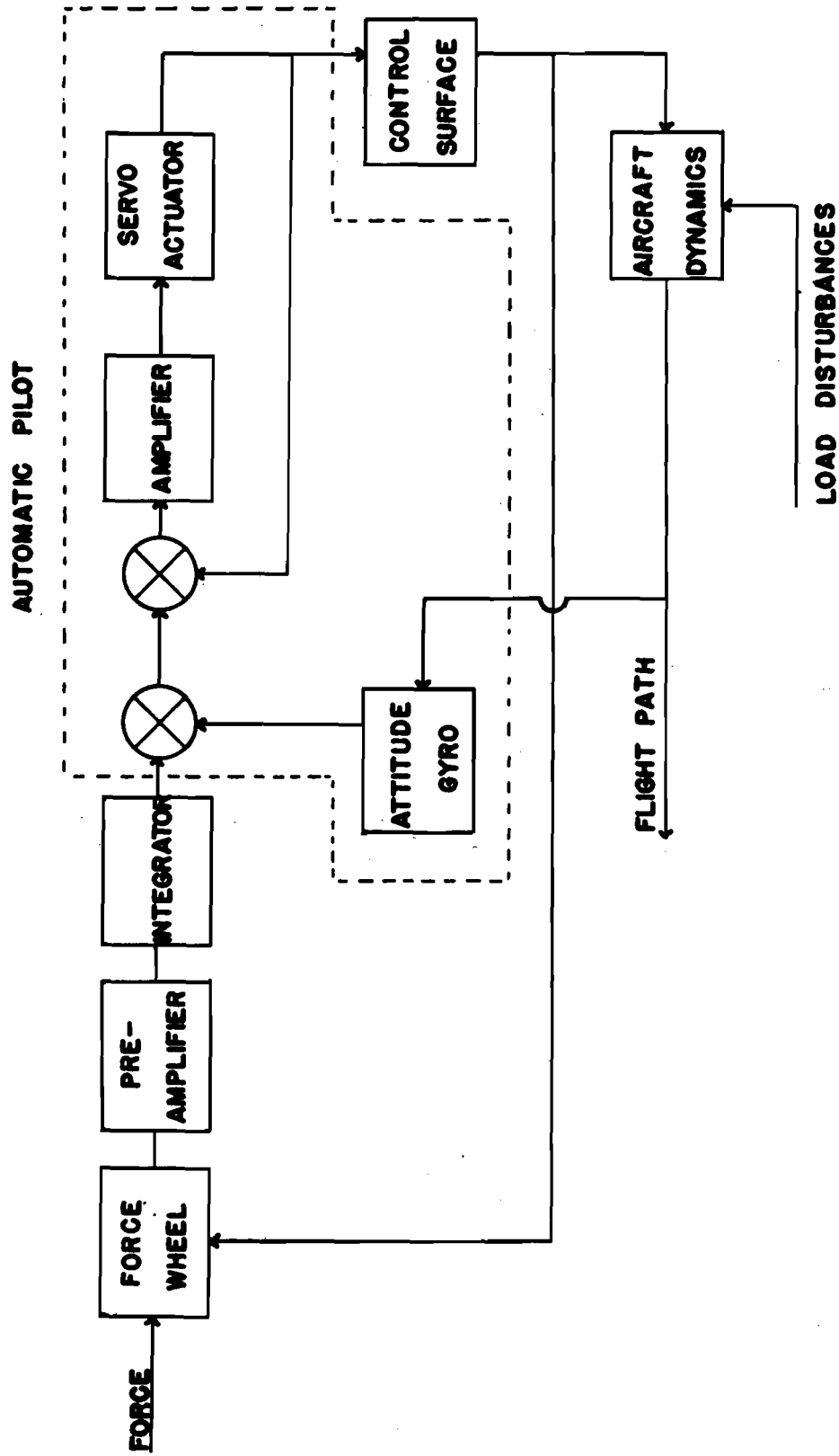


FORCE WHEEL CONTROL SYSTEM
WITH ATTITUDE-TYPE AUTOPILOT

FIGURE 4

control. Unfortunately, the test aircraft was lost before extensive evaluation of the system could be started, and before improvements could be incorporated which would have rendered the artificial stabilization operative at all times.

A similar but improved installation is currently being made in a C-54 type transport aircraft at Wright-Patterson Air Force Base. Unanswered research questions concerning such equipment are legion, and the operational uses to which it may be put remain to be explored.

Consider several possible force wheel configurations. The block diagram of an elementary force wheel system for one aircraft axis is shown in Figure 2. This arrangement operates as a boost only, and no artificial stability is provided. The wheel is rigidly connected to the control surface through the normal control cables. This link, however, does not normally supply an appreciable portion of the hinge moment, but merely acts as a surface position feedback to the pilot. Systems of this type would tend to make the force-displacement gradient of the control wheel relatively independent of airspeed. This was the characteristic of the later B-17 installation.

A somewhat more refined system is shown in block diagram form in Figure 3. In this arrangement, the signal from a sensing element (such as a rate gyro or sideslip indicator) is fed back in such a way as to alter the effective dynamics of the aircraft. Presumably, the system is designed so that the dynamic stability of the aircraft is improved. The rigid link between the control surface and the control wheel is retained. This means that control surface deflections due to both wheel force signals and artificial stability signals are reflected in deflections of the pilot's controls. In some cases, this may be undesirable. The degree of undesirability appears to be a function of the magnitude and frequency content of the artificial stability signals.

If it is necessary to closely approximate normal aircraft feel characteristics, signals proportional to airspeed and "g" force may be introduced to vary the gain of the force wheel preamplifier and therefore alter the force-displacement gradient of the pilot's controls.

Methods whereby the force wheel control system may be used with an attitude-type automatic pilot are shown in Figure 4. In this configuration, a signal proportional to the integral of wheel force is fed into the automatic pilot amplifier in such a way as to command aircraft attitude. All of the stability associated with an attitude-type of automatic pilot is retained during all normal maneuvers. The control wheel therefore becomes a sort of refined pedestal controllers with "feel". The rigid link between the control surface and the control wheel is retained.

36
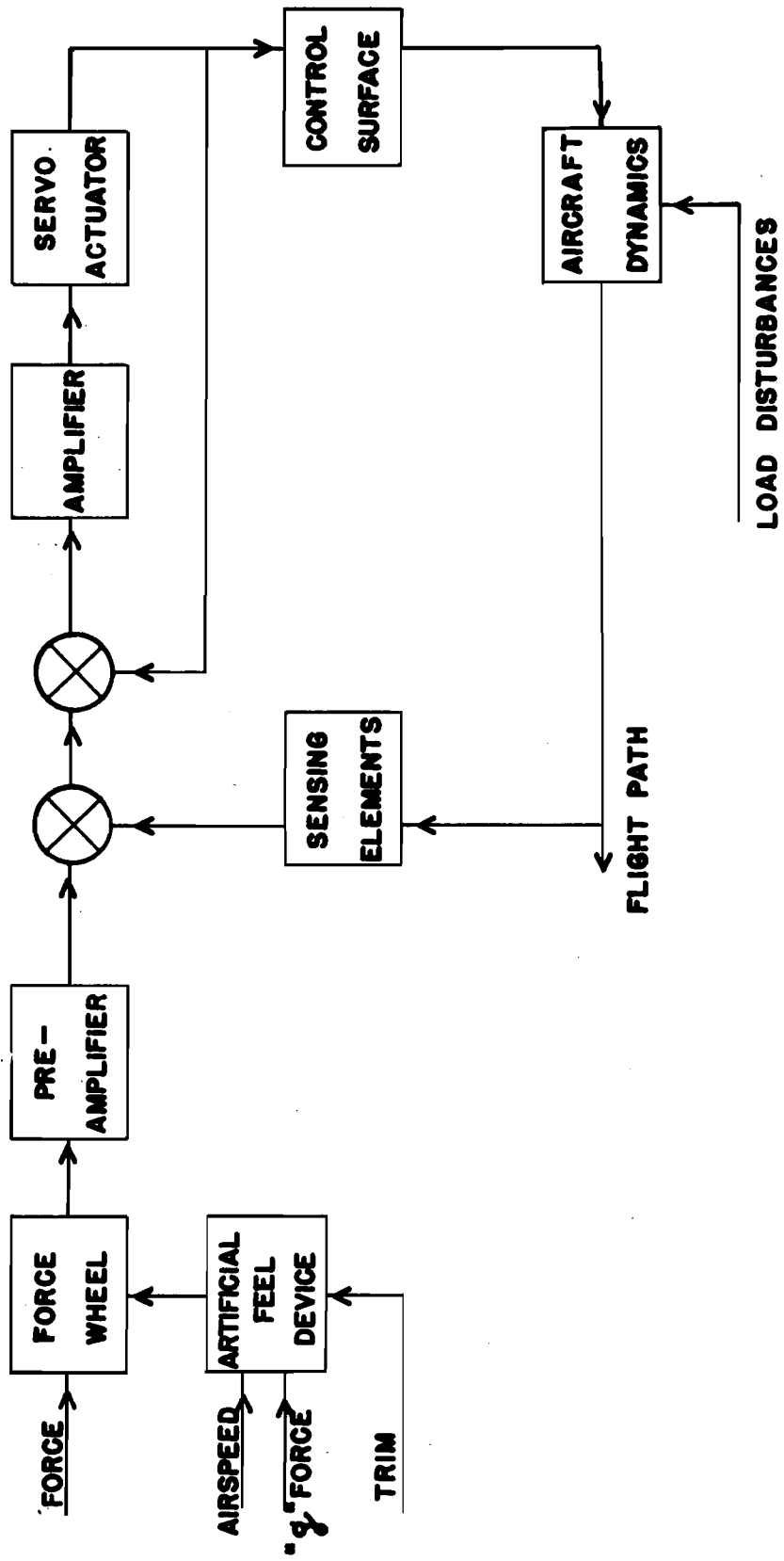
FORCE WHEEL CONTROL SYSTEM
WITH ARTIFICIAL STABILITY
AND ARTIFICIAL FEEL

FIGURE 5
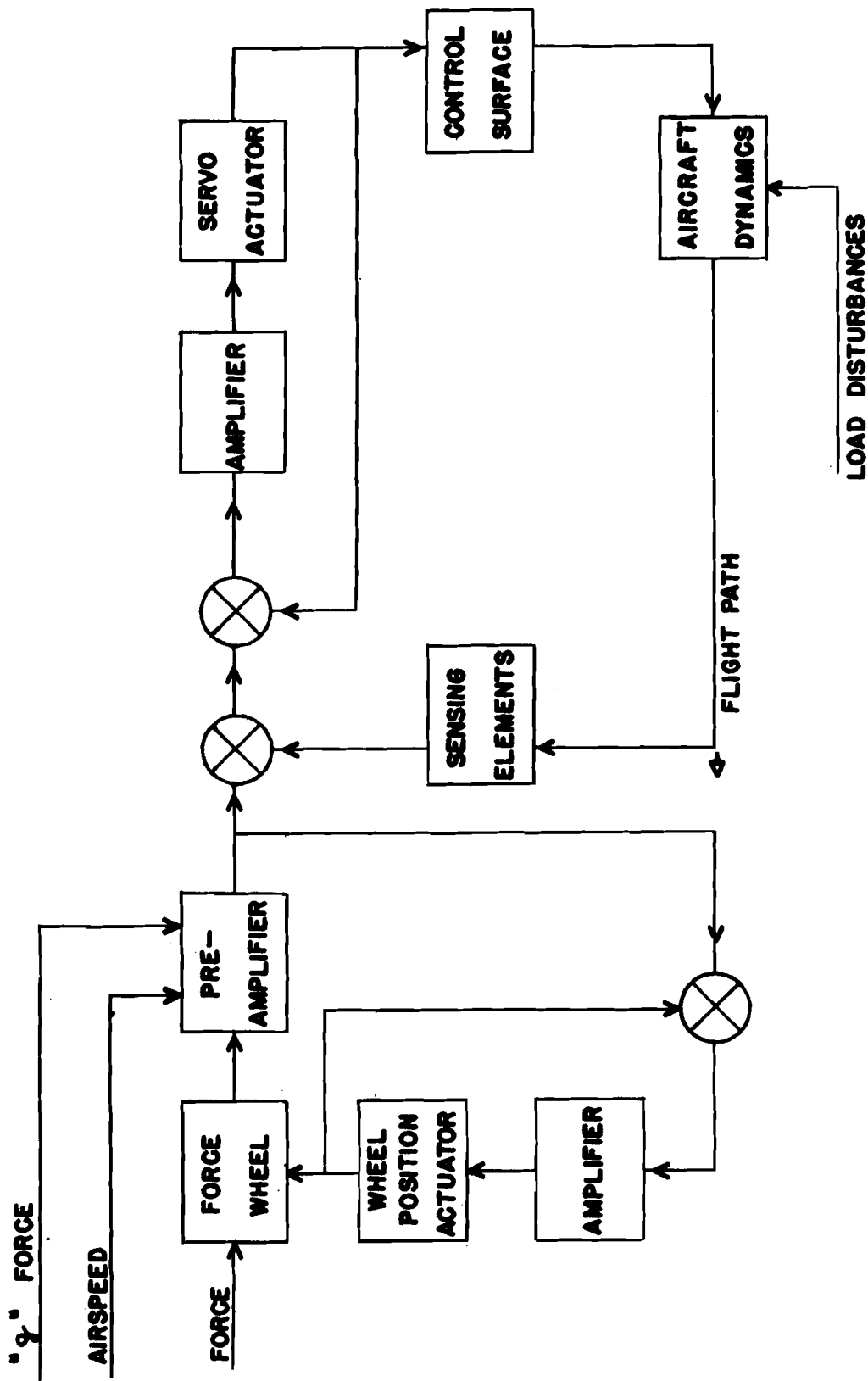
FORCE WHEEL CONTROL SYSTEM
WITH ARTIFICIAL STABILITY
AND ARTIFICIAL FEEL

FIGURE 6

The configuration described above results in a control character-
istic in which, effectively, wheel force commands rate of change of
attitude. If the integrator is removed, the lateral control charac-
teristic becomes similar to that of an automobile, in which wheel
force commands a rate of turn. Integrators for the B-17 installation
were constructed and ground-checked but were never installed. Improved
integrators will be a feature of the C-54 installation.

In Figure 5, the pilot's controls are not connected mechanically to
the control surface, and motions of the control surface induced by arti-
ficial stability signals from the sensing element are not accompanied by
similar motions of the cockpit controls. This means that the pilot is
not subjected to the possibly disconcerting phenomenon of having the
control wheel move about in a manner which he does not command. As far
as the pilot is concerned, he is flying an aircraft which is more stable,
but just as controllable as the same aircraft would be if it had a more
conventional control system.

The force wheel system of Figure 5 is a so-called "full-powered"
system in which none of the power necessary to move the control surfaces
is supplied by the pilot. This is in contrast to the systems previously
described, which are boost systems, since a small portion of the power
necessary to move the control surfaces is supplied by the pilot through
the rigid mechanical connection between the cockpit controls and the
control surfaces.

In a full powered system there is no conventional control "feel"
for the pilot, so it is desirable to include artificial feel in the form
of a bungee spring, and bobweight with provisions for variation of the bungee
characteristics with airspeed. The effect of trim may be simulated by in-
cluding means for varying the cockpit control position at which no force is
experienced. It may be desirable, however, to fix the stick and fly with
forces alone. This was to have been tried on the B-17. In this case
there would be no control position gradient and no displacement of the
stick with varying trim.

Another force wheel system using full-powered control surfaces is
shown in Figure 6. This arrangement is similar to that just described,
except that the artificial feel bungee has been replaced by a wheel position
servo system. The force-displacement gradient may be conveniently adjusted,
and, in fact, may be made nonlinear if desired. Nonlinear gradients are
supposed to be psychologically optimum. Provisions are shown for the in-
troduction of airspeed and "g" force signals into the force wheel preamp-
lifier to simultaneously alter the control surface and wheel force gradi-
ents. This is essentially the system which is to be flown in the C-45.

The force wheel systems mentioned above are only a few of the many possible configurations. Tests with systems similar to those of Figures 4 and 6 will be conducted by the All Weather Branch in coming months.

The use of force wheel control, in conjunction with inboard stabilization of airframe dynamics, makes simultaneous flight path stability and control realizable. All the flexible methods of servo-mechanism loop compensation are placed at the disposal of the airplane handling qualities designer. While many research questions concerning optimum stability and control remain to be investigated in flight, the technical practicability and enthusiastic pilot acceptance of force wheel control have already been demonstrated.

BIBLIOGRAPHY

1. Graham, D.     "Flight Path Stability and Control in Relation to All Weather Flying"   USAF  MR  WCT-2372  29 October 1951

2. Milliken, W. F. "Dynamic Stability and Control Research, Section VIII"  Cornell Aeronautical Laboratory Report No. CAL-39   (Paper presented at the Third International Conference of the R. Ae. S.-I. A. S. Brighton, England  September 3-14 1951)

3. Perkins, C. D. and Graham, D.  "Control Force Instrumentation For Flight Test"  Princeton University Aeronautical Engineering Laboratory   Report No. 107  30 March 1949

4. Orlansky, J.     "Psychological Aspects of Stick and Rudder Controls in Aircraft"  Aeronautical Engineering Review vol. 8 no. 1    January 1949

# AN ANALYSIS OF FULLY-POWERED AIRCRAFT CONTROL SYSTEMS

## Including Some Reference to Flutter Theory

by

D. T. McRUER
G. E. CLICK
J. W. HAGER
of

Northrop Aircraft, Incorporated
Hawthorne, Cal.

### SUMMARY

The overall control system analyzed features an integrally mounted valve-cylinder combination. Among the parameters included in the derivations of the equations are: compressibility of the working fluid, all major system elasticities, all apparent sources of damping, and some aerodynamic effects.

Consideration is given to the effect of the major system parameters upon the dominant frequency modes and upon stability. Possible modifications to the classical flutter theory are also indicated.

## TABLE OF CONTENTS

## INTRODUCTION

This paper presents an analysis of a typical valve-cylinder hydraulic actuator as shown in Fig. 1.
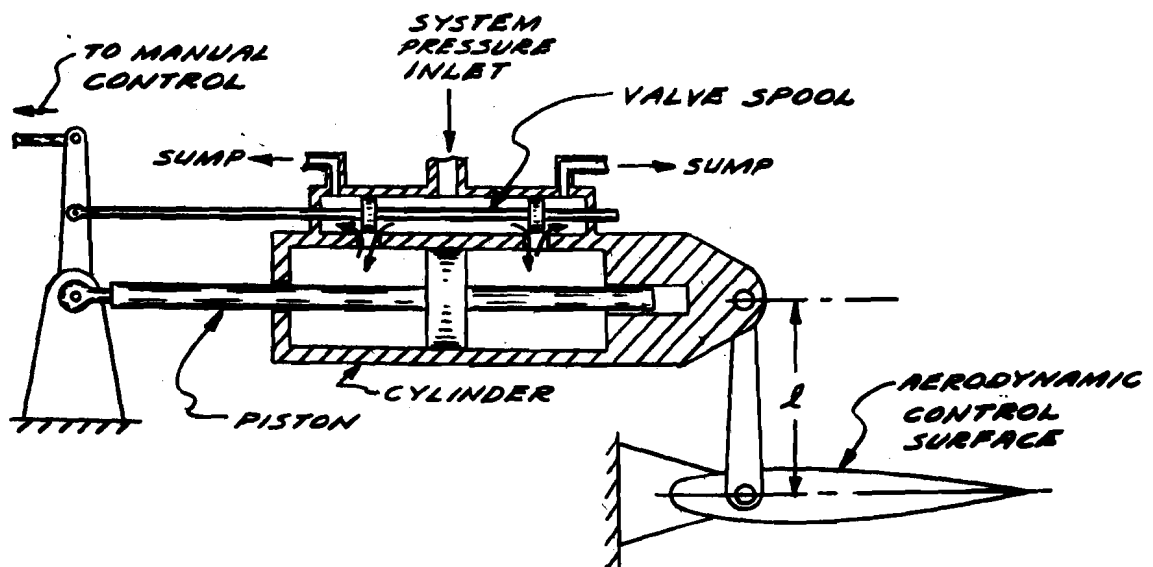


Schematic of Valve-Cylinder Hydraulic Actuator

## Fig. 1

The valve, being integral with the cylinder, provides:

- ~~compression so that the~~ fluid is made more rigid and entrained air will never constitute an appreciable part of the working volume of fluid.

2. Position error as a function of load, common to "open center" systems, assumes negligible proportions because the neutral leakage (region of open center type operation) is confined to extremely small valve displacements. (Fig. 2.)

3. The dead band common to "closed center" systems is eliminated.

4. Extremely high force and power amplification, high efficiency, low time constants, and low thresholds of operation are possible.
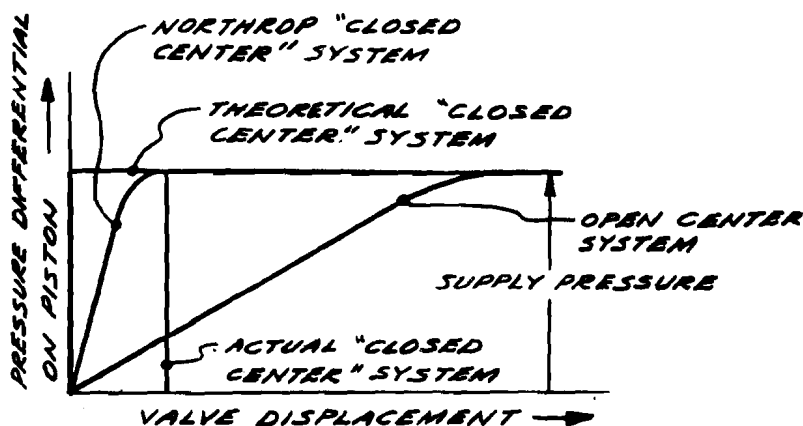


Curves of Resultant Pressure on Piston
for Different Types of Control Systems

Fig. 2

This system has been in use by Northrop Aircraft since about 1943. The difficulty in design of these systems in the past has been due primarily to a lack of knowledge of its stability and of its dynamic action.

It is the primary purpose of this paper to set up a mathematical model of this general type of actuator, present various frequency response data as achieved in practice, and provide the basis of analytical treatment from which the application of normal servomechanism methods can result in achieving a satisfactory system. The present paper is not concerned with the physical manifestations of proper design (see Reference 1), but design practice can readily be based on the conclusions presented or implied herein.

METHOD OF ATTACK

The mechanism under discussion is inherently non-linear for almost all large input amplitudes. Also, the system is complex enough to make a non-linear analysis difficult and lengthy, if not impossible with presently known techniques. Therefore the approach used considers small perturbations about steady state operating points.

The plan is as follows:

1. Derive the flow equations.

2. Derive the simplified system load equations.

3. Combine the two and discuss the simplified system.

4. Discuss the limiting cases of the simplified system.

5. Derive the equations for the general load case including effects on flutter theory.

## ASSUMPTIONS

The following assumptions will govern the analysis:

1. Linearity exists about steady-state operating points.

2. All elements of the system can be replaced by lumped constants.

3. The fluid in the cylinder is always compressed to the extent that cavitation is negligible.

4. The valve is designed in such a way as to make negligible the rate of change of momentum of the fluid as it passes through the valve, thus resulting in the elimination of centering and decentering forces on the valve.

5. The piston is double ended.

6. The valve is symmetrical, i.e., in its neutral position all neutral leakage areas are equal.

7. Sump pressure is essentially zero.

## THE FLOW EQUATIONS

SERVO ERROR - The error, $E$ , of this servomechanism is the difference between the valve displacement relative to fixed structure, $X_v$ , and the cylinder displacement relative to the same fixed structure, $X_e$ . Let the perturbations of the displacements $X_v$ , $X_n$ , and $E$
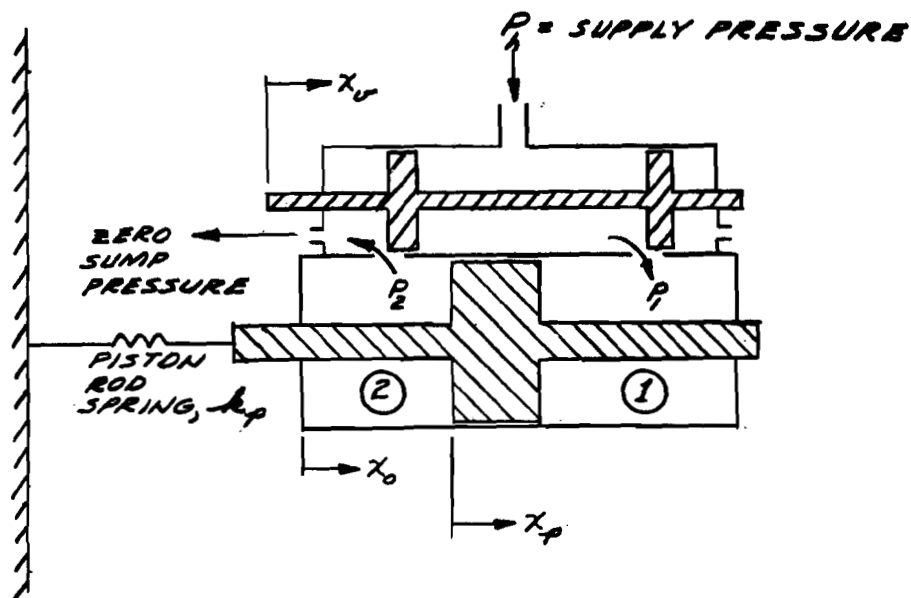
Pressure and Displacement Definitions

<u>Fig. 3</u>

<u>FLOW FROM THE VALVE</u> - The effective flow from the valve tending to move the cylinder is a function of the supply pressure, $P_1$ , the cylinder pressures $P_1$ and $P_2$ , on either side of the piston, and the valve displacement from neutral, $E$ . The functional dependence upon $P_1$ , and $P_2$ is more simply expressed in terms of the pressure difference, $P_c$ = $P_1 - P_2$ ; then, outside the neutral leakage region the flow from the valve into the high pressure side of the cylinder is given by

(2)  $\quad Q = f(E) \sqrt{P_1 - P_c}$

where $Q$ is volume per sec.

and $f(E)$ is a function of orifice area.

NOTE: The above relationship is easily derived from the fundamental orifice equation

$$Q = C a_c \sqrt{2g\left(\frac{\Delta P}{w}\right)}$$

where $\quad C$ = orifice coefficient

$\quad\quad a_c$ = orifice area

$g$ = gravitational constant

$w$ = specific weight of fluid

$\Delta p = P_h - P_l$ = pressure drop across orifice

$P_l = \dfrac{P_h + P_c}{2}$, because of valve symmetry

Inside the neutral leakage region the flow from the valve must be expressed by more complicated functions of the above mentioned variables. However, the object of this short discussion is to emphasize that the flow from the valve is predominantly dependent upon $P_c$ , $E$ , and $P_h$ , and that the relationship is continuous for all practical purposes. Therefore, since

(3) $\qquad Q = Q\,(P_c,\ P_h,\ E)$

the first order Taylor's expansion of the perturbed flow becomes:

(4) $\qquad q = \dfrac{\partial Q}{\partial E}\,\varepsilon + \dfrac{\partial Q}{\partial P_c}\,p_c + \dfrac{\partial Q}{\partial P_h}\,p_h$

where $\varepsilon$ , $p_c$ , and $p_h$ are perturbation quantities. The term $p_h$ is a disturbance entering from the power source, and need not be considered further since this discussion deals only with the surface actuating system. Therefore,

(4a) $\qquad q = \dfrac{\partial Q}{\partial E}\,\varepsilon + \dfrac{\partial Q}{\partial P_c}\,p_c$

Typical variations of valve flow $Q$ with pressure difference $P_c$ , valve displacement $E$ being held constant, and of valve flow with valve displacement, pressure difference $P_c$ being held constant, are shown in Fig. 4. Fig. 4 also shows a typical operating point, the steady state values defining the operating point ( $Q^*$ , $E^*$ , and $P_c^*$ ) and possible values of the perturbed quantities. The partial derivatives of equation (4a) are the slopes of the curves evaluated at the operating point. Note that on Fig. (4a), the first quadrant shows the flow condition for a resisting load, and the second quadrant for an overhauling load.

CYLINDER MOTION     CYLINDER MOTION

LOAD     LOAD

$E = CONSTANT$

$Q$ vs $P_c$ FOR $E \to 0$
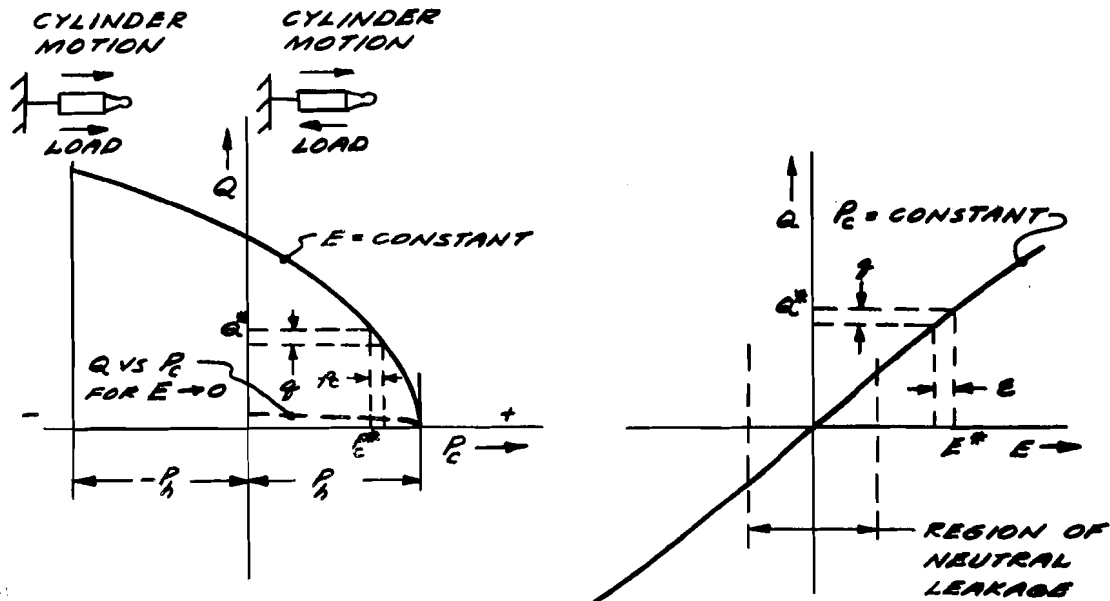
Variation of Valve Flow
with Pressure Drop
Across the Piston
(Valve displacement from
neutral constant)

(a)

$P_c = CONSTANT$

REGION OF
NEUTRAL
LEAKAGE

Variation of Valve Flow
with Valve Displacement
from Neutral
(Pressure drop across
piston constant)

(b)

Fig. 4

Note that $\partial Q / \partial E$ is always positive or zero and that $\partial Q / \partial P_c$ is always negative (or zero), a set of conditions which are almost always a necessity for system stability. It will be advantageous in the development that follows to make the normal signs of these quantities apparent, that is,

(5)    $\dfrac{\partial Q}{\partial E} = C_E$

$\dfrac{\partial Q}{\partial P_c} = -\left| C_p \right|$

Minus sign denotes that slope of Fig. 4 (a) is always negative.

Then equation (4a) may be written

(4b)    $q = C_E E - C_p P_c$

The term $C_p$ is analogous to the slope of the torque-speed curve of a shunt motor, and gives rise to a similar damping action. The term $C_E$ is analogous to the slope of the speed-field current curves of a shunt motor, and gives rise to a similar gain term in the overall system.

$C_p$ varies from zero to infinity as a function of $F$ and of $E$; the zero occurring when the valve is in neutral with no pressure drop across the piston, and the infinity occurring at the system stall.

THE FLOW INTO THE CYLINDER - It now becomes necessary to relate the flow from the valve with cylinder motion, piston motion, and the pressure drop across the piston. In developing the equations for cylinder flow the compressibility of the fluid will be taken into account.

The total mass of fluid on one side of the piston at any time $t$ is:

(6) $\quad m = \rho \gamma$

where $\quad \gamma$ = volume occupied by the mass

and $\quad \rho$ = fluid density at the time

(7) $\quad$ Then $\quad \dfrac{dm}{dt} = \rho \dfrac{d\gamma}{dt} + \dfrac{\gamma}{\rho} \dfrac{d\rho}{dt}$ ,

and the volumetric flow corresponding to this mass flow rate is

(8) $\quad Q = \dfrac{1}{\rho} \dfrac{dm}{dt} = \dfrac{d\gamma}{dt} + \dfrac{\gamma}{\rho} \dfrac{d\rho}{dt}$

The compressibility of any fluid is characterized by the expression,

(9) $\quad N = -\gamma \dfrac{dP}{d\gamma} \bigg/_{m = CONSTANT} = \rho \dfrac{dP}{d\rho}$

or

(10) $\quad \dfrac{d\rho}{\rho} = \dfrac{1}{N} dP$

where $\quad N$ = bulk modulus of fluid (force per unit area)

$\rho$ = instantaneous density (mass per unit volume)

$P$ = instantaneous fluid pressure

Dividing both sides of equation (10) by $dt$ ,

(11) $\quad \dfrac{1}{\rho}\dfrac{d\rho}{dt} = \dfrac{1}{N}\dfrac{dP}{dt}$

and substituting equation (11) into (8)

(12) $\quad Q = \dfrac{dV}{dt} + \dfrac{V}{N}\dfrac{dP}{dt}$

or

(12a) $\quad Q_1 = \dfrac{dV_1}{dt} + \dfrac{V_1}{N_1}\dfrac{dP_1}{dt}$

and

(12b) $\quad Q_2 = \dfrac{dV_2}{dt} + \dfrac{V_2}{N_2}\dfrac{dP_2}{dt}$

where the subscripts, 1 and 2, denote the regions on one and on the other side of the piston respectively (see Fig. 3).

If it is assumed that the instantaneous flow into one side of the cylinder is equal to the instantaneous flow out of the other side, i.e.,

$Q_1 = -Q_2 = Q$ ,

and if it is further assumed that the bulk modulus $N$ is constant and identical for both regions, equations (12a and b) become

(13) $\quad Q = \dfrac{dV_1}{dt} + \dfrac{V_1}{N_1}\dfrac{dP_1}{dt} = -\left(\dfrac{dV_2}{dt} + \dfrac{V_2}{N_2}\dfrac{dP_2}{dt}\right)$

Since $\dfrac{dV_1}{dt} = -\dfrac{dV_2}{dt}$ , it follows that

$V_1\dfrac{dP_1}{dt} = -V_2\dfrac{dP_2}{dt}$

Addition of the quantity $(X_2\ dP/dt)$ to both sides of the last expression yields the relationship

(14) $\dfrac{dP_i}{dt} = \dfrac{\delta_2}{\delta_1 + \delta_2} \dfrac{d}{dt}\left(P_i - P_2\right) = \dfrac{\delta_2}{\delta_1 + \delta_2} \dfrac{dP_c}{dt}$

where $P_c = P_i - P_2$ , the pressure differential across the piston.

Further, the time rate of change of the volume on the high pressure side of the cylinder is

(15) $\dfrac{dV_i}{dt} = A\dfrac{d}{dt}\left(X_o - X_p\right)$

where $X_o$ = cylinder displacement relative to structure

$X_p$ = piston displacement relative to structure (non-rigid piston)

Substituting equations (14) and (15) into (13),

(16) $Q = A\dfrac{d}{dt}\left(X_o - X_p\right) + \dfrac{1}{N}\left(\dfrac{\delta_1 \delta_2}{\delta_1 + \delta_2}\right)\dfrac{dP_c}{dt}$

$= A\dfrac{d}{dt}\left(X_o - X_p\right) + \dfrac{\delta'}{N}\dfrac{dP_c}{dt}$

where $\delta' \equiv \dfrac{\delta_1 \delta_2}{\delta_1 + \delta_2}$ , an effective oil volume [‡]

The above expression is in terms of total quantities, i.e., steady state values plus perturbations. In terms of perturbed flow the expression becomes,

(17) $q = A\dfrac{d}{dt}\left(X_o - X_p\right) + \left(\dfrac{\delta'^* + \Delta\delta'}{N}\right)\dfrac{dp_c}{dt} + \dfrac{\Delta\delta'}{N}\dfrac{dP_c^*}{dt}$

[‡] The physical representation of the cylinder oil as a spring also involves this same effective oil volume. See page 12.

where $q$ , $x_o$ , $x_p$ , $p_c$ , and $\Delta r'$ are perturbed quantities, and $r'^{*}$ and $p_c^{*}$ are steady-state values.

Simplification of equation (17) may be obtained by considering specific operating conditions. For example, since perturbations are being considered about a steady-state cylinder pressure differential, the term $d p_c^{*}/dt$ must be disregarded. Furthermore, it is a recognized fact that hydraulic servos generally are nearest instability at, or near, the no-load condition.* This zero load condition closely corresponds to a faired surfaces position, wherein the volumes of oil on either side of the piston are very nearly equal. The effective oil volume has been previously defined as

$$r' = \frac{\gamma_1 \gamma_2}{\gamma_1 + \gamma_2} ,$$

and since $\Delta \gamma_1 = -\Delta \gamma_2 = \Delta r$

then $\Delta r' \approx \Delta r \left( \frac{\gamma_2 - \gamma_1}{\gamma_1 + \gamma_2} \right)$ ;

so if $\gamma_1 \approx \gamma_2$ , then $\Delta r' = 0$ ,

or $\qquad\qquad\qquad r' \approx$ a constant $= r'^{*}$

The approximate linearized expression for perturbed flow thus obtained under the foregoing conditions is

$$(18) \quad q = A \frac{d}{dt} \left( x_o - x_p \right) + \frac{r'}{N} \frac{d p_c}{dt}$$

or (18a) $\quad q(s) = A s \left[ x_o(s) - x_p(s) \right] + \frac{r'}{N} s p_c(s)$

The physical representation of the oil within the cylinder as a spring is developed as follows:

Consider, first, an open ended cylinder that has been subjected to force $\Delta F$ and compressed a linear displacement $\Delta X$ , as shown in Fig. 5.

---

* The effective damping term, $C_p$ , approaches zero as $p_c$ , and hence the cylinder load, diminishes. See page 8.
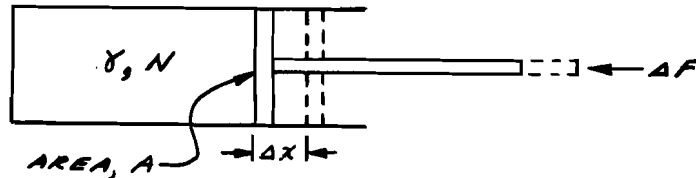
<u>Fig. 5</u>

From equation (9)

(19) $\quad \Delta \gamma = \dfrac{(\Delta P)\gamma}{N}$

The pressure increment is $\quad \Delta P = \dfrac{\Delta F}{A}$

and the volume increment is $\quad \Delta \gamma = A(\Delta x)$

so that,

(20) $\quad \dfrac{\Delta F}{\Delta x} = \dfrac{A^2 N}{\gamma} = K_o \qquad$ = Equivalent spring constant of the oil.

Actually there is oil in both sides of the piston so that effectively there are two springs in parallel; hence the effective spring constant is

$$ k_o = \dfrac{A^2 N}{\gamma_1} + \dfrac{A^2 N}{\gamma_2} = A^2 N \left( \dfrac{\gamma_1 + \gamma_2}{\gamma_1 \gamma_2} \right) $$

(20a) $\quad k_o = \dfrac{A^2 N}{\gamma'}$

where $\quad \gamma' = \dfrac{\gamma_1 \gamma_2}{\gamma_1 + \gamma_2} \qquad$ as in equation (16).

## THE LOAD EQUATIONS

The true load upon the cylinder is rather involved and will be considered later. Due to its complexity it is desirable to use a simplified system to obtain basic understanding and then use the entire system to determine the effect of some of the less important elements upon the system operation. The simplified system is illustrated in Figs. 6 and 7. It will be noted that the piston rod is assumed rigid and that the valve displacement $x_v$ is considered identical to the servo input signal $x_i$ .
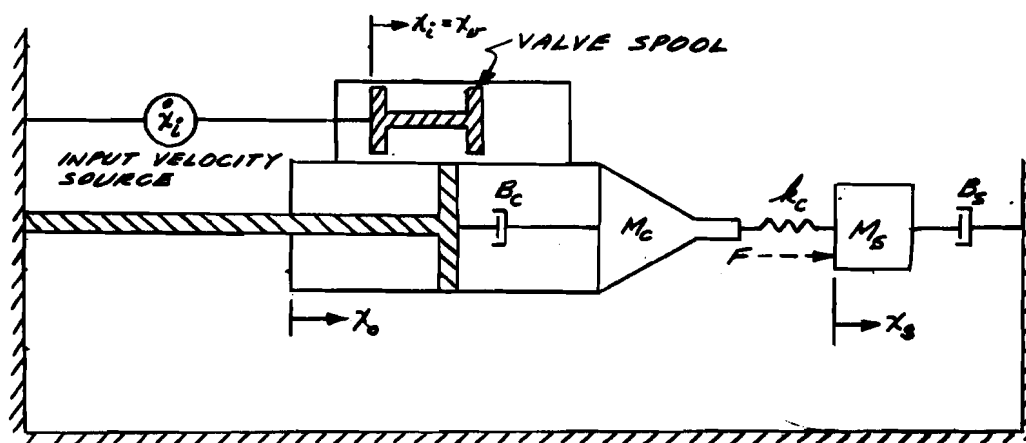
Schematic Load Diagram

Fig. 6
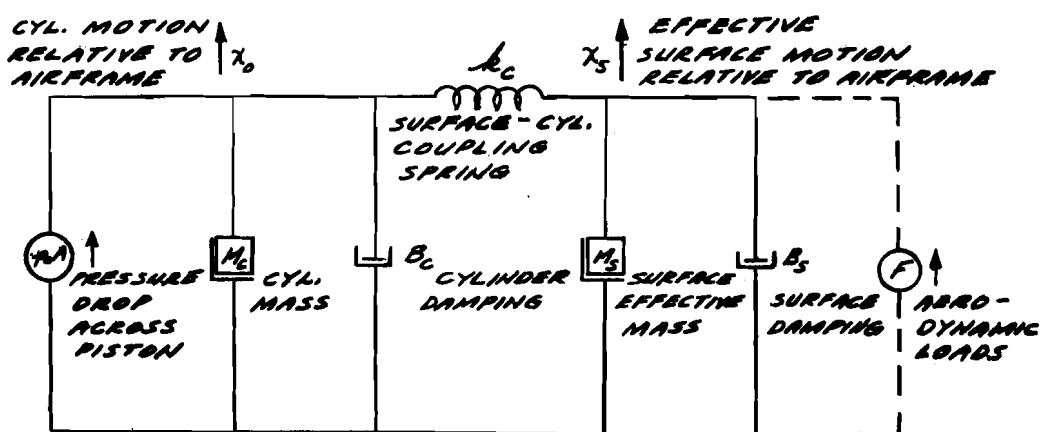


NOTE: All "effective" quantities are referred to the line of action of the cylinder.

Simplified Load System

Fig. 7

The load equations based upon this simplified system are presented below:

(21) $\quad X_o \left( M_c s^2 + B_c s + k_c \right) - k_c X_s - p_c A = 0$

(22) $\quad -k_c X_o + X_s \left( M_s s^2 + B_s s + k_c \right) = F$

The error equation (1), with $x_i = x_{ir}$, becomes

$$(1)' \quad \varepsilon = x_i - x_o$$

also, since the piston displacement $x_p$ is non-existent, the flow equation (18a) becomes

$$(18a)' \quad q = As\, x_o + \frac{\gamma'}{N} s\, p_c$$

The flow equations (4b) (page 7 ) and (18a') combine to form the expression

$$(23) \quad As\, x_o + p_c \left( \frac{\gamma'}{N} s + C_p \right) = C_\varepsilon \varepsilon$$

The simplified load system is now completely defined by equations (21) through (23).

## THE SIMPLIFIED SYSTEM

It now becomes a simple algebraic task to combine equations (21) through (23) into the open loop transfer function of the system. By definition, the open loop transfer function implies that all extraneous inputs, or disturbances, are zero; hence the aerodynamic force $F$ of equation (18) is zero.

$$
(24) \quad \frac{x_o}{\varepsilon} = \frac{C_\varepsilon\, AN}{\gamma'}\left(s^2 + \frac{B_s}{M_s}s + \frac{A_c}{M_s}\right) \left\{ M_c s \left[ s^4 + \left( \frac{B_s}{M_s} + \frac{B_c}{M_c} + \frac{C_p N}{\gamma'} \right) s^3 \right.\right.
$$

$$
+ \left( A_c \left\{ \frac{1}{M_c} + \frac{1}{M_s} \right\} + \frac{B_s B_c}{M_c M_s} + \frac{C_p N}{\gamma'} \left\{ \frac{B_s}{M_s} + \frac{B_c}{M_c} \right\} + \frac{A^2 N}{\gamma' M_c} \right) s^2
$$

$$
+ \left( \frac{A_c}{M_c M_s}\left[ B_s + B_c \right] + \frac{C_p A_c N}{\gamma'}\left[ \frac{1}{M_c} + \frac{1}{M_s} \right] + \frac{C_p N B_s B_c}{\gamma' M_c M_s} \right.
$$

$$
\left. + \frac{A^2 N B_c}{\gamma' M_c M_s} \right) s + \left( \frac{C_p A_c N}{\gamma' M_c M_s}\left[ B_s + B_c \right] + \frac{A^2 N A_c}{\gamma' M_c M_s} \right) \left.\left.\right]\right\}^{-1}
$$

Near valve neutral, with $\ell_c^* = 0$ , the open loop transfer function becomes simple, since $C_p \approx 0$ . (See Fig. 4.) Making this substitution plus the relationship $A_0 = A^2 N / \delta'$ (the effective spring due to oil compressibility), equation (24) becomes:

$$(25) \quad \frac{x_o}{\varepsilon} = \frac{\frac{C_E A_o}{A}\left[s^2 + \frac{B_s}{M_s}s + \frac{A_c}{M_s}\right]}{s\left\{s^4 + \left[\frac{B_s}{M_s} + \frac{A_c}{M_c}\right]s^3 + \left[A_c\left(\frac{1}{M_c} + \frac{1}{M_s}\right) + \frac{A_o}{M_c} + \frac{B_s A_c}{M_c M_s}\right]s^2 + \left[\frac{A_c(B_s + A_c)}{M_c M_s} + \frac{A_o B_s}{M_c M_s}\right]s + \frac{A_o A_c}{M_c M_s}\right\}}$$

Equation (25), though representative of a simplified system, is still quite complex. It is therefore of considerable value to attempt approximate factorization, and to consider limiting cases.

Equations (24) and (25) are of the form

$$(26) \quad \frac{x_o}{\varepsilon} = \frac{K \omega_1^2 \omega_\varepsilon^2}{\omega_3^2} \frac{(s^2 + 2 \zeta_3 \omega_3 s + \omega_3^2)}{s(s^2 + 2 \zeta_1 \omega_1 s + \omega_1^2)(s^2 + 2 \zeta_2 \omega_2 s + \omega_2^2)}$$

By assuming that the denominator frequencies are widely separated, it is possible to obtain an approximate factorization of the denominator in general terms. (See Table I.) The method originally developed by Lin (Reference 2) is employed for the factorization; it is assumed that the first trial solution converges immediately. In this situation, the Bode diagrams of the simplified system will appear as shown in Fig. 8. Experimental points are plotted on top of the calculated values for a typical physical system.

| | $C_p = 0$ | $C_p \neq 0$ | $C_p = 0$ {FURTHER APPROXIMATION} |
|---|---|---|---|
| $2\zeta_1\omega_1$ | $\dfrac{k_c(B_s+B_c)+k_0 B_s}{k_c(M_c+M_s)+k_0 M_s + B_s B_c}$ | $\dfrac{B_s\left[1+\frac{k_c}{k_0}\left(1+\frac{B_c}{B_s}\right)+\frac{C_p}{A^2}B_s\left[\frac{k_c}{B_s}(M_s+M_c)+B_c\right]\right]}{M_s\left[1+\frac{C_p}{A^2}\left(B_s\frac{M_c}{M_s}+B_c\right)+\frac{B_s B_c}{k_0 M_s}+\frac{k_c}{k_0}\left(1+\frac{M_c}{M_s}\right)\right]}$ | $\dfrac{B_s+\left(\frac{k_c}{k_0}\right)(B_s+B_c)}{M_s+\left(\frac{k_c}{k_0}\right)(M_s+M_c)}$ |
| $\omega_1^2$ | $\dfrac{k_c}{M_s\left(1+\frac{k_c}{k_0}\right)+\frac{B_s B_c}{k_0}+M_c\frac{k_c}{k_0}}$ | $\dfrac{k_c\left[1+\frac{C_p}{A^2}(B_s+B_c)\right]}{M_s\left[1+\frac{C_p}{A^2}\left(B_s\frac{M_c}{M_s}+B_c\right)+\frac{B_s B_c}{k_0 M_s}+\frac{k_c}{k_0}\left(1+\frac{M_c}{M_s}\right)\right]}$ | $\dfrac{1}{M_s}\left(\dfrac{k_0 k_c}{k_0+k_c}\right)$ |
| $2\zeta_2\omega_2$ | $\dfrac{k_c\left(\frac{M_c}{M_s}+B_c\frac{k_c}{M_c}\right)+B_s B_c\left(\frac{B_s}{M_s}+\frac{B_c}{M_c}\right)+k_0 B_c\frac{M_s}{M_c}}{k_c(M_c+M_s)+k_0 M_s + B_s B_c}$ | ⟶ SAME | |
| $\omega_2^2$ | $\dfrac{1}{M_c}\left(k_0+k_c\right)+\dfrac{k_c}{M_s}+\dfrac{B_s B_c}{M_c M_s}$ | ⟶ SAME | $\dfrac{1}{M_c}\left(k_c+k_0\right)+\dfrac{k_c}{M_s}$ |
| $2\zeta_3\omega_3$ | $\dfrac{B_s}{M_s}$ | $\dfrac{B_s}{M_s}$ | |
| $\omega_3^2$ | $\dfrac{k_c}{M_s}$ | $\dfrac{k_c}{M_s}$ | |
| $k$ | $\dfrac{C_e}{A}$ | $\dfrac{C_e}{A}$ | |

TABLE I

Bode Diagram & Experimental Verification
of Simplified System

Fig. 8

## LIMITING CASES OF THE SIMPLIFIED SYSTEM

COMPRESSIBILITY ZERO - (Bulk Modulus infinite.) For the limiting case in which the compressibility of the fluid becomes very small, the open loop transfer function becomes:

$$(27) \quad \frac{x_o}{\varepsilon} = C_\varepsilon A \left( M_s s^2 + B_s s + k_c \right) \left\{ s \left[ C_p M_c M_s s^3 + \left( C_p \{ B_s M_c + B_c M_s \} + A^2 M_s \right) s^2 \right. \right. $$
$$\left. \left. + \left( C_p k_c \{ M_s + M_c \} + C_p B_s B_c + A^2 B_s \right) s + \left( C_p k_c \{ B_c + B_s \} + A^2 k_c \right) \right] \right\}^{-1}$$

Around the neutral position, with $C_p = 0$ , the open loop transfer function reduces to a very simple expression.

$$(28) \quad \frac{x_o}{\varepsilon} = \frac{C_\varepsilon}{A s}$$

Equation (28) will be recognized as the conventional expression used in the analysis of hydraulic amplifiers when used with mechanisms having large lags at frequencies much lower than those of the hydraulic amplifier. Equation (28) is also recognized as that of perfect integrator and zero position error servo. The reason for this is, of course, that in this case there are no spring or friction loads. If the hydraulic amplifier itself is stable, this approximation is an excellent one when the other elements of a control loop such as an autopilot and airframe serve to lower the possible gain crossover frequency, $\omega = C_\varepsilon / A$ . For use in such analyses, then, the hydraulic system is adequately described as

$$(29) \quad \frac{x_o}{x_i} = \frac{1}{\frac{A}{C_\varepsilon} s + 1}$$

The time constant $A/C_\varepsilon$ is capable of being made quite small with proper design, down to the order of 1/100 second in the authors' experiences.

COMPRESSIBILITY INFINITE (Bulk Modulus Zero.) If valve damping, $B_v$ (between the valve spool and the valve housing), is included as an extension to the simplified load system, the open loop transfer function, equation (25), can be shown to be

$$(25)' \quad \frac{x_o}{\varepsilon} = \frac{\frac{B_v}{M_c} \left[ s^2 + \frac{C_\varepsilon k_o}{B_v A} \right] \left[ s^2 + \frac{B_s}{M_s} s + \frac{k_c}{M_s} \right]}{s \left\{ s^4 + \left[ \frac{B_s}{M_s} + \frac{B_c}{M_c} \right] s^3 + \left[ k_c \left( \frac{1}{M_c} + \frac{1}{M_s} \right) + \frac{k_o}{M_c} + \frac{B_c B_s}{M_c M_s} \right] s^2 + \right.}$$

$$\left. \left[ \frac{k_c (B_c + B_s)}{M_c M_s} + \frac{k_o B_s}{M_c M_s} \right] s + \frac{k_o k_c}{M_c M_s} \right\}$$

For the case with infinite compressibility, the above open loop transfer function becomes

$$(30) \quad \frac{x_o}{\varepsilon} = \frac{\frac{B_{cr}}{M_c}\left[s^2 + \frac{B_s s}{M_s} + \frac{k_c}{M_s}\right]}{s^3 + \left[\frac{B_s}{M_s} + \frac{B_c}{M_c}\right]s^2 + \left[k_c\left(\frac{1}{M_c} + \frac{1}{M_s}\right) + \frac{B_s B_c}{M_s M_c}\right]s + \left[\frac{k_c}{M_s M_c}(B_s + B_c)\right]}$$

Input motion is coupled to output motion only because of the viscous drag of the valve on the cylinder. The system is no longer a zero position error device. Physically, the use of the relationship of equation (30) appears when two hydraulic systems are connected in parallel, with the power to one system shut down, or on a single actuator installation with power off. If there is no viscous friction coupling between valve and cylinder, the transfer function becomes zero, and there is no motion transmitted from input to output.

COUPLING SPRING $k_c$ ZERO - The situation occasionally arises where backlash occurs between the cylinder and the surface load. It is then desirable to investigate the stability of the system within the backlash region, though it must be remembered that stability inside the backlash region does not necessarily rule out the possibility of a limit cycle occurring due primarily to the backlash.

The open loop transfer function with $k_c = 0$ then becomes:

$$(31) \quad \frac{x_o}{\varepsilon} = \frac{\frac{C_E k_o}{A M_c}\left[s + \frac{B_s}{M_s}\right]}{s\left\{s^3 + \left[\frac{B_s}{M_s} + \frac{B_c}{M_c} + \frac{C_p k_o}{A^2}\right]s^2 + \left[\frac{B_c B_s}{M_c M_s} + \frac{C_p k_o}{A^2}\left(\frac{B_c}{M_c} + \frac{B_s}{M_s}\right) + \frac{k_o}{M_c}\right]s + \left[\frac{C_p k_o B_c B_s}{A^2 M_c M_s} + \frac{k_o B_s}{M_c M_s}\right]\right\}}$$

which, when $C_p = 0$, reduces to

$$(32) \quad \frac{x_o}{\varepsilon} \approx \frac{\frac{C_E k_o}{A M_c}}{s\left(s^2 + \frac{B_c}{M_c}s + \frac{k_o}{M_c}\right)}$$
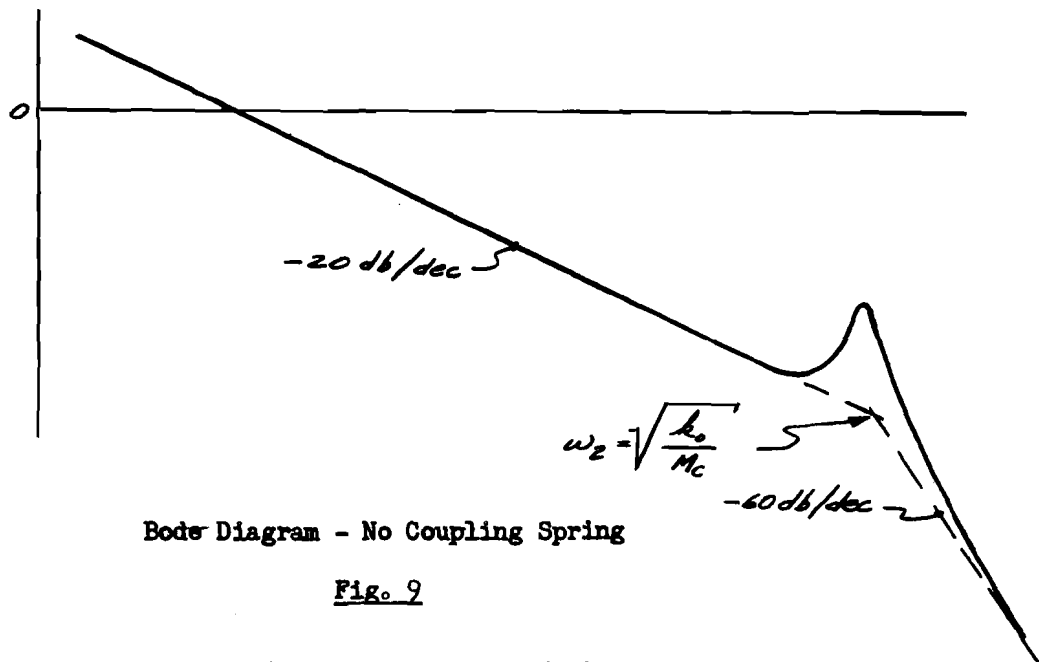
Bode Diagram - No Coupling Spring

**Fig. 9**

Comparing equation (32) with equation (25), and also comparing the Bode charts of Figures 8 and 9, it is apparent that stability of the hydraulic system outside the backlash region assures stability inside the backlash region.

DAMPING COEFFICIENTS $\mathcal{B}_c$ , $\mathcal{B}_s$ , AND $\mathcal{B}_\nu << C_p$ - When the surface loading produces high hinge moments, the pressure drop, $\mathcal{R}$ , across the cylinder approaches the system pressure, $\mathcal{R}_4$ . This condition corresponds to a very steep slope of the flow-pressure curve (Fig. 4(b)), and, hence, the gradient $C_p$ is very large compared to all other system damping.

The open loop transfer function then becomes:

$$(33) \quad \frac{x_o}{e} = \frac{C_c \, k_o \left( s^2 + \frac{k_c}{M_s} \right)}{M_c A s \left\{ s^4 + \frac{C_p k_o}{A^2} s^3 + \left[ k_c \left( \frac{1}{M_c} + \frac{1}{M_s} \right) + \frac{k_o}{M_c} \right] s^2 + \left[ \frac{C_p k_c k_o}{A^2} \left( \frac{1}{M_c} + \frac{1}{M_s} \right) \right] s + \frac{k_o k_c}{M_c M_s} \right\}}$$

Approximate factorization of the denominator yields the undamped natural frequencies:

$$(34) \quad \omega_1^2 = \frac{k_c}{M_s} \left[ \frac{1}{1 + \frac{k_c}{k_o} \left( 1 + \frac{M_c}{M_s} \right)} \right]$$

$$(35) \quad \omega_2^2 = \frac{k_c}{M_s} + \frac{1}{M_c} \left( k_o + k_c \right)$$

Note that $\omega_2$ is identical to $\omega_2$ listed in Table I.

SPRING CONSTANTS AND MASSES EQUAL - A large portion of the fore-
going discussion has to be based upon the assumption that approximate
factorization of the transfer function denominator is possible. This
tacitly assumes that the $\sqrt{k_c/M_c}$ and $\sqrt{k_c/M_s}$ are con-
siderably separated. If these quantities are not separated by a wide
margin, there are no means available to determine the effect of change of
an individual parameter upon the system except by the use of numerical
values.

It is, however, valuable to investigate a limiting case where the
values of $\sqrt{k_c/M_s}$ and $\sqrt{k_o/M_c}$ are close together, the
case for which $k_c = k_o = k$ and $M_c = M_s = M$ . For
simplification it is also assumed that the valve damping, $B_v$ , is
zero. The open loop transfer function then becomes:

$$(36) \quad \frac{x_o}{\varepsilon} = \frac{\dfrac{C_E k_o}{AM}\left[s^2 + \dfrac{B_s}{M}s + \dfrac{k}{M}\right]}{s\left\{s^4 + \left[\dfrac{B_s + k_c}{M}\right]s^3 + \left[k\left(\dfrac{3}{M}\right) + \dfrac{B_s k_c}{M^2}\right]s^2 + \left[\dfrac{k}{M^2}\left(2B_s + k\right)\right]s + \dfrac{k^2}{M^2}\right\}}$$

which, with approximate factors becomes:

$$(37) \quad \frac{x_o}{\varepsilon} = \frac{\dfrac{C_E k_o}{AM}\left[s^2 + \dfrac{B_s}{M}s + \dfrac{k}{M}\right]}{s\left\{\left(s^2 + \dfrac{2B_s + B_c}{3M}s + \dfrac{k}{3M}\right)\left(s^2 + \dfrac{\tfrac{3}{2}B_s + \tfrac{3}{2}B_c}{M}s + \dfrac{3k}{M}\right)\right\}}$$

The Bode diagram of this system is shown in Fig. 10.
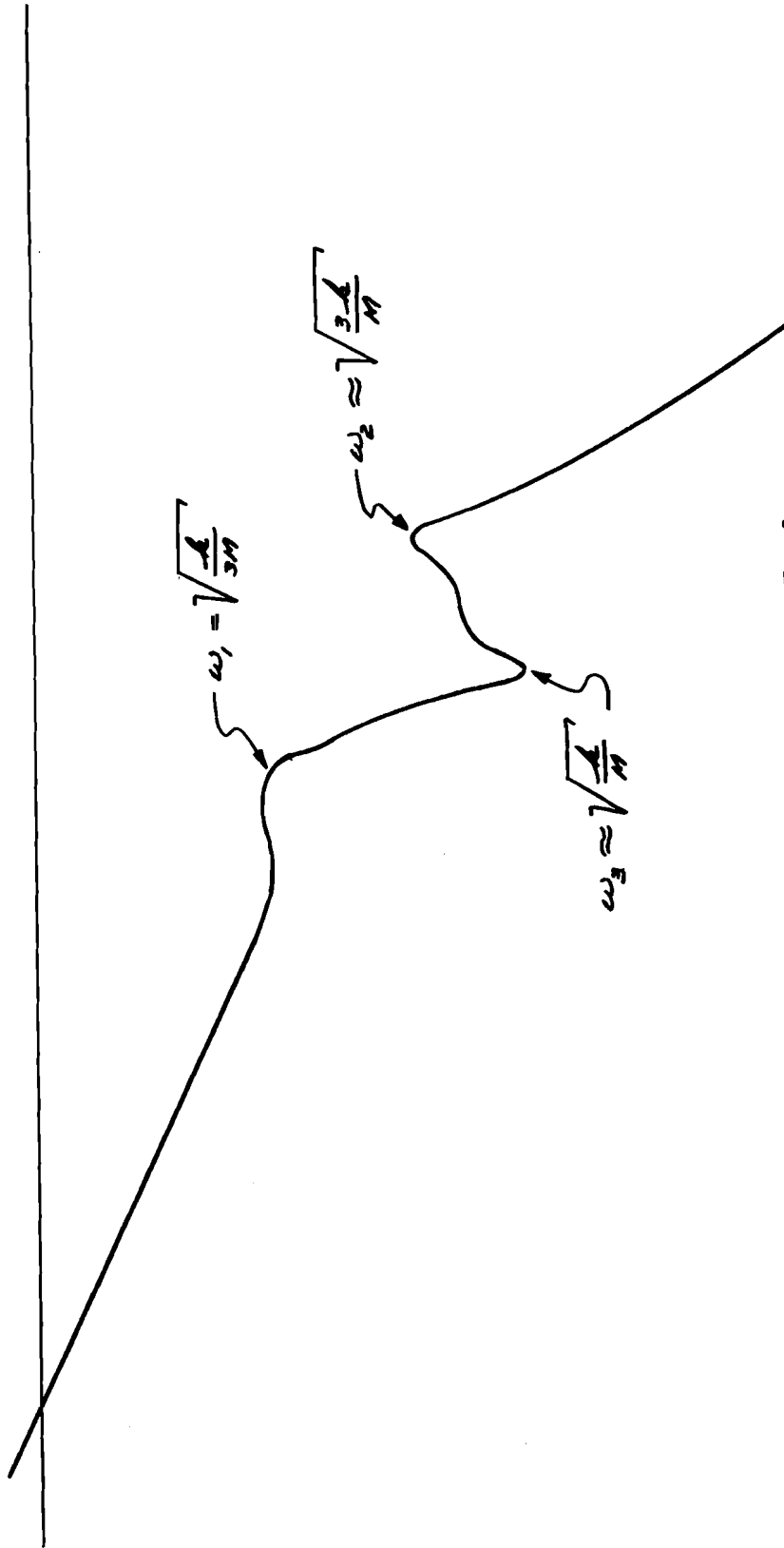
Bode Diagram - Masses and Springs Equal

Fig. 10

$$\omega_1 = \sqrt{\frac{k}{3M}}$$

$$\omega_2 \approx \sqrt{\frac{3k}{M}}$$

$$\omega_3 \approx \sqrt{\frac{k}{M}}$$

**EFFECT OF ADDING A SPRING LOAD AT THE SURFACE** (See Fig. 7.) -
The entire system analysis to this point has separated the hydraulic system
from external systems at the portion of the load schematic where the
load $F$ appears. The underlying reason for this procedure was to provide
a means of handling the flutter analysis of the hydraulic system. How-
ever, in the operation of a hydraulic system under flight conditions, the
force $F$ will be the major load, and a portion of this force may be a
definite function of $X_s$ . When such a force exists, the force $F$
ceases to be purely an external disturbance and becomes a primary element
of the inner loop. The simplest example of this situation exists when
$F = -k_s X_s$ , or a pure spring load such as a static hinge moment
gradient is applied to the system. In this event:

$$(38) \quad \frac{X_\rho}{\epsilon} = \left[\frac{C_\epsilon k_o}{A M_c}\left(s^2 + \frac{B_s}{M_s}s + \frac{k_c + k_s}{M_s}\right)\right]\left\{s^5 + \left[\frac{k_c}{M_c} + \frac{B_s}{M_s} + \frac{C_p k_o}{A^2}\right]s^4\right.$$

$$+ \left[k_c\left(\frac{1}{M_c} + \frac{1}{M_s}\right) + \frac{k_s}{M_s} + \frac{k_o}{M_c} + \frac{C_p k_o}{A^2}\left(\frac{B_s}{M_s} + \frac{B_c}{M_c}\right) + \frac{k_c B_s}{M_c M_s}\right]s^3$$

$$+ \left[\frac{k_c(B_c + B_s) + k_s B_c}{M_c M_s} + \frac{C_p k_o}{A^2}\left(\frac{k_c}{M_c} + \frac{k_c + k_s}{M_s} + \frac{k_c k_s}{M_c M_s}\right) + \frac{k_o B_s}{M_c M_s}\right]s^2$$

$$+ \left[\frac{k_c k_s}{M_c M_s} + \frac{C_p k_o}{A^2}\left(\frac{k_c(B_c + B_s) + k_s k_c}{M_c M_s}\right) + \frac{k_o(k_c + k_s)}{M_c M_s}\right]s$$

$$\left. + \frac{C_p k_o}{A^2}\frac{k_c k_s}{M_c M_s}\right\}^{-1}$$

An approximate value of the nominal lowest undamped natural frequency is,
with $C_p = 0$ .

$$(39) \quad \omega_l^2 = \frac{(k_c + k_s)k_o}{k_c(M_c + M_s) + k_s M_c + k_o M_s}$$

Normally $k_s$ is much less than $k_o$ , so that the lowest undamped
natural frequency is essentially unchanged.

**THE GENERAL LOAD CASE**

The purpose of this section is to present the equations for the
hydraulic system with all of the terms taken into account, to indicate
the use of the hydraulic system data in flutter calculations and to in-
vestigate the effects of various structural components upon the lowest
undamped natural frequency of the open loop transfer function.

64

The load equations, (40) through (43), are written from Fig. 11 (but with $C_{\nu}$ and $C_c = O$ ) as follows: (See Fig. 11).

(40) $\quad X_o\left[M_c s^2 + (A_c + B_\nu)s + k_c\right] - B_\nu s X_\nu - B_c s X_p - A_c X_s - f_c A = O$

(41) $\quad -B_\nu s X_o + X_\nu\left[M_\nu s^2 + (B_\nu + B_i)s + k_\nu\right] \qquad\qquad = k_\nu X_i$

(42) $\quad -B_c s X_o \qquad\qquad + X_p\left[M_p s^2 + (A_c + A_p)s + k_p\right] + f_c A = O$

(43) $\quad -A_c X_o \qquad\qquad + X_s\left[M_s s^2 + A_s s + k_c\right] = F$

In addition to the above load equations, one further expression is necessary for the analysis of the complete hydraulic-aerodynamic system:

(44) $\quad X_o(As + C_e) - C_e X_\nu - As X_p + f_c\left(\frac{r'}{N}s + C_p\right) = O$

This equation is obtained from the relationships given by equations (1), (4b), and (18a).

The characteristic determinant for the above array is:

$$(45)\quad \Delta_D = \begin{vmatrix} X_o & X_\nu & X_p & X_s & f_c \\[2mm] M_c s^2 + (A_c + B_\nu)s + k_c & -B_\nu s & -B_c s & -A_c & -A \\[2mm] -B_\nu s & M_\nu s^2 + (B_\nu + B_i)s + k_\nu & O & O & O \\[2mm] -B_c s & O & M_p s^2 + (A_c + A_p)s + k_p & O & +A \\[2mm] -A_c & O & O & M_s s^2 + A_s s + k_c & O \\[2mm] As + C_e & -C_e & -As & O & \frac{r'}{N}s + C_p \end{vmatrix}$$

SCHEMATIC DIAGRAM OF GENERAL
SYSTEM
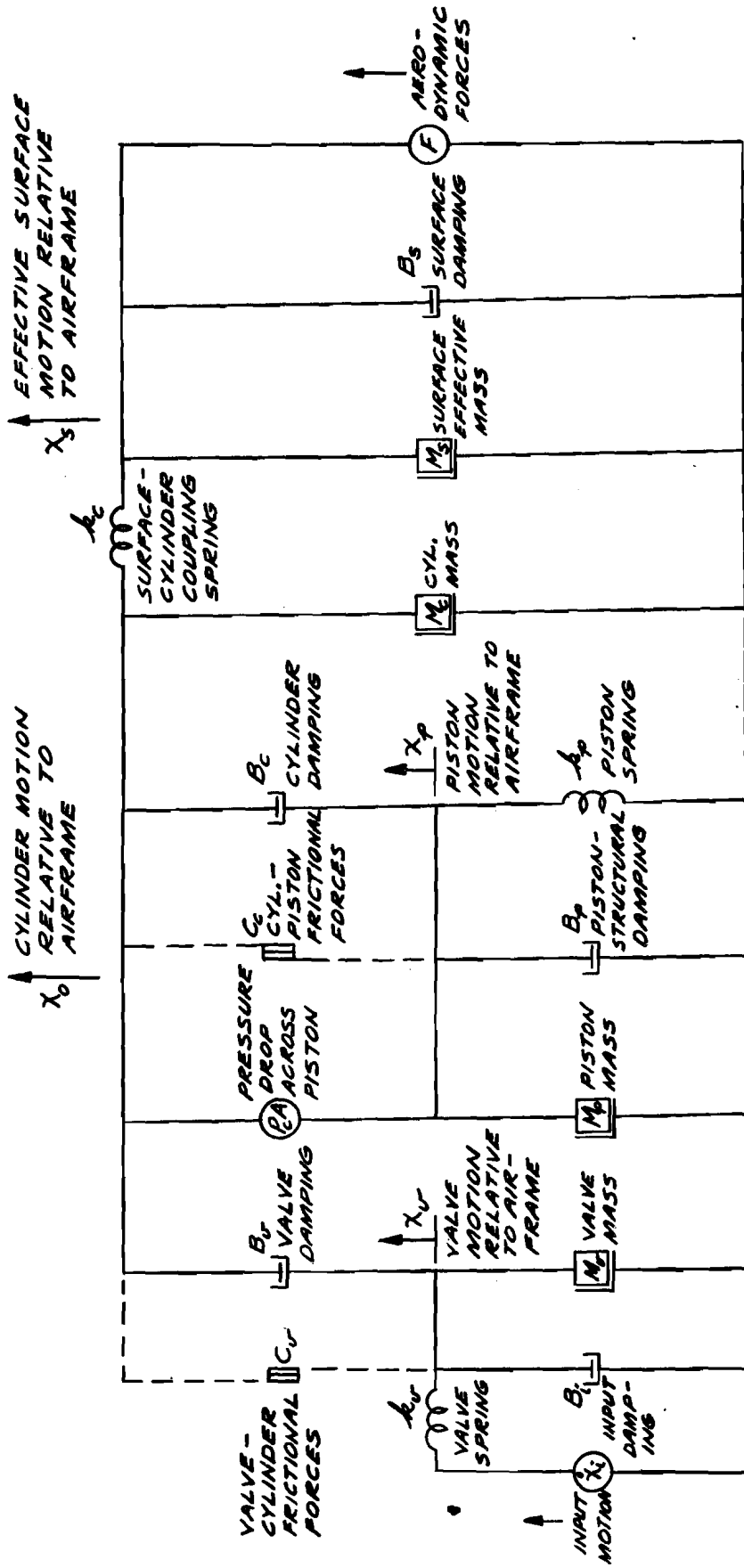
FIG. 11

GENERAL LOAD SYSTEM

FIG. 11a

The output $\chi_o$ is then

(46) $\quad \chi_o = -k_v \chi_i \dfrac{\Delta_{21}}{\Delta_D} - F \dfrac{\Delta_{41}}{\Delta_D}$

Equation (44) may be rewritten,

(44a) $\quad \chi_o (As) - As \chi_p + f_c \left( \dfrac{r'}{N} s + C_P \right) = C_E \, \varepsilon$

in which case (46) becomes:

(46a) $\quad \chi_o = C_E \, \varepsilon \, \dfrac{\Delta'_{51}}{\Delta'_D} - F \dfrac{\Delta'_{41}}{\Delta'_D} - k_v \chi_i \dfrac{\Delta'_{21}}{\Delta'_D}$

(The "primes" denote the new form of $\Delta_D$ after substitution of equation (44a) for (44).)

(46b) $\quad \chi_o = Y_E \, \varepsilon + Y_F \, F + Y_i \, \chi_i$

where $\quad Y_E = C_E \dfrac{\Delta'_{51}}{\Delta'_D}$

$\qquad\qquad Y_F = - \dfrac{\Delta'_{41}}{\Delta'_D}$

$\qquad\qquad Y_i = -k_v \dfrac{\Delta'_{21}}{\Delta'_D}$

Recalling that

$\qquad \varepsilon = \chi_v - \chi_o \qquad\qquad$ (Equation (1))

and $\quad \chi_v = \dfrac{k_v \chi_i + B_v s \chi_o}{M_v s^2 + (B_v + B_i) s + k_v} \qquad\qquad$ (Equation (41)),

Block Diagram of Complete Hydraulic-Aerodynamic System

Fig. 12

The system is greatly simplified if the valve damping, $B_v$, can be reduced to an insignificant magnitude† ; note that with $B_v = 0$, the transfer function $Y_i$ also disappears. The simplified block diagram under this assumption is shown in Fig. 13
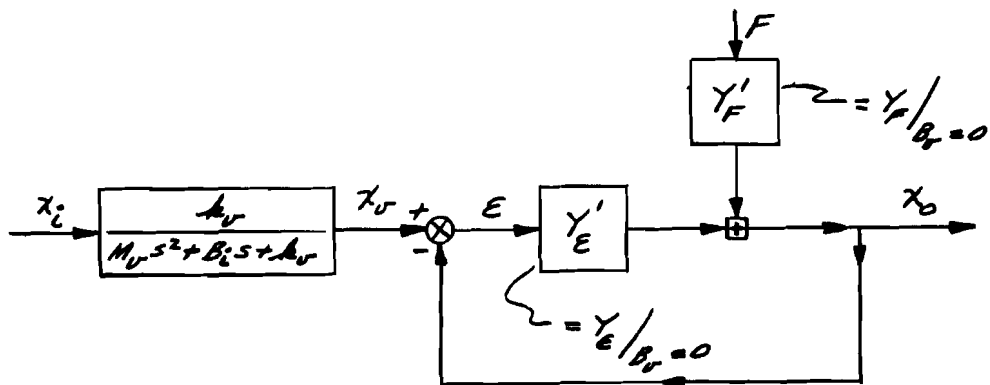


Simplified System

Fig. 13

The open loop transfer function becomes

(47) $\quad \dfrac{X_o}{\mathcal{E}} = Y_{\mathcal{E}}' = C_{\mathcal{E}} \dfrac{\Delta_{s1}'}{\Delta_b'} \Big/_{B_v = 0}$

Expansion of the terms $\Delta_{s1}'/\Delta_b'$ for $C_p = 0$ leads to the rather complex expression

(47a) $\quad \dfrac{X_o}{\mathcal{E}} = \dfrac{k_b C_{\mathcal{E}} \left[ (M_p s^2 + B_p s + k_p)(M_s s^2 + B_s s + k_c) \right]}{A s (a\, s^6 + b\, s^5 + c\, s^4 + d\, s^3 + e\, s^2 + f\, s + g)}$

† Recall that this was one of the assumptions for the simplified lead case.

where $a = M_c M_p M_s$

$$b = B_c M_c M_s + B_p M_c M_s + B_c M_p M_s + B_s M_c M_p$$

$$c = M_c M_s (k_o + k_p) + k_c M_p (M_c + M_s) + k_o M_p M_s + B_c (B_p M_s + B_s M_c + B_s M_p) + B_p B_s M_c$$

$$d = k_c M_s (B_c + B_p) + k_p (B_c M_s + B_s M_c) + k_c M_c (B_c + B_p) + k_c M_p (B_s + B_c) + k_o B_s (M_p + M_c) + B_p (k_o M_s + B_c B_s)$$

$$e = k_c k_o (M_p + M_c + M_s) + k_c k_p (M_s + M_c) + k_o k_p M_s + B_c B_s (k_p + k_c) + B_p k_c (B_s + B_c) + k_p B_s k_o$$

$$f = k_c k_p (B_s + B_c) + k_o k_c (B_p + B_s) + k_o k_p B_s$$

$$g = k_o k_c k_p$$

It will be noted that if the piston spring constant, $k_p$, becomes very large compared to all other system constants, equation (47a) reduces to the simplified expression, equation (25). When $k_p$ is of the same order of magnitude as the oil spring constant, $k_o$, and the coupling spring constant, $k_c$, the more complex open loop expression, equation (47a), must be employed for the stability analysis.

Open loop techniques require that the valve damping, $B_v$, must always be negligible. If this assumption is not made, the vastly more complicated system shown in Fig. 12 must be analyzed by considering the complete closed loop expression $x_o/x_i$. Valve damping, entirely aside from complicating the stability analysis, usually represents an unwanted input load requiring excessive pilot force and/or too large an autopilot servo motor.

It is of interest to examine the lowest approximate undamped natural frequency of the denominator of equation (47a) to gain a certain amount of insight into the effects of the system elements upon system stability. This is done in the same manner as was done previously with the simplified case: The lowest undamped natural frequency is approximately obtained by letting all damping assume negligible proportions in the quotient $g/e$ :

(48) $\quad \dfrac{g}{e} \approx \omega_n^2 \approx \dfrac{k_o\, k_c\, k_p}{M_s(k_c\, k_p + k_i\, k_p + k_c\, k_i) + M_c(k_o\, k_p + k_c\, k_i) + M_p(k_c\, k_o)}$

$\quad = \dfrac{1}{M_s\left(\dfrac{1}{k_c} + \dfrac{1}{k_o} + \dfrac{1}{k_p}\right) + M_c\left(\dfrac{1}{k_o} + \dfrac{1}{k_p}\right) + M_p\left(\dfrac{1}{k_p}\right)}$

and when $\quad M_s >> M_c \quad$ and $M_p$

(48a) $\quad \omega_n^2 \approx \dfrac{1}{M_s\left(\dfrac{1}{k_c} + \dfrac{1}{k_o} + \dfrac{1}{k_p}\right)} = \dfrac{k_r}{M_s}$

where $k_r$ is the series equivalent spring constant as seen by the surface mass, $M_s$ .

## HYDRAULIC SYSTEM DATA IN FLUTTER CALCULATIONS:

The general equations should also be used in flutter calculations. The transfer function $F/x_s$ is easily formed, and used to replace the customary inertia, damping, and spring looking into the surface. The tacit assumption restricting this usage is that bending and torsion do not couple with the hydraulic system. Referring again to equations (40) through (45) it is apparent that the surface motion may be expressed by

$$x_s = F \frac{\Delta_{44}}{\Delta_D} + k_v x_i \frac{\Delta_{24}}{\Delta_D}$$

Since the overall system is now being viewed from a flutter standpoint, i.e., looking from the surface into the system, the hydraulic system input, $x_i$, is merely a disturbance and may be considered zero.

The characteristic determinant may also be expressed,

$$\Delta_D = k_c \Delta_{14} + \left( M_s s^2 + B_s s + k_c \right) \Delta_{44}$$

Then the complete transfer function relating surface load and surface motion (with $x_i = 0$) is:

$$(49) \quad \frac{F}{x_s} = \frac{\Delta_D}{\Delta_{44}} = k_c \frac{\Delta_{14}}{\Delta_{44}} + \left( M_s s^2 + B_s s + k_c \right)$$

where

$$\frac{\Delta_{14}}{\Delta_{44}} = \frac{-k_c Z_v \left( h s^3 + i s^2 + j s + k \right)}{\left( \ell s^7 + m s^6 + n s^5 + n_2 s^4 + t s^3 + u s^2 + v s + w \right)}$$

and where

$$Z_v = M_v s^2 + \left( B_v + B_i \right) s + k_v$$

$$h = \frac{A^2}{C_p} M_p$$

$$i = k_o M_p + \frac{A^2}{C_p} \left( B_c + B_p \right)$$

$$j = k_o \left( B_c + B_p \right) + \frac{A^2}{C_p} \left( k_o + k_p \right)$$

$$k = k_o k_p$$

$$\ell = \frac{A^2}{C_p} M_C M_v M_p$$

$$m = \frac{A^2}{C_p} \lambda + k_0 M_C M_p M_v$$

where: $\lambda = M_C M_v (B_c + B_p) + M_c M_p (B_v + B_i) + M_v M_p (B_c + B_v)$

$$n = \frac{A^2}{C_p}\left[\Omega + \eta + k_0 M_v (M_c + M_p)\right] + k_0 \lambda$$

where: $\Omega = k_c M_p M_v + k_p M_c M_v + k_v M_c M_p$

$$\eta = M_c(B_c + B_p)(B_v + B_i) + M_p\left[B_v(B_c + B_i) + B_i B_c\right] + M_v\left[B_i(B_c + B_p) + B_p B_c\right]$$

$$r = \frac{A^2}{C_p}\left\{ \xi + k_0\left[(M_c + M_p)(B_v + B_i) + M_v(B_v + B_p)\right] + \zeta \right\} + k_0(\Omega + \eta) + \frac{AC_E}{C_p} k_v M_v M_p$$

where: $\xi = k_c\left[M_v(B_c + B_p) + M_p(B_v + B_i)\right] + k_p\left[M_v(B_c + B_v) + M_c(B_v + B_i)\right]$

$$\qquad + k_v\left[M_c(B_c + B_p) + M_p(B_c + B_v)\right]$$

$$\zeta = B_c B_p(B_v + B_i) + B_v B_i(B_c + B_p)$$

$$t = \frac{A^2}{C_p}\left\{ k_0\left[M_v k_p + k_v(M_p + M_c) + M_v k_c + B_v(B_c + B_p) + B_i B_p\right] \right. $$
$$\left. + \phi + \psi \right\} + k_0\left[\xi + \zeta + \frac{AC_E}{C_p}(M_v k_p + M_p B_i)\right]$$

where: $\phi = M_v k_c k_p + M_p k_v k_c + M_c k_v k_p$

$$\gamma = k_c(B_v + B_i)(B_c + B_p) + k_p\left[B_v B_c + B_i(B_c + B_v)\right] + k_v\left[B_v B_c + B_p(B_v + B_c)\right]$$

$$u = \frac{A^2}{C_p}\left\{ \sigma + k_0\left[k_v(B_v + B_p) + k_c(B_v + B_i)\right] \right\} + k_0\left\{ \phi + \gamma + \frac{AC_E}{C_p}\left[(M_v k_p + M_p k_i) \right.\right.$$
$$\left.\left. + B_i k_p\right] \right\}$$

where: $\sigma = k_c k_p(B_v + B_i) + k_c k_v(B_c + B_p) + k_v k_p(B_c + B_p)$

$$v = \frac{A^2}{C_p}\left[ k_p k_v(k_c + k_0) + k_c k_0 k_v\right] + k_0 \sigma + \frac{AC_E}{C_p} k_0 k_p(B_v + B_i)$$

$$w = k_0 k_p k_v\left(k_c + \frac{AC_E}{C_p}\right)$$

74

It will now be shown that the quadratic term of equation (49) includes the only dynamical parameters considered in the normal flutter analyses, where as the first term, $\Delta_c$ $\Delta_{i+}/\Delta_{++}$ , represents the correction that must be added to take into account the heretofore disregarded characteristics of the hydraulic-flutter system.

In ordinary flutter calculations it is the practice to use Theodorsen's differential equations of motion. The equation expressing the equilibrium of the moments on a movable surface is given by:

$$\ddot{\alpha}\left[I_\beta + \mathcal{L}(c-a)S_\beta\right] + \ddot{\beta}\,I_\beta + \beta\,C_\beta + \ddot{\mathcal{L}}\,S_\beta = M_\beta$$

or

(50) $\alpha(s)\,s^2\left[I_\beta + \mathcal{L}(c-a)S_\beta\right] + \beta(s)\left[I_\beta\,s^2 + C_\beta\right] + \mathcal{L}(s)\left[S_\beta\,s^2\right] = M_\beta(s)$

where     $\alpha$ = angle of attack

$\beta$ = surface angular deflection

$\mathcal{L}$ = vertical coordinate of axis of rotation of airfoil

$I_\beta$ = moment of inertia per unit length of surface (about hinge line)

$S_\beta$ = static moment of surface (in slugs-feet) per unit length (about hinge line)

$C_\beta$ = torsional stiffness of surface per unit length (about hinge line)

$M_\beta$ = total aerodynamic moment on surface per unit length (about hinge line)

$a$ = coordinate of axis of rotation of airfoil (percent of airfoil half chord length)

$\mathcal{L}$ = half chord length of airfoil

$c$ = coordinate of surface hinge line (percent of airfoil half cord length)

Fig. 14 Illustrates the geometrical parameters of the airfoil-surface combination.
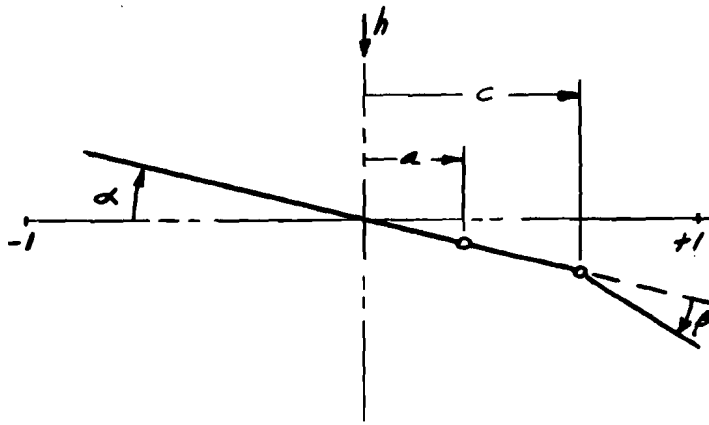
Parameters of Airfoil-Surface Combination

Fig. 14

Of especial concern is that portion of the total aerodynamic moment which is related to $\beta$ and its derivatives alone. Designating this moment component by $M_F$ ,

(51) $\quad M_F = \beta\left[ I_\beta s^2 + C_\beta \right]$

The above equation, obviously, does not include the dynamical characteristics of the hydraulic system, but, rather, represents a surface inertia tied to a spring, as illustrated below.
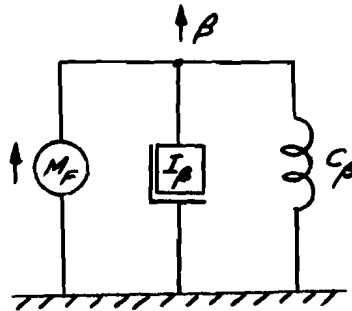


Fig. 15

Since $\quad M_F = \dfrac{F \cdot l}{d}$

$I_\beta = \dfrac{M_S \cdot l^2}{d}$

$$C_\beta = \frac{\mathcal{A}_c \mathcal{L}^2}{d}$$ ($\mathcal{A}_c$ includes all flexibility from the hydraulic cylinder to the effective mass center of the surface)

$$\rho = \frac{x_s}{\ell}$$

$\mathcal{L}$ = surface horn radius

$d$ = surface span

then in lineal terms, equation (51) becomes:

(52) $$\frac{F}{x_s} = M_s s^2 + \mathcal{A}_c = \frac{M_F d}{\beta \ell^2}$$

Comparison of equation (52) with (49) clearly shows that the complete expression for the hydraulic-flutter system is far more complex than the simple situation shown in Fig. 14.

Thus

(53) $$M_F = \beta \frac{\ell^2}{d} \left( \frac{F}{x_s} \right)$$

$$= \beta \left[ \frac{\ell^2}{d} \frac{\Delta_o}{\Delta_{FF}} \right]$$

The above component of the total aerodynamic moment related to $\beta$ and its derivatives alone now replaces the original incomplete term in equation (50); therefore the differential equation of motion is more precisely expressed,

(54) $$\alpha(s) \left[ I_\beta s^2 + \mathcal{A}(c-a) S_\beta \right] + \beta(s) \left[ \frac{\ell^2}{d} \frac{\Delta_o}{\Delta_{FF}} \right] + \mathcal{A}(s) S_\beta s^2 = M_\beta(s)$$

The diagrammatic representation of the corrected component is seen in Fig. 16.
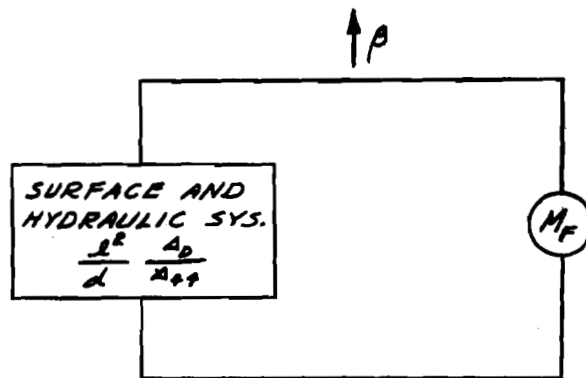
Fig. 16

Recalling that equation (49) expressed the term $P/x_s$ $(= \Delta_p/\Delta_{qq})$ as the sum of the separate components individually due to the surface dynamics and the hydraulic system dynamics, then an equalivalent representation of Fig. 16 may be visualized schematically as shown below.
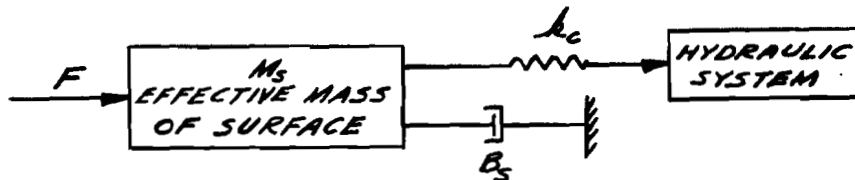


from the system, i.e., the valve mass, $M_v$ , and its attached spring, $k_v$ , are uncoupled from the network. The term $z_v/x_v = 0$ then becomes, as a logical consequence, a perfect factor of the seventh order denominator, and all terms related to valve motion vanish from the expression.

The following transfer function results:

$$(55) \quad \frac{F}{x_s} = -k_c^2 \left\{ B_{cp} M_p s^3 + \left[ k_0 M_p + B_{cp}(B_c + B_p) \right] s^2 + \left[ B_{cp}(k_0 + k_p) \right. \right.$$

$$\left. + (B_c + B_p)k_0 \right] s + k_0 k_p \right\} \left\{ B_{cp} M_c M_p s^5 + \left\{ B_{cp} \left[ (B_c + B_p) M_c \right. \right. \right.$$

$$\left. + B_c M_p \right] + k_0 M_c M_p \right\} s^4 + \left\{ B_{cp} \left[ (k_0 + k_p) M_c + (k_c + k_0) M_p \right. \right.$$

$$\left. + B_c B_p \right] + \left[ (B_c + B_p)k_0 M_c + k_0 M_p B_c \right] \right\} s^3 + \left\{ B_{cp} \left[ (B_c + B_p) k_c \right. \right.$$

$$\left. + B_p k_0 + B_c k_p \right] + k_0 \left[ k_p M_c + (k_c + k_f) M_p + B_c B_p \right] \right\} s^2$$

$$+ \left\{ B_{cp} \left[ k_c(k_0 + k_p) + k_0 k_p \right] + k_0 \left[ (B_c + B_p) k_c + B_p k_f \right. \right.$$

$$\left. + B_c k_p \right] \right\} s + k_0 k_p (k_c + k_f) \right\}^{-1} + \left( M_s s^2 + B_s s + k_c \right)$$

where the newly introduced constants, $B_{cp}$ and $k_f$ are defined:

$$B_{cp} = \frac{A^2}{C_p} \quad \text{and} \quad k_f = \left( \frac{A C_E}{C_p} \right)^{\ddagger}$$

---

‡ The concept of the constant, $k_f$ , may be visualized by referring to the plot of piston pressure differential vs valve displacement, Fig. 2, Page 3. Piston load could have been plotted rather than pressure, and assuming bilateral relationships, it follows that:

$$\frac{\partial P_c A}{\partial E} = A \frac{\partial P_c}{\partial E} = A \frac{\left| \frac{\partial a}{\partial E} \right|}{\left| \frac{\partial a}{\partial E} \right|} = A \frac{C_E}{C_p} \equiv k_f$$

A desirable feature of any well designed hydraulic actuator installation is that the piston and mounting structure are as rigid as possible. Normally, then, the piston spring constant is large compared to all other spring constants, including that of the hydraulic fluid. With this important assumption, the quadratic $[M_p s^2 + (A_c + A_p)s + A_{cp}]$ becomes an approximate factor of the numerator and denominator of the $A_{cp}/A_{cp}$ portion of equation (55), reducing it to:

$$(56) \quad \frac{F}{x_s} = \left\{ \frac{-A_c^2(B_{cp}s + A_o)}{B_{cp}M_c s^3 + [B_{cp}B_c + A_o M_c]s^2 + [B_{cp}(A_c + A_o) + B_c A_o]s + A_o(A_c + A_f)} \right\}$$
$$+ (M_s s^2 + B_s s + A_c)$$

Very little more can be done to simplify the above expression; actual values of the constants must be substituted and the expression numerically factored. Experience with typical Northrop-type hydraulic systems, however, has shown that the denominator cubic has an approximate quadratic factor, $(M_c s^2 + B_c s + A_c + A_o)$; this implies that the constant $B_{cp}$ is very large (i.e., $C_p$ is very small), which is the case for valve positions near neutral. Thus,

$$(57) \quad \frac{F}{x_s} \approx \left\{ \frac{-A_c^2(B_{cp}s + A_o)}{\left[B_{cp}s + \frac{A_o(A_c + A_f)}{(A_c + A_o)}\right]\left[M_c s^2 + B_c s + A_c + A_o\right]} \right\} + (M_s s^2 + B_s s + A_c)$$

The term in the braces, to reiterate, is the corrective term which must be added to (or subtracted from) the quadratic, $(M_s s^2 + B_s s + A_c)$, to obtain the proper transfer function between the aerodynamic force, $F$, and the corresponding surface deflection, $x_s$. This corrective term is of the form,

$$Y_{CORR} = \frac{K \omega_n^2 (\tau_1 s + 1)}{(\tau_2 s + 1)(s^2 + 2\zeta \omega_n s + \omega_n^2)}$$

where
$$K = \frac{-A_c^2}{A_c + A_f}$$
$$\tau_1 = \frac{B_{cp}}{A_o}$$
$$\tau_2 = \frac{B_{cp}(A_c + A_o)}{A_o(A_c + A_f)}$$
$$2\zeta \omega_n = \frac{B_c}{M_c}$$
$$\omega_n^2 = \frac{A_c + A_o}{M_c}$$

A generic frequency response plot of this relation is shown in Fig. 18.
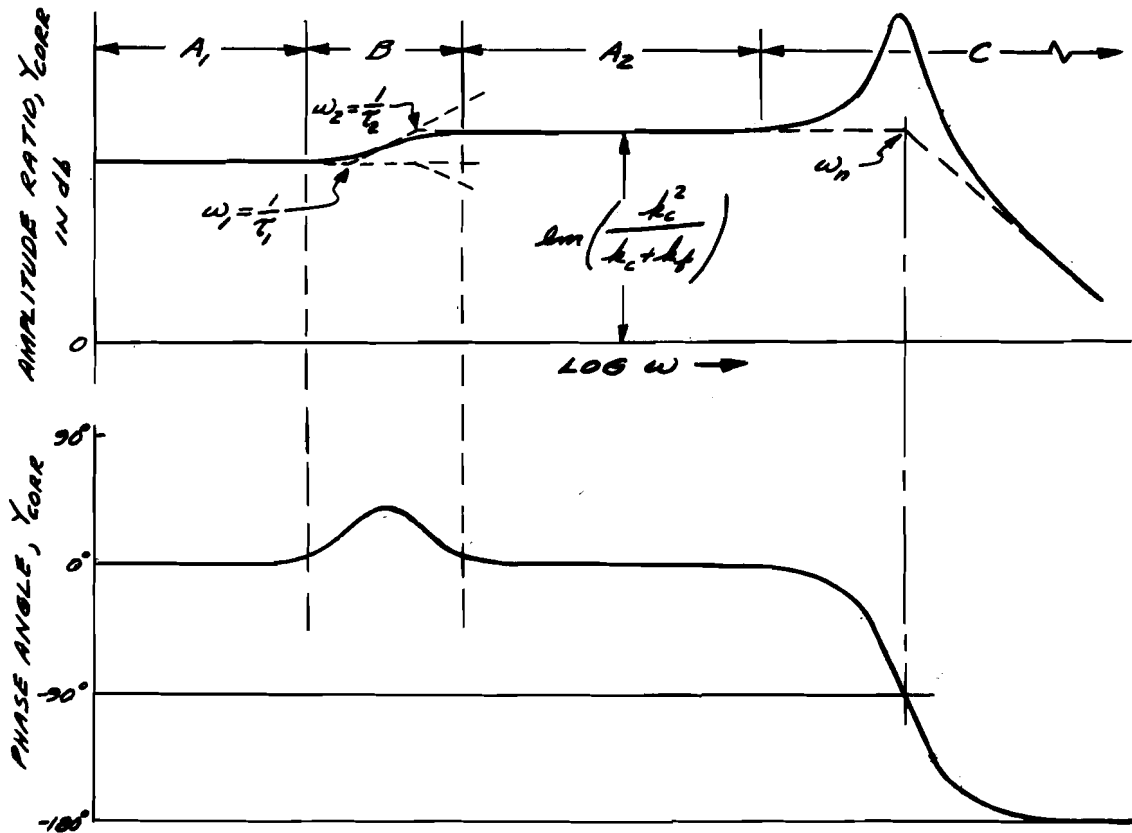


Frequency Response of $Y_{CORR}$

Fig. 18

Another prerequisite of a fully-powered hydraulic servo is that it must be capable of resisting large hinge moments with relatively small valve displacements. It follows that the slope of the pressure vs valve error curve must be rather steep, or that the value of the spring constant $k_f (= A G_c / C_p)$ is high. On the other hand, the oil spring constant $k_c (= A^2 N / r')$ is restricted by the cylinder size that can be installed in a thin airfoil section. So, in general, $k_f$ will be greater than $k_c$; thus

$$\omega_2 = \frac{(k_c + k_f) k_o}{B_{cp}(k_c + k_f)} > \omega_1 = \frac{k_o}{B_{cp}}$$

Also, since the effective damping constant $\mathcal{L}_f$ is very large (or $C_f$ very small) compared to the cylinder mass $M_c$ ,

$$\omega_n = \sqrt{\frac{k_c + k_s}{M_c}} \gg \omega_s$$

Fig. 18 reflects the above orders of magnitude of the frequencies involved. In the regions marked $A_1$ and $A_2$, the corrective terms contain essentially zero phase angle modification to be applied to the complex vector $(M_s s^2 + k_s s + k_c)$ , and, hence, may be considered pure spring corrections. The region marked $B$ is a transition range between $A_1$ and $A_2$ ; its upper limit is determined primarily by the value of the servo gain term, $C_\epsilon$ , which is inherent in the spring $k_f$ . (The larger the value of $k_f$ , the higher becomes the frequency $\omega_s$ ; the range $B$ terminates slightly beyond that frequency.) In the range $C$ the correction factor is composed of all three mechanical elements, i.e., masses and dampers as well as spring combinations. The resonant peak, $\omega_n = (k_c + k_o / M_c)^{\frac{1}{2}}$ , fortunately occurs at a very high frequency, and generally will not affect the flutter analysis.

At sufficiently low frequencies, i.e., approaching static or steady-state load conditions, the aerodynamic load transfer function becomes a pure spring constant formed by the series linkage of the coupling spring, $k_c$ , and the effective hydraulic servo spring $k_f$ .

$$(58) \qquad \frac{F}{x_s}\bigg|_{\omega \to 0} \approx \frac{-k_c^2}{k_c + k_f} + k_c = \frac{k_c k_f}{k_c + k_f} \equiv k_{A_1}$$

The spring $k_{A_1}$ , is effective over the frequency range $A_1$ and its value is derivable from any one of the equations (55), (56), or (57).

Since flutter itself implies a dynamical condition, the major region of interest lies above the range $A_1$ . In fact, the transition region $B$ also includes frequencies which are still well below those of the most commonly encountered flutter modes. The range $A_2$ , therefore, is the one most pertinent to the analysis. The exact transfer function $F/x_s$ cannot be obtained merely by adding a corrective spring term to the quadratic $(M_s s^2 + k_s s + k_c)$ ; however numerical calculations for typical systems have shown that the equivalent spring in the dynamical range $A_2$ is essentially the series spring combination that would be obtained if the hydraulic system were viewed as a passive network. In other words, at sufficiently high frequencies the servo action of the system is greatly suppressed, and the effective spring in the range $A_2$ is

$$(59) \qquad k_{A_2} \approx \frac{k_c k_o}{k_c + k_o}$$

or, if the piston spring $k_p$ is finite,

$$(60) \qquad k_{A_2} \approx \frac{k_c \, k_o \, k_p}{k_c \, k_o + k_c \, k_p + k_o \, k_p}$$

Normal static tests (i.e., loading the surface and measuring its deflections) will not provide a satisfactory means for obtaining the above spring constant.

To summarize, the following conclusions regarding Northrop type hydraulic-flutter systems may be made:

1. A hydraulic system correction factor must be added vectorially to the normal surface quadratic ( $M_s \, s^2 + c_s \, s + k_c$ ) to obtain the proper load transfer function.

2. Only the range $A_2$ of Fig. 18 is of interest in the problem since the regions $A_1$ and $B$ are well below and the range $C$ is far above the normally encountered flutter frequencies.

3. In the range of interest, $A_2$ , the hydraulic system may be viewed essentially as a pure spring, as far as the absence of phase lag terms in the correction factor is concerned.

The magnitude of this spring constant is approximately that of the series combination of (1) the spring coupling, the hydraulic cylinder and the surface, (2) the hydraulic oil spring, and (3) the piston rod spring (if finite).

# NOMENCLATURES

|  |  | Dimensions |
|---|---|---|
| $A$ = | cylinder area. | $L^2$ |
| $a$ = | coordinate of axis of rotation of airfoil. | (Zero Dim.) |
| $a_c$ = | orifice area | $L^2$ |
| $\alpha$ = | angle of attack. | (Zero Dim.) |
| $B_c$ = | cylinder-piston damping coefficient. | $FL^{-1}T$ |
| $B_i$ = | input damping | $FL^{-1}T$ |
| $B_p$ = | piston-structure damping coefficient. | $FL^{-1}T$ |
| $B_{c\rho}$ = | synthetic damping coefficient | $FL^{-1}T$ |
| $B_s$ = | surface-structure damping coefficient. | $FL^{-1}T$ |
| $b$ = | half chord length of airfoil. | $L$ |
| $B_v$ = | valve-cylinder damping coefficient. | $FL^{-1}T$ |
| $\beta$ = | surface angular deflection. | (Zero Dim.) |
| $a$ = | orifice coefficient. | (Zero Dim.) |
| $C_\beta$ = | torsional stiffness of surface per unit length (about hinge line). | $F$ |
| $C_\xi$ = | slope of the flow-valve displacement curve. | $L^2F^{-1}$ |
| $C_p$ = | slope of the flow-pressure differential curve. | $F^{-1}L^5T^{-1}$ |
| $C_c$ = | cylinder-piston coulomb frictional forces. | $F$ |
| $C_v$ = | valve-cylinder coulomb frictional forces. | $F$ |
| $c$ = | coordinate of surface hinge line. | (Zero Dim.) |
| $E$ = | valve displacement from neutral. | $L$ |
| $E^*$ = | steady state valve displacement (operating point). | $L$ |
| $\mathcal{E}$ = | valve displacement perturbation. | $L$ |
| $F$ = | aerodynamic load at surface. | $F$ |
| $g$ = | gravitational constant. | $LT^{-2}$ |

| | | |
|---|---|---|
| $h$ = | vertical coordinate of axis of rotation of airfoil. | $L$ |
| $I_\beta$ = | moment of inertia per unit length of surface (with respect to surface hinge line). | $FT^2$ |
| $K$ = | gain constant. | $T^{-1}$ |
| $k$ = | gain constant | $T^{-1}$ |
| $k_c$ = | cylinder-surface coupling spring constant. | $FL^{-1}$ |
| $k_f$ = | effective hydraulic servo spring constant. | $FL^{-1}$ |
| $K_o$ = | equivalent spring constant of the oil. | $FL^{-1}$ |
| $k_o$ = | effective spring constant of oil within cylinder. | $FL^{-1}$ |
| $k_p$ = | piston spring constant. | $FL^{-1}$ |
| $k_s$ = | aerodynamic surface spring constant. | $FL^{-1}$ |
| $k_r$ = | series equivalent spring constant | $FL^{-1}$ |
| $k_v$ = | valve spring constant. | $FL^{-1}$ |
| $d$ = | span of surface | $L$ |
| $\ell$ = | surface-cylinder effective moment arm. | $L$ |
| $M$ = | mass. | $FL^{-1}T^2$ |
| $m$ = | mass. | $FL^{-1}T^2$ |
| $M_c$ = | cylinder mass. | $FL^{-1}T^2$ |
| $M_p$ = | piston mass. | $FL^{-1}T^2$ |
| $M_s$ = | surface mass. | $FL^{-1}T^2$ |
| $M_v$ = | valve mass. | $FL^{-1}T^2$ |
| $M_\beta$ = | total aerodynamic moment. | $FL^{-1}T^2$ |
| $N$ = | bulk modulus of fluid. | $FL^{-2}$ |
| $P$ = | instantaneous pressure. | $FL^{-2}$ |
| $P_c$ = | pressure differential across piston. | $FL^{-2}$ |
| $P_c^m$ = | steady state pressure differential. | $FL^{-2}$ |
| $p_c$ = | pressure differential perturbation. | $FL^{-2}$ |

|  |  | Dimensions |
|---|---|---|
| $P_s$ = | supply pressure. | $FL^{-2}$ |
| $P_{o,R}$ = | pressure on either side of piston. | $FL^{-2}$ |
| $\eta_{o,R}$ = | perturbed pressure on either side of piston. | $FL^{-2}$ |
| $\Delta p$ = | pressure drop across orifice | $FL^{-2}$ |
| $Q$ = | volumetric flow from valve or flow into cylinder. | $L^3T^{-1}$ |
| $Q^*$ = | steady state volumetric valve flow. | $L^3T^{-1}$ |
| $q$ = | volumetric valve flow perturbation. | $L^3T^{-1}$ |
| $\rho$ = | fluid density. | $FL^{-4}T^2$ |
| $s$ = | Laplace operator. | $T^{-1}$ |
| $S_\alpha$ = | static moment per unit length of airfoil (with respect to axis of rotation of airfoil). | $FL^{-1}T^2$ |
| $S_\beta$ = | static moment per unit length of surface, (with respect to surface hinge line). | $FL^{-1}T^2$ |
| $t$ = | time. | $T$ |
| $V_i$ = | input velocity. | $LT^{-1}$ |
| $v_i$ = | input velocity perturbation. | $LT^{-1}$ |
| $w$ = | specific weight of fluid. | $FL^{-3}$ |
| $\dot{x}_i$ = | input velocity perturbation (velocity source). | $LT^{-1}$ |
| $X_i$ = | input displacement relative to structure. | $L$ |
| $x_i$ = | input displacement perturbation. | $L$ |
| $X_o$ = | cylinder displacement relative to structure. | $L$ |
| $x_o$ = | cylinder displacement perturbation. | $L$ |
| $X_p$ = | piston displacement relative to structure. | $L$ |
| $x_p$ = | piston displacement perturbation. | $L$ |
| $X_s$ = | surface displacement relative to structure. (measured at cylinder horn). | $L$ |

| | | Dimensions |
|---|---|---|
| $X_s$ = | surface displacement perturbation. | L |
| $X_\nu$ = | valve displacement relative to structure. | L |
| $X_\nu$ = | valve displacement perturbation. | L |
| $\forall$ = | volume. | $L^3$ |
| $\forall'$ = | effective oil volume within cylinder. | $L^3$ |
| $\forall'^*$ = | steady state oil volume. | $L^3$ |
| $\forall_{1\atop 2}$ = | volume on either side of piston. | $L^3$ |
| $\mathcal{T}$ = | time constant. | T |
| $\omega$ = | angular frequency. | $T^{-1}$ |
| $\omega_n$ = | natural angular frequency. | $T^{-1}$ |
| $\mathcal{S}$ = | damping ratio | (Zero Dim.) |

NOTE: All displacements, velocities, acceleration, masses, spring constants, etc., are effective values measured coincident with or parallel to line of action of cylinder.

## REFERENCES

(1) Feeney, T. A., "Powered Controls Design Practice at Northrop Aircraft", Northrop Aircraft, Inc., 1949.

(2) Lin, S. N., "A Method of Successive Approximations of Evaluating The Real and Complex Roots of Cubic and Higher Order Equations", Journal of Mathematics and Physics, Volume XX No. 3, August 1941.

(3) Theordorsen, T., "General Theory of Aerodynamic Instability and the Mechanism of Flutter", NACA TR 496, 1934.

(4) McRuer, D. T., "An Analysis of Northrop Aircraft Powered Flight Controls", Northrop Aircraft, Inc., 1949.

(5) Analysis of Type F-5 Automatic Pilot Applied to the Type F-89 Aircraft and Control System -- Contract AF 33(038)-6946, Northrop Aircraft, Inc., 1950.

# PARAMETERS FOR THE DESIGN OF HIGH- SPEED HYDRAULIC SERVOMOTORS

by HAROLD GOLD
EDWARD W. OTTO
VICTOR L. RANSOM
of
National Advisory Committee for Aeronautics
Lewis Flight Propulsion Laboratory
Cleveland, O.

## INTRODUCTION

The servomotor dealt with in this paper is a power amplifying, positioning device of the type used in such applications as control valve positioners, flight controls and power steering devices. The hydraulic servomotor as a device has been known for approximately one hundred years. Its application to high speed machinery, however, appears to be relatively recent. There is consequently very little published literature on the dynamics of this servomotor in spite of its long history. Nevertheless, when properly designed, the hydraulic servomotor is particularly suited for high speed service because of the extremely high force-mass ratios that can be obtained and because the device inherently is heavily damped.

This paper is based on an experimental and analytical study of the dynamics of the hydraulic servomotor recently completed by the authors at Lewis laboratory and soon to be published by the NACA (reference 1.) The results of this study have shown that although the response of the servomotor is essentially nonlinear and discontinuous, the response may be closely approximated with relatively simple linear equations. The present paper presents data demonstrating the nonlinear, discontinuous nature of the dynamic response of the servomotor and includes a derivation of the basic analytical expressions for describing the response. The derivations which are presented in the "Analysis" section of this paper are essentially an abstract of the detailed derivations given in reference 1.

The derived analytical expressions are summarized in the form of charts. By means of these charts the rational design of the servomotor to meet specifications on either the transient or the frequency response characteristics is made possible.

## DEFINITIONS AND INITIAL ASSUMPTIONS

Straight line servomotor. - The elements of the straight line hydraulic servomotor are shown schematically in figure 1. In the neutral position, the spool member of the pilot valve closes the passages

## HYDRAULIC SERVOMOTOR

ERROR

PISTON

OUTPUT SHAFT

INPUT LEVER
(A)

DRAIN

SUPPLY PRESSURE

DRAIN

NACA
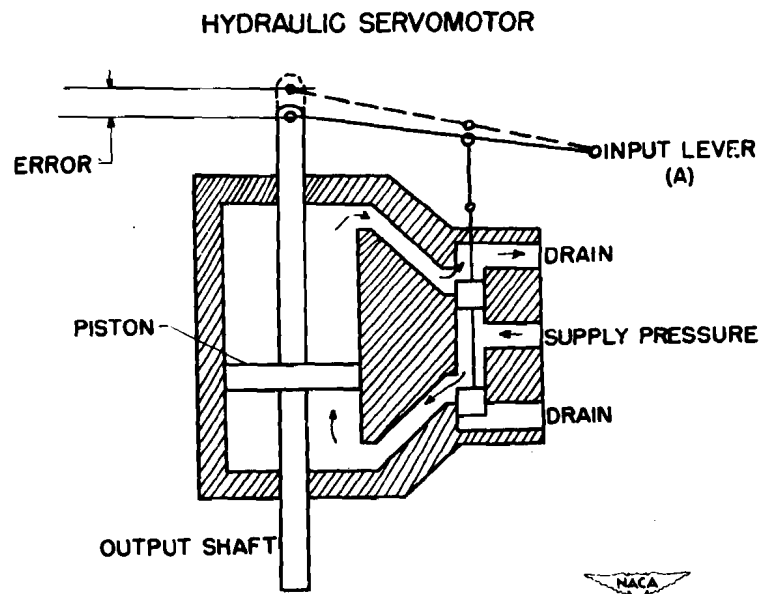
## ROTARY HYDRAULIC SERVOMETER

ERROR

VANE

$(P_2)$

$(P_1)$

$L_2$

$L_1$

DRAIN
$(P_d)$

SUPPLY
PRESSURE
$(P_s)$

SUPPLY
PRESSURE
$(P_s)$

PILOT VALVE &
INPUT SHAFT

OUTPUT SHAFT

NACA
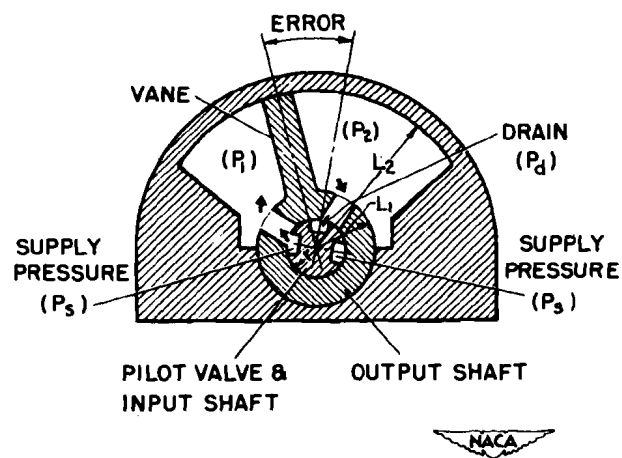
## FIGURE 1

to the piston. When the spool member is displaced from the neutral position by movement of the input lever at point (A), the flow of fluid through the pilot valve causes the piston to move in the direction which returns the spool to the neutral position. It follows from the geometry of the linkage that for every position of the linkage point (A) there is a corresponding equilibrium position of the piston. The description of several other forms of pilot valving and feedback linkage is available in the literature.

Rotary servomotor. - The rotary servomotor is also shown schematically in figure 1. Rotation of the pilot valve with respect to the output shaft opens a pressure passage to one side of the vane and a drain passage to the opposite side of the vane. The vane is thereby caused to rotate in the same direction as the pilot valve. In the neutral position of the valve the passages to either side of the vane are closed.

Initial assumptions. - The analysis which follows is developed with the following initial assumptions:

1. The area of opening of the pilot valve varies linearly with the motion of the valve.

2. At fixed input, the ratio of pilot valve movement to piston movement is constant.

3. At all positions of the pilot valve the inlet and discharge openings are equal.

4. The supply and drain pressure are constant.

5. The compressibility and mass of the hydraulic fluid are negligible.

6. Structure and mechanical linkage are rigid.

7. Mechanical friction is negligible.

8. Fluid friction losses in motor passages are negligible.

9. Leakage is negligible.

## DYNAMICS OF THE SERVOMOTOR

### Response to a Step Input

Basic dynamic considerations. - Under the condition of no load on the output shaft and negligible internal motor mass, the pressure drop across the piston will be zero. The fluid flow through the cylinder is therefore

essentially unobstructed. The flow of fluid is then proportional to the area of the valve opening and the flow coefficient. At constant flow coefficient therefore the piston velocity is directly proportional to the valve opening. With rectangular valve ports the open area of the valve is directly proportional to the error of the piston position. The velocity of the piston is consequently proportional to the error. In the no load case therefore, the servomotor will exhibit a transient response that is characterized by a linear first order system.

The pressure drop across the motor is divided equally between the inlet and drain valve ports.

Based on a constant flow coefficient, the piston velocity may then be equated to the flow through the valve ports by the following relation:

$$A_p \dot{x} = \left[ CRW \sqrt{\frac{P_s - P_d}{2}} \right] (S-x) \tag{1}$$

Equation (1) may be written in the form

$$T\dot{x} + x = S \tag{2}$$

where

$$T = \frac{\sqrt{2} \, A_p}{CRW\sqrt{P_s - P_d}} \tag{3}$$

The analysis of the response of the servomotor under an inertia load is considerably more complex than in the no load case. Under an inertia load the piston is accelerated from zero velocity. There is consequently an initial period in the response during which the flow through the valve ports is laminar, as a result of which the flow coefficient is subject to large variations. After the piston has reached the maximum velocity in the transient, the momentum of the load may cause the flow of fluid into the upstream side of the cylinder to cavitate. The variation of the pressure drop across the piston is therefore not describable by a continuous function and consequently a single differential equation cannot be written for the entire transient.

In spite of the complex nature of the response there are basically only two phases in the transient: the acceleration phase and the deceleration phase. This conclusion, particularly with reference to a continuous deceleration phase without overshoot or oscillation, is based on the assumption of rigid oil and structure and zero leakage. Under these assumptions the cylinder pressures during the deceleration phase are finite but may exceed physical limits.

Figure 2 shows an oscillographic record of the response of a servo-motor to a step input under a relatively heavy inertia load. The traces shown are: position response, timing mark, downstream cylinder pressure, and upstream cylinder pressure. The characteristic acceleration phase and dead heat deceleration phase are quite clearly demonstrated. It will be noted that the downstream cylinder pressure exceeds the supply pressure in the deceleration phase and at the same time the upstream cylinder pressure is driven to zero (cavitation occurs).

Linear equation for approximation of the acceleration phase of the response. - It is indicated by the measured response of hydraulic servo-motors under inertia loads that the acceleration phase may be approximated by a linear second order system. The general form of a second order differential equation with constant coefficient may be written

$$a\ddot{x} + b\dot{x} + x = S \qquad (4)$$

At no load the servomotor responds as a first order system. Equation (4) should therefore reduce to equation (1) for the inertialess case. Therefore:

$$b = T$$

At the start of the transient $(t = + 0)$, the upstream cylinder pressure is equal to the supply pressure and the downstream cylinder pressure is equal to the drain pressure. Hence when

$$t = + 0$$

$$x = 0$$

$$\dot{x} = 0$$

$$\ddot{x} = \frac{(P_s - P_d)A_p}{M}$$

Substituting these values in equation (4)

$$a = \frac{MS}{(P_s - P_d)A_p}$$

The differential equation that approximates the acceleration phase is then

$$\frac{MS}{(P_s - P_d)A_p} \ddot{x} + T\dot{x} + x = S \qquad (5)$$

Equation (5) may be defined in terms of the no-load time constant T and the reciprocal of the damping ratio. This quantity is here designated the "inertia index - E." The new term is employed in this paper because the term "damping ratio" or other terms sometimes associated with the reciprocal of the damping ratio would have no meaning in the type of transient associated with the hydraulic servomotor.

Equation (5) expressed in terms of the parameters T and E is

$$\frac{T^2E^2}{4}\frac{\ddot{x}}{s} + T\frac{\dot{x}}{s} + \frac{x}{s} = 1 \tag{6}$$

Equating like coefficients in equations (5) and (6)

$$E = \frac{2}{T}\sqrt{\frac{MS}{(P_s-P_d)A_p}} \tag{7}$$

Substituting equation (3) in equation (7) the general expression for E is obtained:

$$E = \frac{\sqrt{2}\ CRW\ \sqrt{MS}}{A_p^{3/2}} \tag{8}$$

Linear equation for approximation of the deceleration phase. - In the deceleration phase of the transient the pilot valve areas are reduced to small values. Consequently the flow rate through the valves is affected to a far greater degree by the reducing value area than by variations in the pressure drop across the valve. For this reason the response in the deceleration phase does not deviate significantly from the no-load response. Equation (2) may therefore be used to approximate the deceleration phase.

Evaluation of coefficient for the rotary servomotor. - By means of a parallel development expressions for T and E can be obtained for the rotary motor. These expressions are given below.

$$T = \frac{h(L_2^2-L_1^2)}{\sqrt{2}\ CRW\ \sqrt{P_s-P_d}} \tag{9}$$

$$E = \frac{4\ CRW\ \sqrt{\theta J}}{\left[h(L_2^2-L_1^2)\right]^{3/2}} \tag{10}$$

Application of equations. - The method of applying equations (2) and (6) to the calculations of the transient is presented in figure 3. As shown in figure 3, the end of the acceleration phase is defined by the inflection point of the solution of equation (6) for $E > 1$. For $E < 1$, the second order equation may be used to approximate the entire transient and therefore the inflection point need not be evaluated. Figure 4 is a plot of rise time against no-load time constant for a range of values of inertia index. The chart is computed from the relations shown in figure 3. The rise time is defined as the time to reach 90 percent of the final value.

Experimental response. - Figure 5 shows the characteristic agreement between calculated and measured responses (reported in reference 1) in a series of runs in which the factors that determine the parameters T and E have been varied. As can be seen, the calculated responses have provided a close approximation of the actual responses over a wide range of conditions. It may be of particular interest to note that the effect of magnitude of the input step as predicted by the approximating equations is evident in the measured responses.

Peak cylinder pressure during a transient. - In a transient under a heavy load, the downstream cylinder pressure may exceed the supply pressure. For this reason an evaluation of the peak cylinder pressure is significant from a structural standpoint. It is shown in reference 1 that the ratio of the maximum cylinder pressure to the supply pressure is a function solely of the inertia index. The relation derived in reference 1 is plotted in figure 6. Also shown in figure 6 are experimental values reported in reference 1.

## Response to a Sinusoidal Input

Basic dynamic considerations. - It has been shown that under an inertia load, the transient response of the servomotor is nonlinear. The basic character of the transient response has been shown to vary with time in the transient. It can therefore be expected that the frequency response will also exhibit nonlinear characteristics and that the basic character of the response will vary with the frequency of the input.

Low frequency amplitude attenuation and phase shift. - At low fre-
quencies the forces that act on the mass of the system are small and

94

# HYDRAULIC SERVOMOTOR TRANSIENT RESPONSE
## UNDER HEAVY INERTIA LOAD

OUTPUT TRACE

START OF TRANSIENT

0.2 SEC

TIME

250 LB/SQ IN — UPSTREAM CYLINDER PRESSURE

0

DOWNSTREAM CYLINDER PRESSURE

250 LB/SQ IN

0
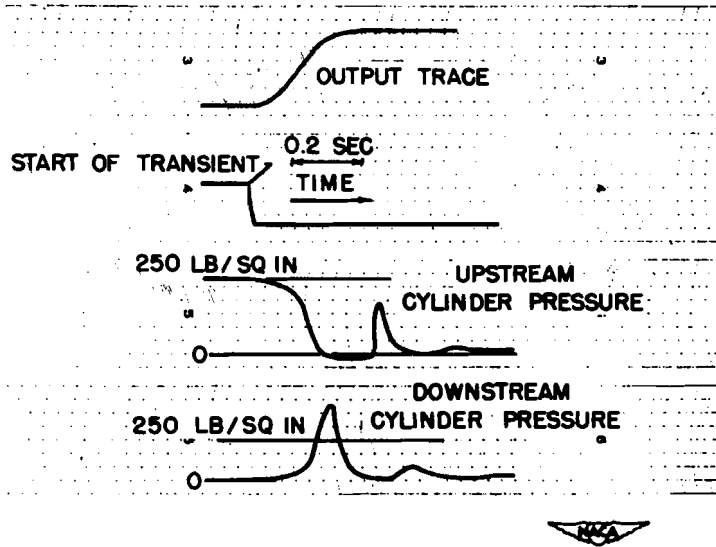
**FIGURE 2**

## SUMMARY OF LINEAR RELATIONS FOR THE TRANSIENT RESPONSE
## OF HYDRAULIC SERVOMOTORS WITH MECHANICAL FEEDBACK

$E<1$ $\quad \frac{x}{s} = 1 - \frac{1}{2}\left[1 + \frac{1}{\sqrt{1-E^2}}\right] e^{\left[\frac{-2}{TE^2} + \frac{2\sqrt{1-E^2}}{TE^2}\right]t} - \frac{1}{2}\left[1 - \frac{1}{\sqrt{1-E^2}}\right] e^{-\left[\frac{2}{E^2T} + \frac{2\sqrt{1-E^2}}{TE^2}\right]t}$

$E=1$ $\quad \frac{x}{s} = 1 - e^{\frac{-2t}{T}}\left[1 + \frac{2t}{T}\right]$

$E>1$ $\quad \frac{x}{s} = 1 - \frac{E^2}{\sqrt{E^2-1}}e^{\frac{-2t}{E^2T}}\left[\cos\left(\frac{2\sqrt{E^2-1}}{E^2T}\right)t - Tan^{-1}\frac{1}{\sqrt{E^2-1}}\right]$ $\quad \frac{x}{s} = 1 - \left(1 - \frac{x_1}{s}\right)e^{-\left(\frac{t-t_1}{T}\right)}$

OUTPUT TRAVEL ($\frac{x}{s}$)

$\frac{x}{s}$

$\frac{x}{s} = 1 - \frac{2t}{E}e^{-\left\{\frac{Tan^{-1}\sqrt{E^2-1}}{\sqrt{E^2-1}}\right\}}$

$t_1 = \frac{TE^2}{2\sqrt{E^2-1}}Tan^{-1}\sqrt{E^2-1}$

TIME (t)

STRAIGHT LINE SERVOMOTOR

$T = \frac{\sqrt{2}\,A\rho}{CRW\sqrt{P_s - P_d}}$ $\qquad E = \frac{\sqrt{2}\,CRW\sqrt{M_s}}{A\rho^{3/2}}$

ROTARY SERVOMOTOR

$T = \frac{h(L_s - L_1)}{\sqrt{2}\,CrW\sqrt{P_s - P_d}}$ $\qquad E = \frac{4CrW\sqrt{I}}{(h(L_s - L_1))^{3/2}}$
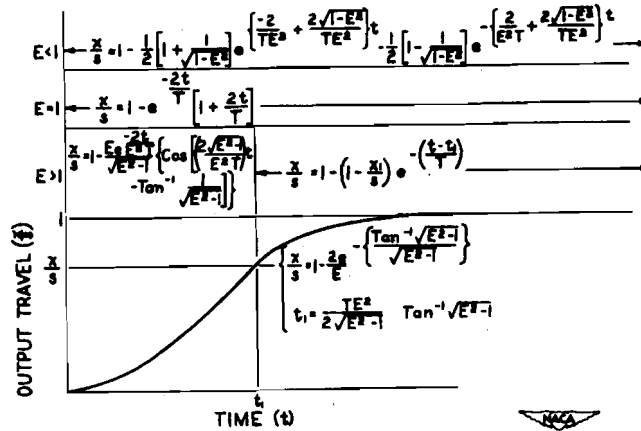
**FIGURE 3**

CHART FOR DETERMINATION OF TIME TO REACH
90 PERCENT OF FINAL VALUE. HYDRAULIC SERVOMOTOR
WITH MECHANICAL FEED BACK
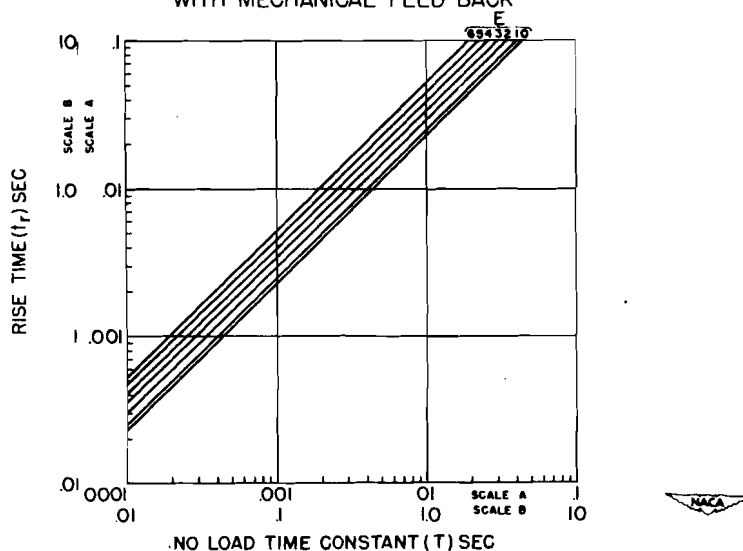


**FIGURE 4**

MEASURED AND CALCULATED TRANSIENT RESPONSES
OF A HYDRAULIC SERVOMOTOR
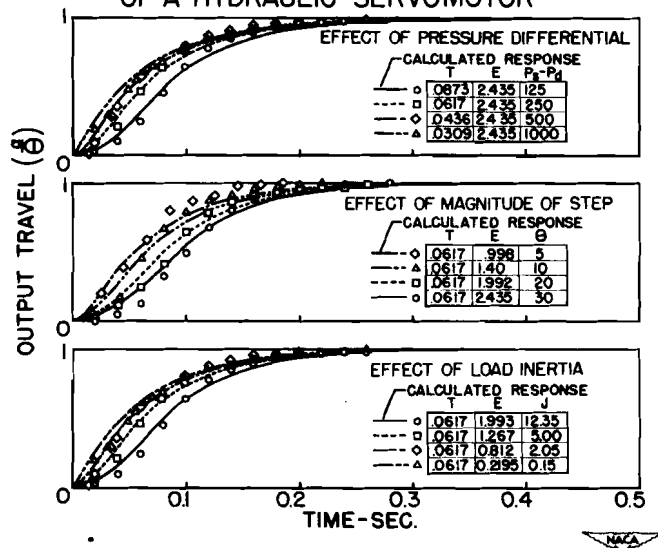


**FIGURE 5**

$$\dot{x} = \frac{S' \cos \omega t - x}{T} \tag{11}$$

The solution to equation (11) is

$$A \, e^{i\phi} = \frac{1}{1 + i\omega T} \tag{12}$$

The term $Ae^{i\phi}$ is a vector quantity having an amplitude $A$ and a phase angle $\phi$. From equation (12)

$$A = \frac{1}{\sqrt{1+T^2\omega^2}} \tag{13}$$

$$\phi = - \tan^{-1} T\omega \tag{14}$$

High frequency amplitude attenuation. - At no-load the piston velocity is at all times proportional to the valve opening; therefore in the response to a sinusoidal input at no-load the pilot valve area is zero at the ends of the output travel (the velocity being zero). Under an inertia load the piston velocity is not linearly proportional to the pilot valve opening and hence in the response to a sinusoidal input the valve area is not necessarily zero at the ends of the output travel. If at high frequencies, the response of the servomotor is assumed to be essentially sinusoidal, the maximum acceleration can be considered to occur at the limits of the output travel and hence when the piston velocity is zero. Under the condition of negligible mass of the hydraulic fluid, the pressure difference across the piston at any instant when the piston velocity is zero and the pilot valve area is greater than zero, is the pressure difference across the servomotor. Above some frequency the system may then be approximated by a linear system wherein the pressure difference across the piston varies sinusoidally with an amplitude of $(P_s-P_d)$ and with the frequency of the input. On the basis of this approximation the acceleration of the piston is

$$\ddot{x} = \frac{(P_s-P_d)A_p}{M} \sin \omega t \tag{15}$$

Integrating equation (15) and introducing the condition that $x$ varies about zero and neglecting changes in sign

$$x = \frac{(P_s-P_d)A_p}{M\omega^2} \sin \omega t \tag{16}$$

Dividing both sides of equation (16) by the output amplitude at zero
frequency, the equation relating the amplitude ratio and the frequency is:

$$A = \frac{(P_s - P_d)A_p}{S'M\omega^2}$$ (17)

The dimensionless quantity, inertia index, may be defined for the
frequency response by replacing the magnitude of the step (S) with the
term amplitude of the output sine wave at zero frequency (S'). Rewriting
equation (8) and introducing the symbol (S') in place of (S) the expres-
sion for the inertia index for the frequency response is obtained:

$$E' = \frac{\sqrt{2} \ CRW \ \sqrt{MS'}}{A_p^{3/2}}$$ (18)

Equation (3) and (18) substituted in equation (17) yield the general
expression for the amplitude attenuation

$$A = \frac{4}{(E')^2 T^2 \omega^2}$$ (19)

High frequency phase shift. - The derivation of equation (19) does
not provide relations by which the phase shift may be computed. The
amplitude attenuation expressed by equation (19), is, however, the
asymptotic relation of a linear second order system. The phase shift in
the high frequency band may therefore be considered to be described by a
linear second order system. It can be shown further that equation (6)

Straight line representation. - The straight line approximation of
the frequency response relations is presented in figure 7. In the low
frequency band the amplitude is expressed by the asumptotes of equa-
tion (13)

$$A = 1$$

and

$$A = \frac{1}{T\omega}$$

RATIO OF PEAK TRANSIENT CYLINDER PRESSURE TO SUPPLY PRESSURE AS A FUNCTION OF INERTIA INDEX. HYDRAULIC SERVOMOTOR WITH MECHANICAL FEEDBACK
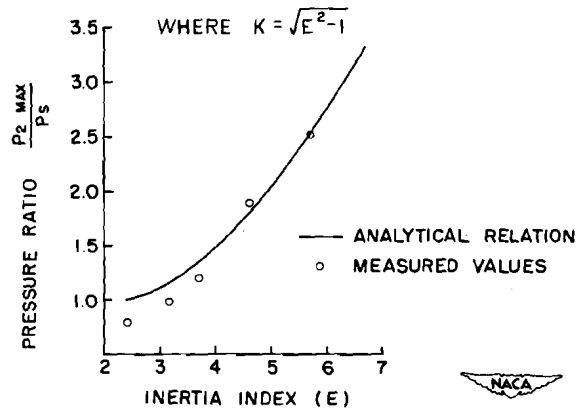
FIGURE 6



SUMMARY OF LINEAR RELATIONS FOR THE FREQUENCY RESPONSE OF HYDRAULIC SERVO-MOTORS WITH MECHANICAL FEEDBACK

FIGURE 7

The high frequency attenuation is expressed by the relation of equation (19). The cross-over frequency is defined by the intersection of the low and high frequency asymptotes.

Phase shift is represented by straight lines on semilogarithmic coordinates in figure 7. The slope of the low frequency line is defined by the slope of the first order system (equation (14)) at $\phi = 45^{\circ}$. The slope of the high frequency line is defined by the slope of the second order system (equation (20)) at $\phi = 90^{\circ}$. The low frequency phase shift line passes through $\phi = 45^{\circ}$ at the low frequency band break frequency ($f_1$). The high frequency phase shift line is oriented by the cross-over frequency. In figure 7 the cross-over frequency is shown to occur after the low frequency phase shift line has reached the $90^{\circ}$ limit. The orientation of the high frequency phase shift line for other relative locations of the cross-over frequency is shown in connection with the experimental responses.

Experimental responses. - Figure 8 shows the experimentally and analytically determined effect on the frequency response of the hydraulic servomotor of the parameters:   load inertia and input amplitude.

Figure 8(a) shows the effect of load inertia on the amplitude attenuation and on the phase shift. An increase in load inertia results in a reduction in the frequency at which the attenuation becomes rapid. In the analytical expression developed in this paper (summarized in fig. 7) this effect is evident in the increased value of $E'$ with increasing load inertia and the consequent reduction in the values of $f_2$ and $f_3$.

Figure 8(b) shows the effect of input amplitude on the frequency response. The increase in input amplitude is seen to have an effect similar to that of increasing load inertia. This effect is made evident in the analysis by equation (17).

In both amplitude and phase shift the agreement between the measured responses and the analytical straight line approximations is in general well within the experimental accuracy. The slopes of the attenuation and phase data clearly demonstrate the first order characteristics of the response in the low frequency band the the second-order characteristics of the response in the high frequency band. The transition from first to second order characteristics at the calculated break frequency is quite pronounced.

## APPLICATION TO DESIGN

### Design Relations

From equations (3) and (8) the following expressions for the piston area and the product of the feedback ratio and port width of a straight line servomotor can be derived:

$$A_p = \frac{4MS}{(P_s-P_d)T^2E^2} \tag{21}$$

$$RW = \frac{2MS}{C\left(\frac{P_s-P_d}{2}\right)^{3/2}T^3E^2} \tag{22}$$

Equations (21) and (22) are written in terms of transient response parameters but apply to frequency response parameters by replacing S and E with S' and E', respectively. The corresponding equations for the various sizes of a rotary servomotor in terms of the various design parameters may be obtained from equations (9) and (10) in a similar manner.

Equation (21) expresses the relation between the motor inertia (proportional to $A_p$) and the various response parameters. Equation (22) expresses the relation between the input inertia (proportional to RW) and the various response parameters. The motor inertia and the input inertia are significant factors in the design of high speed servomotors. The following paragraphs will discuss methods for aiding in the selection of optimum designs to meet specifications on either the transient or frequency response characteristics.

## Determination of Design Parameters

Load mass. - The value of M in the design equations includes the mass of the output part of the servomotor as well as the load mass. In high-speed applications the motor mass may be a significant percentage of the total mass. For this reason the estimated mass of the output part of the motor should be added to the known load mass. It is obvious from the character of the response of hydraulic servomotors of this type that the response characteristics for a given size are always improved by reductions in the load mass.

Pressure differential across servomotor. - In general the size of a servomotor for a given response is reduced by an increase in pressure differential. The reduction in weight, however, is modified by the need for larger sections to withstand the increased pressure. The determination of the optimum pressure is beyond the scope of this paper. The no-load time constant varies inversely as the square root of the pressure differential whereas the inertia index is independent of the pressure differential. Therefore in a given servomotor the break frequencies ($f_1$ and $f_3$) are proportional to the square root of the pressure differential, and the rise time is approximately inversely proportional to the square root of the pressure differential.

Magnitude of the desired output. - Because the character of the
response is determined by the magnitude of the desired output, a value
of the output magnitude must be selected for design purposes. In general
this information is obtained from the process which the servomotor is
varying and consists of an estimation of the maximum percent change in
the process that is required to occur in a given transient or sine wave
oscillation. This variation should then be translated into the output
stroke required of the servomotor to produce such a change. The total
stroke of the servomotor will usually be larger than the design value
of S or S' and corresponds to the steady state range through which
the process is carried. If a step change or sine wave oscillation larger
than S or S' is introduced the resulting inertia index will be larger
than that assumed in the design with the consequent possibility of damage
from high peak cylinder pressures. Protection against such damage can
be obtained by restricting the length of the pilot valve lands.

Selection of no-load time constant and inertia index for frequency
response requirements. - If the frequency response requirements of the
servomotor are known they in general will take the form of the first
break frequency $(f_1)$ and the crossover frequency $(f_3)$. The equations
for T and E' in terms of these two frequencies are as follows:

$$T = \frac{1}{2\pi f_1} \qquad (23)$$

$$E' = 2\sqrt{f_1/f_3}$$

As shown in the analysis the response of a servomotor of this type is
characterized in both attenuation and phase shift by a first order rela-
tion up to the crossover frequency. The phase shift in this frequency
band is therefore limited to a maximum value of $90°$. The crossover fre-
quency $f_3$ can therefore be selected on the basis of sufficient amplitude
attenuation at $90°$ phase shift to insure stability in the control loop.
With $f_1$ and $f_3$ defined, the dimensions of the servomotor are estab-
lished. Substituting equations (23) and (24) in equation (21) the fol-
lowing relation is obtained:

$$A_p = \frac{4MS'\pi^2 f_1 f_3}{P_s - P_d} \qquad (25)$$

From equation (25) it can be seen that at a fixed value of $f_1$ an increased
margin for $f_3$ can only be obtained by a proportionate increase in piston
area.

Selection of no-load time constant and inertia index for transient
response requirements. - Transient response requirements can be expressed
in terms of the time to reach 90 percent of the final value. The

variation of this rise time with  T  and  E  was presented in figure 4.
It can be seen from figure 4 that a given value of rise time can be
obtained at various combinations of  T  and  E.  The relation presented
graphically in figure 4 may be expressed approximately by the following
equation:

$$t_r = T\left(2 + \frac{E}{2}\right) \tag{26}$$

Equation (26) combined with equation (21) yields a general relation for
the variation of piston area with inertia index.  This relation is:

$$A_p = \frac{4MS}{(P_s-P_d)t_r^2}\left(\frac{2}{E} + \frac{1}{2}\right)^2 \tag{27}$$

Equation (26) combined with equation (22) yields a general relation for
the variation of the product of the feedback ratio and the port width
with inertia index as follows:

$$RW = \frac{2MS}{c\left(\frac{P_s-P_d}{2}\right)^{3/2} t_r^3}\left[E\left(\frac{2}{E} + \frac{1}{2}\right)^3\right] \tag{28}$$

The terms  $\left(\frac{2}{E} + \frac{1}{2}\right)^2$  and  $E\left(\frac{2}{E} + \frac{1}{2}\right)^3$  in the above equations are proportional
to  $A_p$  and  RW, respectively.  Thus the numerical values of these terms
plotted as a function of  E  will indicate the variation of the size of
the servomotor with inertia index.  The resulting plot is shown in fig-
ure 9.  As a further aid in the choice of a value of  E  the maximum
cylinder pressure which is a function of  E  is also shown.

Figure 9 indicates .that values of  E  above 6 do not materially
reduce the size of the servomotor and result in large values of maximum
cylinder pressure.  Values of  E  below 1 result in large servomotors and
in general would be used only if it is desirable to make the response
substantially first order.  In this respect the above curves indicate
that it would be very difficult to reduce  E  to values close to zero
because the motor size and thus the mass of its parts become large, which
will tend to increase  E.  Values of  E  in the range from 2 to 4 should
result in a servomotor that is very satisfactory both from a size stand-
point and from a response standpoint.

EFFECT OF LOAD INERTIA ON THE FREQUENCY RESPONSE
OF A HYDRAULIC SERVOMOTOR WITH MECHANICAL FEEDBACK



CALCULATED STRAIGHT LINE APPROXIMATIONS

| | J | T | E' | $f_1$ | $f_2$ | $f_3$ |
|---|---|---|---|---|---|---|
| —— □ | 12.35 | .085 | 1.44 | 1.87 | 2.56 | 3.52 |
| ---- ▲ | 19.70 | .085 | 1.82 | 1.87 | 2.03 | 2.20 |
| —·— ○ | 27.05 | .085 | 2.13 | 1.87 | 1.73 | 1.73 |
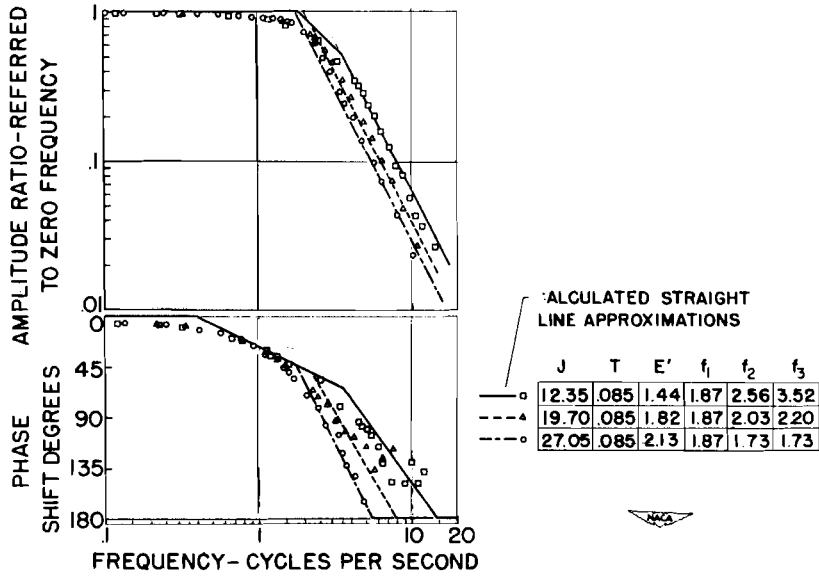
FIGURE 8

EFFECT OF AMPLITUDE ON THE FREQUENCY RESPONSE
OF A HYDRAULIC SERVOMOTOR WITH MECHANICAL FEEDBACK



CALCULATED STRAIGHT LINE APPROXIMATIONS

| | θ' | T | E' | $f_1$ | $f_2$ | $f_3$ |
|---|---|---|---|---|---|---|
| —— ○ | 10° | .085 | .917 | 1.87 | 4.03 | 8.68 |
| ---- ◇ | 15° | .085 | 1.124 | 1.87 | 3.29 | 5.78 |
| —·— ▲ | 20° | .085 | 1.298 | 1.87 | 2.85 | 4.32 |
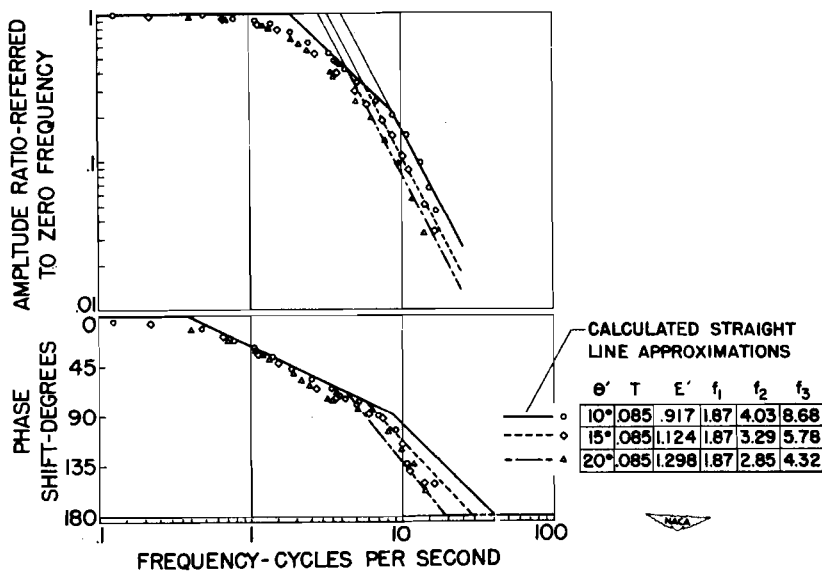
FIGURE 9

CHART ILLUSTRATING EFFECT OF INERTIA INDEX E
ON SERVOMOTOR SIZE
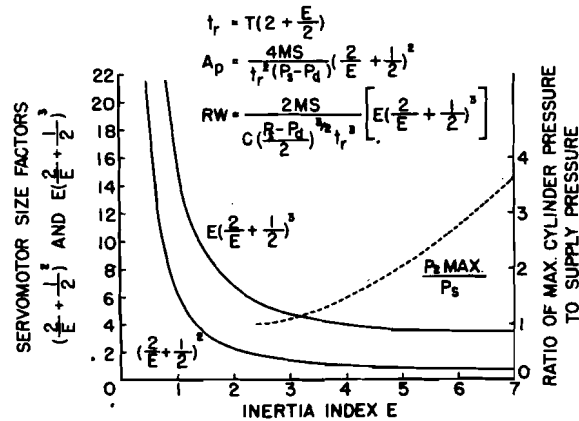


**FIGURE 10**

## CONCLUDING REMARKS

The discussion has shown that the response characteristics of hydraulic servomotors with mechanical feedback may be represented by linear equations. These equations are defined in terms of the size of the servomotor and the load conditions. From these relations, equations which define the dimensions of the servomotor in terms of the known load, and desired response characteristics can be obtained. By means of these relations the rational design of the servomotor to meet specifications on either the transient or frequency response characteristics is made possible.

## REFERENCE

1. NACA Report. Dynamics of Mechanical Feedback-Type Hydraulic Servomotor under Inertia Loads, by Harold Gold, Edward W. Otto, and Victor L. Ransom (soon to be published).

## APPENDIX - SYMBOLS

The following symbols are used in this analysis:

A    ratio of output amplitude at a given frequency to the output amplitude at zero frequency

$A_p$    piston area, sq in.

a    constant

b    constant

E    inertia index (transient response)

E'    inertia index (frequency response)

$f_1$    low frequency band break frequency, cycles/sec

$f_2$    high frequency band break frequency, cycles/sec

$f_3$    cross-over frequency, cycles/sec

h    width of vane, rotary servomotor, in.

J    polar moment of inertia, lb-in. $sec^2$/rad

$L_1$    inner radius, rotary servomotor vane, in.

$L_2$    outer radius, rotary servomotor vane, in.

M    load mass, lb $sec^2$/in.

$P_1$    upstream cylinder pressure, lb/sq in. abs

$P_2$    downstream cylinder pressure, lb/sq in. abs

$P_d$    drain pressure, lb/sq in. abs

$P_s$    supply pressure, lb/sq in. abs

R    ratio of valve travel to piston travel at fixed input

r    ratio of valve travel to vane shaft rotation at fixed input, in./rad

S    magnitude of step (measured at output), in.

S'    amplitude of output sine wave at zero frequency, in.

T     no load time constant, sec

t     time from start of transient, sec

W     width of valve port (measured perpendicular to axis of valve travel), in.

x     instantaneous position of output measured from position at t=0, in.

$x_m$     value of x at point of maximum deceleration in transient response, in.

$\omega$     angular frequency, rad/sec

$\theta$     magnitude of step (measured at output), rad

$\theta'$     amplitude of output sine wave at zero frequency, rad

$\alpha$     instantaneous position of output measured from poistion at t=0, rad

C     dimensional constant in fliud flow equation ($95.1 \frac{sq\ in}{sec\ \sqrt{lbs}}$ based on 0.851 sp gr and flow coefficient of 0.59)

# IMPROVEMENT OF POWER SURFACE CONTROL SYSTEMS
# BY STRUCTURAL DEFLECTION COMPENSATION

by

JAMES J. RAHN
EVERETT W. KANGAS

of

Boeing Aircraft Corporation
Seattle, Washington

# IMPROVEMENT OF POWER SURFACE CONTROL SYSTEMS
# BY STRUCTURAL DEFLECTION COMPENSATION

## INTRODUCTION

Power controls for operation of aircraft control surfaces have
become a necessity as a result of increased airplane size, speed,
range and control requirements. The direct feedback linkage type
of powered surface controls presents the problem of stability
versus response. This is especially true when a large surface
inertia is coupled with a relatively low structural spring rate.
Although these systems may be satisfactory for manual operation,
they may prove marginal or unsatisfactory when used with automatic
flight control equipment.

A means for improving the performance of a mechanical-hydraulic
control system having high surface inertia and low structural
spring rates has been developed and has proven quite successful
on an airplane installation. In this discussion we will first
cover a basic type powered surface control system. Then it will
be shown how a structural deflection feedback linkage can be added
to the system to improve performance.

## A BASIC TYPE POWER OPERATED CONTROL SYSTEM

A powered surface control system operating a high inertia surface
which has a low reaction spring rate may be limited in performance.
To retain stability of the system the gain must be kept low, re-
sulting in slow response which may make the system inadequate for
satisfactory airplane control. This problem was encountered in
the development of a rudder control system which is described be-
low and shown in figure 1. Operation of the pilot's pedals rotates
the torque tube $X_1$ by means of cables. A differential linkage is
located at the upper end of the torque tube. Since the surface is
initially stationary, the movement of the torque tube causes move-
ment of the error link $X_v$ which is connected to the hydraulic control
valve. Displacement of the control valve admits pressure to one
side of the piston and opens the other side to return. The result-
ing pressure differential supplies the force to move the rudder
against inertia, friction, damping and air load. The follow-up or
feedback link $X_o$ connected to the rudder and to the differential
then moves the differential to reduce the error to a minimum and
closes the hydraulic control valve. When the error is a minimum, the
valve is in neutral and the fluid trapped on both sides of the
piston holds the rudder in one position against variable loads.

This system as first installed in the airplane, figure 2, proved
to be unstable. Any disturbance to the control surface or to the
pilot input resulted in a continuous oscillation of the system.
To overcome this instability the system was slowed down by reduc-
ing control valve gain. The net result was a deterioration in
performance and excessive phase lag. The combined lag of the
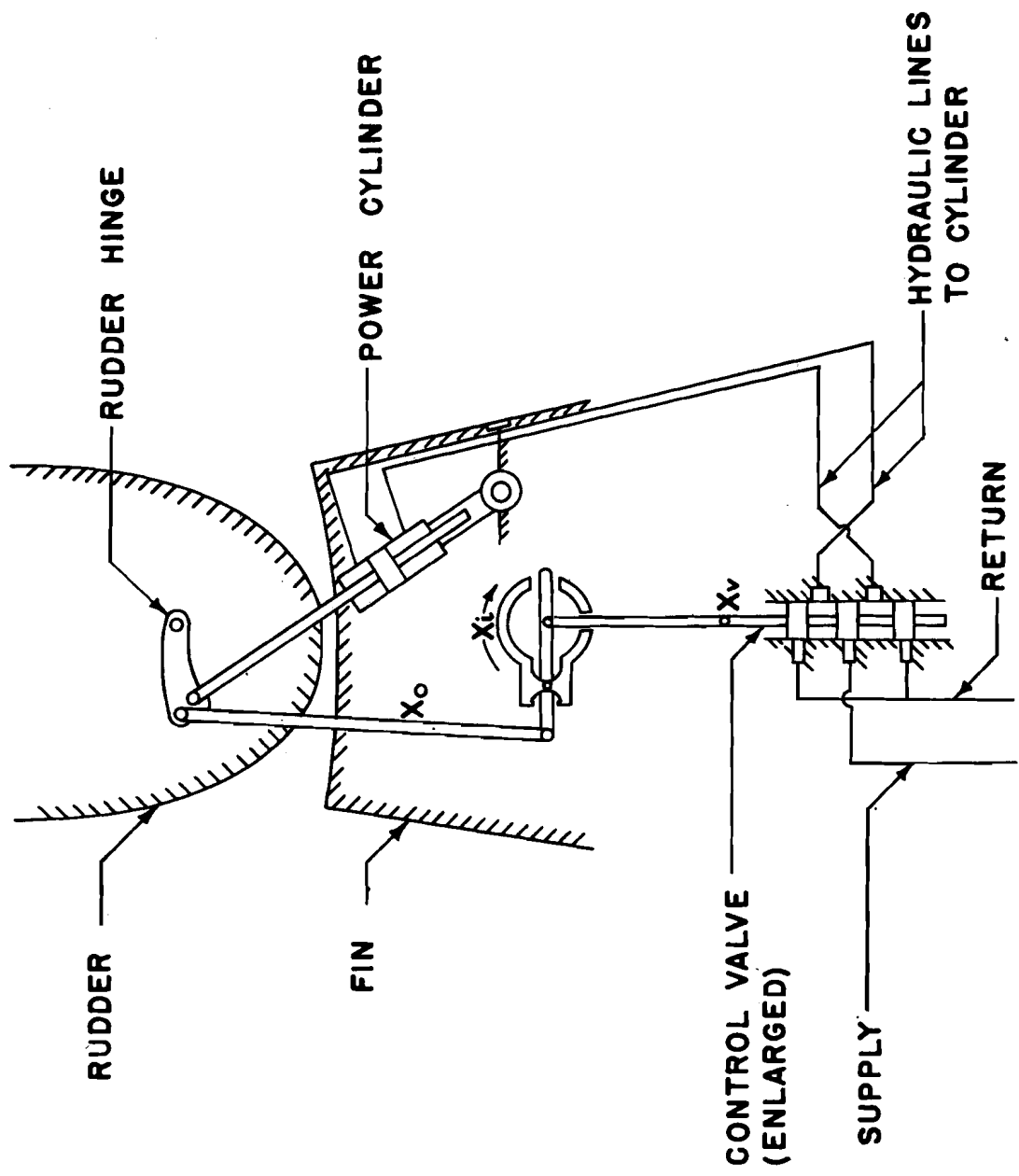
FIG. 1 - DIAGRAMATIC - TYPICAL POWER OPERATED RUDDER CONTROL SYSTEM

110
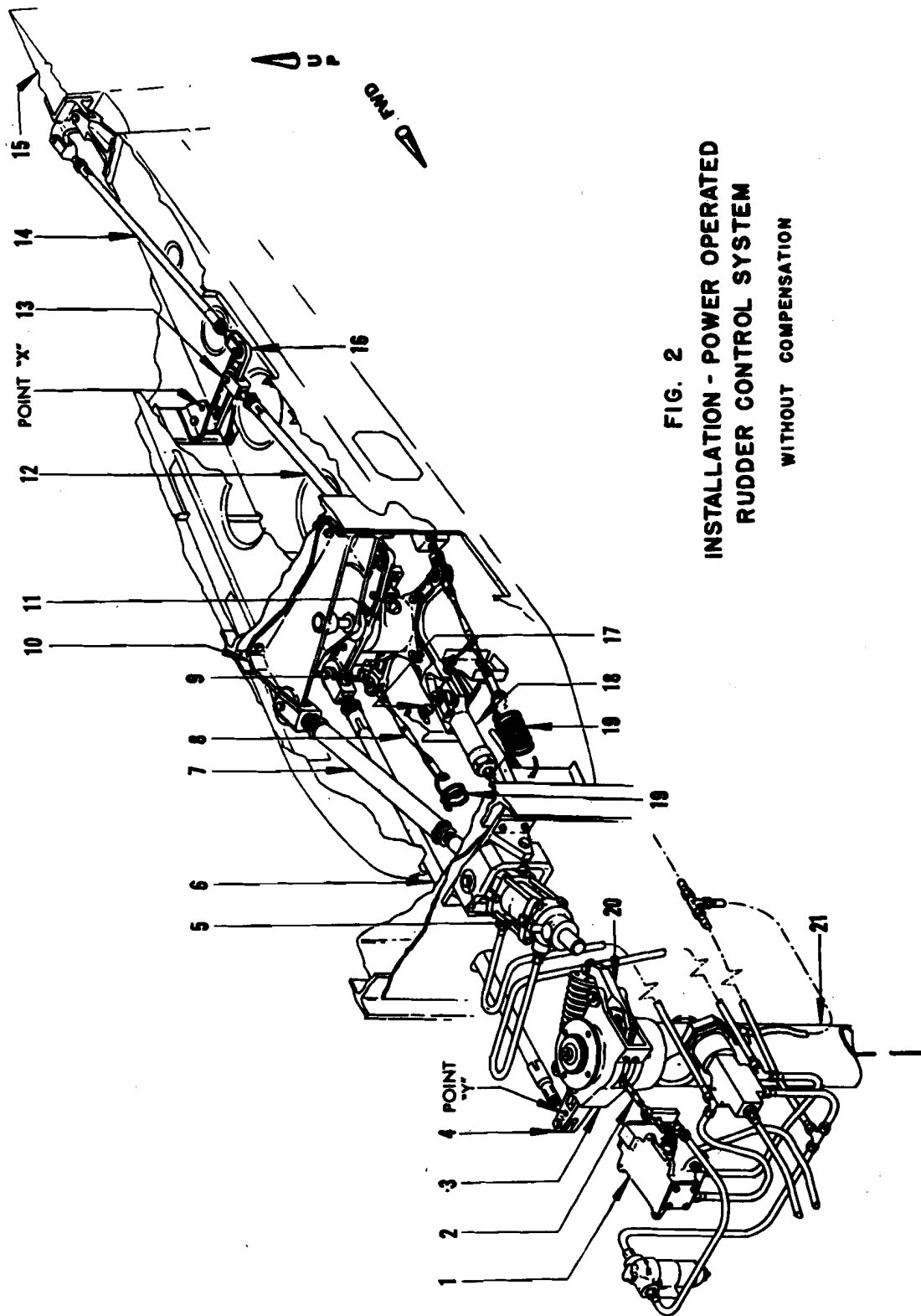


FIG. 2
INSTALLATION - POWER OPERATED
RUDDER CONTROL SYSTEM
WITHOUT COMPENSATION

power operated system and that of the airplane made pilot opera-
tion difficult and operation with the automatic pilot unsatis-
factory.

An analysis of the problem indicated that the difficulty could be
attributed primarily to the reaction spring rates of the system.
The structure of the reaction system had been designed for strength
in accordance with anticipated loads and not for rigidity and thus
accounted for a large portion of the elasticity. The compressi-
bility of the oil along with expansion of the power cylinder,
hydraulic tubing and other components also contributed to the
low overall spring rate of the system. Bending of arms and link-
ages in the feedback system and entrained air in hydraulic oil
were recognized as other factors involved.

It was also found that the original valve, although providing
required gain at higher amplitudes, caused too high gain at low
amplitudes resulting in instability. Other problems included
backlash and play in the system which was attributed primarily to
bearings and the movement of the power cylinder piston "O" ring
in its "standard" groove.

Various changes to the system were made in an effort to improve
performance. These included the design of a control valve whose
gain varied as the square of valve displacement, use of close
tolerance bearings and bolts throughout, and use of more rigid
feedback and control linkages. The reaction structure was also
strengthened locally, but it was found that a large portion of
the fin contributed to the spring rate.

Although some improvement was realized from this effort, it was
apparent that the performance was still less than desired. Fig-
ure 3 shows the frequency response curves of amplitude ratio and
phase of the system with these improvements.

The natural frequency of the airplane upon which this control
system was being used is shown by the dashed vertical line on
figure 3. It can be seen that the powered surface control sys-
tem phase lag was $70^\circ$ for 1 1/4 degree surface amplitude. For
smaller surface amplitudes the phase lag increased rapidly. In
this range of amplitudes the combined phase lag of the control
system and that of the airplane approached a value so high that
sufficient phase lead could not be realized from an automatic
pilot to keep the closed loop system stable. To be on the safe
side the powered control system should have less than 45 degrees
phase lag, for any amplitude at which the rudder is effective,
at a frequency 5 times that of the airplane natural frequency.
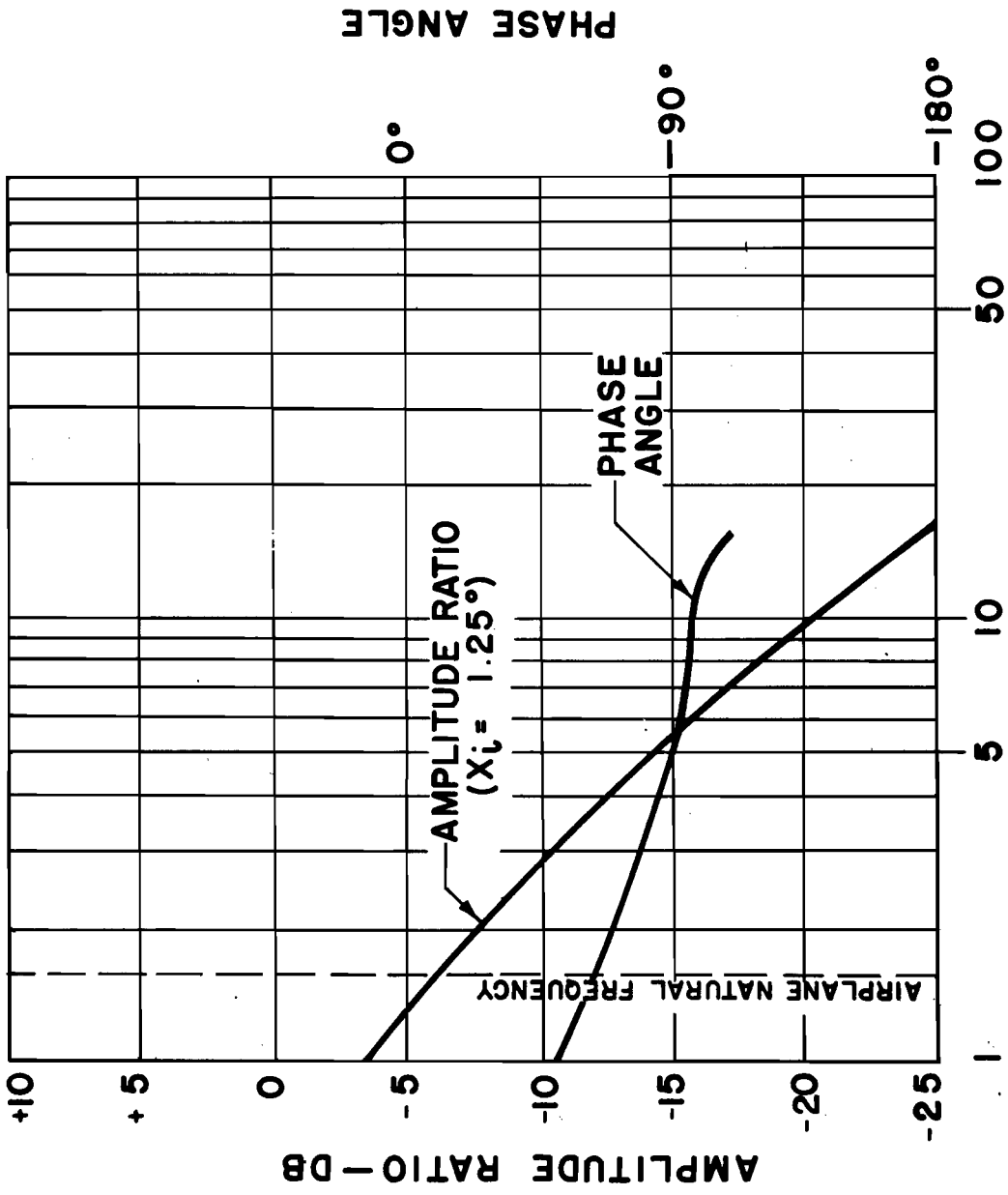
FIG.3-FREQUENCY RESPONSE-WITHOUT COMPENSATION

Additional means were tried in laboratory tests to improve perform-
ance. Damping in the feedback loop was tried, although better re-
sults were obtained, the installation complications did not warrant
its use. The use of a double "O" ring piston also helped to reduce
phase lag by reducing backlash of the system. Although the improve-
ment did not reach the magnitude desired, the double "O" ring piston
was installed since backlash will deteriorate any system.

The main problem, that of low spring rates of the system, still
remained, and prevented necessary increase in system gain to obtain
better response. This problem can be illustrated by referring to
a basic type power operated control system using a direct feedback
linkage as shown schematically in figure 4. It can be seen that
any external disturbance to the control surface or mass results in
deflection of the reaction structure. If the input system is held
fixed while the reaction structure is deflected, the followup link-
age opens the control valve in a direction to oppose this disturb-
ance. If the system has high gain, the control valve may admit
enough energy to cause the system to over correct the surface posi-
tion. Due to the inertia of the surface the over correction causes
a deflection of the structure in the opposite direction which in
turn again opens the valve and again excess energy is admitted and
the cycle is repeated. If the energy admitted per cycle is equal
to or greater than that extracted by aerodynamic damping and fric-
tion of the system, the surface will continue to oscillate. The
amount of energy that is added to the system is primarily deter-
mined by the flow characteristics of the metering valve and may be
kept small if the flow per unit deflection is small. Stability
may, therefore, be achieved by use of a low gain valve. This
improvement in stability of the system is obtained at the expense
of speed of response.

As very little can be done about the hydraulic spring rate and as
the structure stiffness can be increased only to a limited degree,
it was evident that some other means should be considered to comp-
ensate for all of the system spring rates.

## ADDITION OF STRUCTURAL COMPENSATION TO THE BASIC TYPE SYSTEM

High performance of a servomechanism cannot be obtained if lack of
stability limits the allowable gain. Therefore, the stability of
the system is the governing factor. Improvement can be obtained by
increasing either spring rate or damping or by reducing the mass.
For this system the mass could not be reduced and adding damping to
the output was not considered practical or desirable, leaving the
reaction spring rate as the factor to be considered in order to
improve stability.

114

The overall reaction spring rate is due to a series of springs. In the schematic figure 4, they were grouped into 2 main springs, $K_s$ structural spring rate and $K_h$ hydraulic and other spring rates. The first problem is to find a means for measuring the spring deflection then second to find a means of using this spring deflection to stabilize the system.

The structural deflection is a conveniently measurable quantity. It can be used to represent the entire spring system deflection if the proper ratio is applied. How this deflection is used will be shown analytically. However, in order to provide the basis for the analytical treatment of the subject, the system and its operation will be explained first. Proof for this explanation will then be given.

In this system a mechanical linkage is used to modify the system error in accordance with the deflection of the reaction structure. The basic system of figure 4 with the addition of structural deflection compensation is shown in figure 5. An external disturbance to the control surface or mass will deflect the reaction structure. The follow-up linkage will move the control valve to oppose the disturbance in the same manner as illustrated for the uncompensated system. The compensation linkage, however, now also adds to the valve signal. The direction of the valve movement due to the compensation linkage is opposite to the valve movement introduced through the follow-up linkage. By the proper arrangement of the ratio between the reaction compensating linkage and the follow-up linkage the direction and magnitude of control valve movement can be varied. The movement of the control valve as a result of an external disturbance can be made to reduce the amount of energy added to the system or to extract energy from the system. For a special linkage arrangement, energy will be neither added to or extracted from the system. The added linkage can be made to stabilize the system regardless of the magnitude, direction or origin of the disturbing force. This permits an increase in system gain to obtain improved performance.

An analysis of the system shows that the system stability is dependent on a derived term which will be referred to as the "Compensation Factor."

$$C_f = \frac{\frac{c}{d}}{\left(\frac{K_s}{K_h} + 1\right)} \frac{b}{a}$$
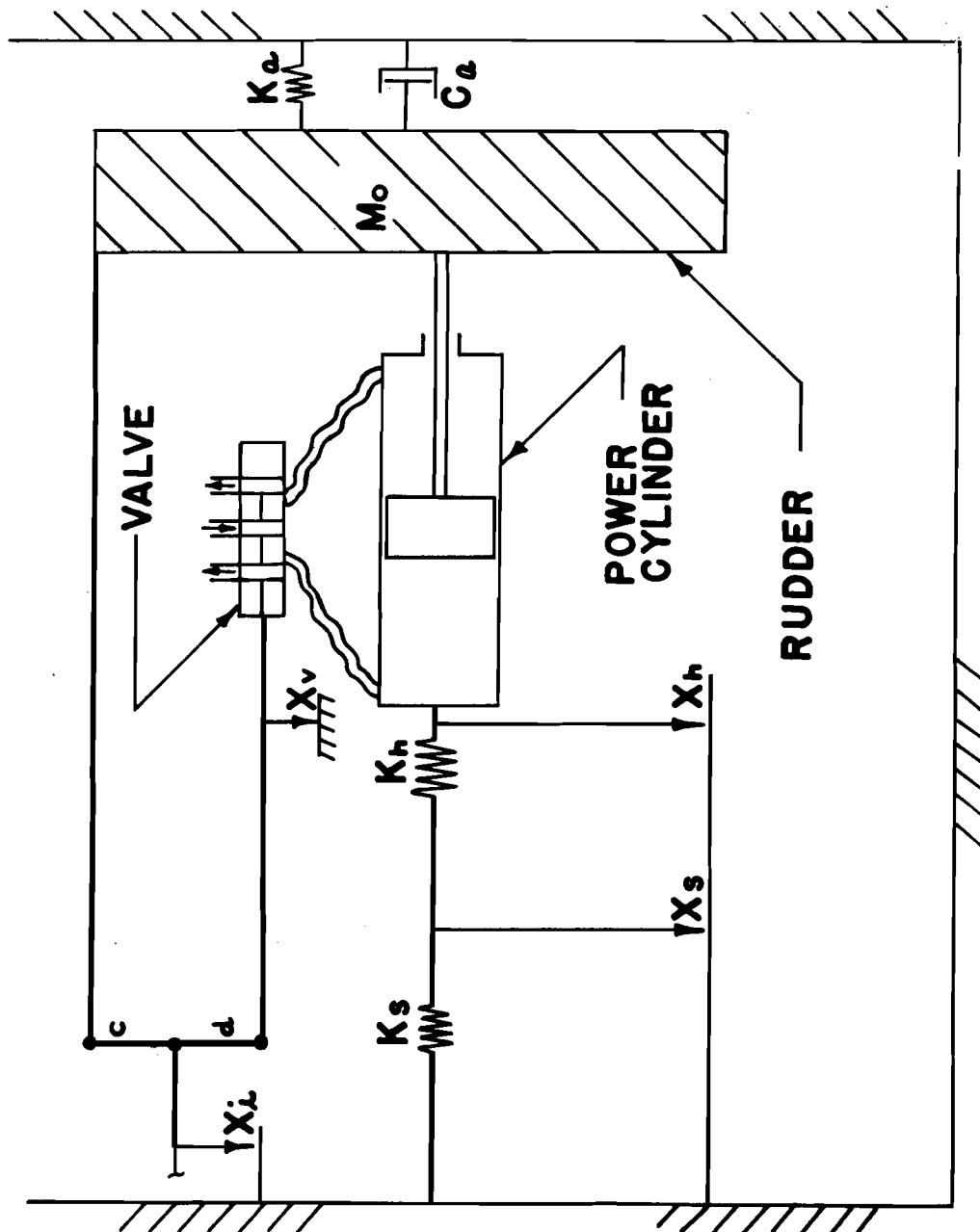
FIG. 4 — SCHEMATIC — BASIC TYPE POWER OPERATED
CONTROL SYSTEM — WITHOUT COMPENSATION
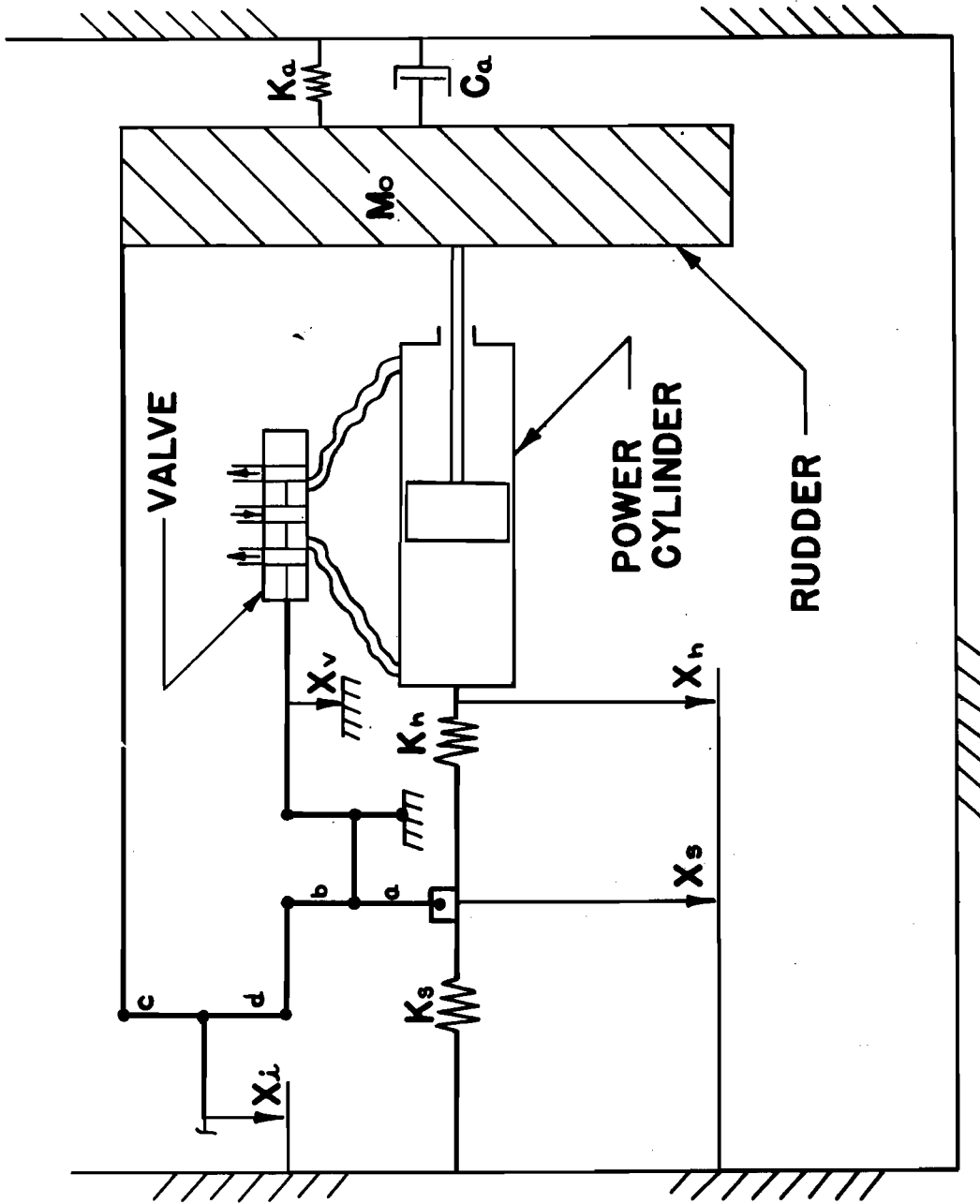
**FIG. 5 – SCHEMATIC – BASIC TYPE POWER OPERATED CONTROL SYSTEM – REACTION COMPENSATED**

In general, the value of $K_s$ and $K_f$ remain constant for a given system. The value of c and d are usually defined by the geometry of the mechanical input system and cannot be changed. By combining these terms the Compensation Factor reduces to a constant times the reaction compensation linkage ratio.

To obtain a stable system the value of $C_f$ must be equal to or greater than 1. Actually the system becomes less unstable and improvement is obtained even for values of $C_f$ less than and approaching 1.

The above derived term for the Compensation Factor and the criteria for stability can be arrived at mathematically as is shown by the following analysis. The symbol definitions are included on page 12 and refer to figure 5.

The differential and algebraic equations for the system are written as follows:

Summation of forces on the output member

$$M_o \ddot{X}_o + C_a \dot{X}_o + K_a X_o = K_h (X_h - X_s) \tag{1}$$

Summation of forces on the reaction system

$$K_s X_s + K_h (X_s - X_h) = O \tag{2}$$

From the geometry of the linkage system

$$X_v = X_L \frac{c+d}{c} - X_s \frac{b}{a} - X_o \frac{d}{c} \tag{3}$$

From the equation of continuity of hydraulic flow

$$X_v K_v = A_c (\dot{X}_o + \dot{X}_h)$$

$$X_v = \frac{A_c}{K_v} (\dot{X}_o + \dot{X}_h) \tag{4}$$

Substituting equation (3) into equation (4)

$$\frac{A_c}{K_v} (\dot{X}_o + \dot{X}_h) = X_L \left(\frac{c+d}{c}\right) - X_s \frac{b}{a} - X_o \frac{d}{c}$$

OR $\quad \dot{X}_o + \dot{X}_h = \frac{K_v}{A_c} \left[ \left( \frac{c+d}{c} \right) X_i - \frac{b}{a} X_s - \frac{d}{c} X_o \right]$ (5)

From equation (2)

$$X_h = X_s \left( 1 + \frac{K_s}{K_h} \right)$$

$$\dot{X}_h = \dot{X}_s \left( 1 + \frac{K_s}{K_h} \right)$$

Substituting these equations into (1) and (5)

$$M_o \ddot{X}_o + C_a \dot{X}_o + K_a X_o = K_h X_s \left( 1 + \frac{K_s}{K_h} \right) - K_h X_s$$

$$M_o \ddot{X}_o + C_a \dot{X}_o + K_a X_o = K_s X_s$$ (6)

$$\dot{X}_o + \left( 1 + \frac{K_s}{K_h} \right) \dot{X}_s = \frac{K_v}{A_c} \frac{d}{c} \left[ \frac{c+d}{d} X_i - \frac{c}{d} \frac{b}{a} X_s - X_o \right]$$ (7)

Equations (6) and (7) are the differential equations of motion for the system. In order to simplify these equations the following new coefficients are defined.

$$K_1 = \frac{c+d}{d}$$
ratio of followup to input linkage

$$K_2 = \frac{c}{d} \frac{b}{a}$$
ratio of followup to compensating linkage

$$G_o = \frac{K_v}{A_c} \frac{d}{c}$$
Velocity gain of the system referred to the output.

With these substitutions into equation (7) the differential equations
for the system become

$$M_o \ddot{X}_o + C_a \dot{X}_o + K_a X_o = K_s X_s \qquad (8)$$

$$\dot{X}_o + \left(1 + \frac{K_s}{K_h}\right) \dot{X}_s = G_o \left[ K_1 X_i - K_2 X_s - X_o \right] \qquad (9)$$

The solution of these equations provides the transfer function of
the system in operator form

$$\left[ \frac{X_o}{X_i} \right] = K_1 \frac{G_o \, \omega_r^2}{S^3 + [2 \, \varphi_a \omega_o + G_o C_f] S^2 + [\omega_o^2 + G_o C_f 2 \, \varphi_a \omega_o] S + G_o [\omega_r^2 + \alpha_f^2 C_f]} \qquad (10)$$

An examination of this characteristic equation by means of Rouths
criterion, and by assuming that aerodynamic damping is zero
although it tends to stabilize the system, it can be shown that
the stability of the system is dependent upon the "Compensation
Factor". The factor is defined as

$$C_f = \frac{K_2}{\left(\frac{K_s}{K_h} + 1\right)} = \frac{\frac{c}{d}}{\left(\frac{K_s}{K_h} + 1\right)} \frac{b}{a}$$

for the system being analyzed. For the system to be stable the
value of $C_f$ must be greater than 1. Neutral stability is obtained
when $C_f$ equal 1.

By proper selection of linkage ratios the value of $C_f$ can, of course,
be varied. For the special case of $C_f$ equal to 1 there will be zero
deflection of control valve slide relative to the sleeve for any
disturbance of the system. If $C_f$ is less than 1, the control valve
slide movement will be in the direction to oppose the external
disturbance, adding energy to the system and tending to destabilize
the system. This approaches the uncompensated system which has $C_f$
equal to zero. A linkage ratio resulting in $C_f$ being greater than 1
will cause the control valve to move in a direction not opposing
the disturbance. This indicates a loss of energy from the system and

will result in a damping effect on the power control system.

Obviously, where the stability of the system is of importance, only values of the compensation factor $C_f$ equal to or greater than 1 are of interest.

To illustrate the application of the Compensation Factor to obtain a linkage ratio for a stable system having $C_f$ equal to 1, assume the following values:

$$K_s = 1$$

$$K_h = 2$$

$$c = 3$$

$$d = 4$$

Then

$$C_f = 1 = \frac{\frac{3}{4}}{\left(\frac{1}{2} + 1\right)} \frac{b}{a}$$

$$\frac{b}{a} = \frac{2}{1}$$

Theoretically as the ratio of b to a becomes larger, the system damping becomes greater, and as the ratio gets smaller it tends to destabilize the system.

The uncompensated system theoretically is assumed to be irreversible. Reversibility here is referred to as displacement of the output member and bears no relationship to the proportional pilot feel of control surface load commonly referred to in boost systems. Actually it is reversible as the valve deadspot and leakage cannot be reduced to zero, backlash cannot be entirely eliminated, and there will always be a finite elasticity in the system linkage. The compensated system is theoretically reversible. The degree of reversibility under static conditions will be equal to $C_f$ times the reversibility of the reaction system. For instance, assuming $C_f$ equal to 1 the reversibility of the system being discussed is approximately .9 degree for maximum load. Under normal conditions with the surface at or near streamline position, the surface loads will actually be a small percent of the maximum load and the reversibility will be proportionally smaller.

Although only one type of power control system has been discussed here, it should be pointed out that the theory of structural deflection compensation applies equally well to any basic positioning system.

## APPLICATION OF STRUCTURAL COMPENSATION
## IN AN AIRPLANE POWER CONTROL SYSTEM

Analysis of the system has shown that the stability of the system is primarily dependent upon linkage ratios. An evaluation of a system for a desired compensation factor will provide an approximate value for the required linkage ratio. In an actual installation, it may be difficult to accurately determine the spring rates of the system, and tests may be required to obtain the best linkage ratio as governed by desired system performance. This procedure was used in arriving at the optimum linkage ratio for the installation discussed in this paper.

A diagramatic sketch of the basic power control system with the addition of the compensated linkage is shown in Figure 6. In the actual installation as shown in figure 7 it was necessary to add five links to the original system. The number of links required is primarily controlled by the physical location of components in the system. The application of this type linkage into a system already designed may be more difficult than for a new system which can be designed to include the simplest and most effective arrangement.

The improvement in stability of this system with the addition of the compensating linkage permitted use of a higher gain valve with a nearly linear flow versus displacement characteristic. This resulted in a higher performance system for all amplitudes. The value of the compensation factor for this system as installed in the airplane was approximately 1.1.

The degree of improvement of the actual airplane installation is shown in figure 8. This is a representation of the power control system performance. It can be seen that the phase characteristics of the system have been improved considerably over the uncompensated system as shown in figure 3. For better comparison, figures 3 and 8 are both shown in figure 9. It should be noted that the amplitude at which the compensated system was tested was only ±1/4 degree as compared to ±1-1/4° for the uncompensated system. This serves to show even more the degree of improvement which was obtained, as the response of a system generally becomes poorer with a decrease in amplitude.

RUDDER HINGE

RUDDER

FIN

POWER CYLINDER

CONTROL VALVE

SUPPLY

HYDRAULIC LINES
TO CYLINDER

RETURN

FIG. 6 – DIAGRAMATIC – TYPICAL POWER OPERATED RUDDER CONTROL SYSTEM
REACTION COMPENSATED

123

2. RUDDER-BOOST VALVE CONTROL ARM
1. RUDDER ACTUATOR ARM
.40 TO .60
BY-PASS VALVE
SHUTOFF VALVE
POINT Y
3. FIN
23. ROD
5. TAB LINKAGE ROD
SEE DETAIL I
7. SUPPORT POINT X
8. ARM
10. ROD
9. TAB
6. RUDDER
SEE DETAIL II
12. TAB-LOCK ARM
TURNBUCKLES
13. TAB SPRINGS
14.
RUDDER ACTUATING CYLINDER
15.
HYDRAULICALLY-OPERATED RUDDER-ARM LOCK
4.
CAM
16. RUDDER-CONTROL TORQUE TUBE
LINK
FILTER
18. RUDDER-BOOST METERING VALVE
ACCUMULATOR
17. TURNBUCKLE ROD

FIG. 7
INSTALLATION POWER OPERATED
RUDDER CONTROL SYSTEM
REACTION COMPENSATED

FIG. 8 — FREQUENCY RESPONSE — REACTION COMPENSATED

**PHASE ANGLE**

0°

90°

180°

100

50

AMP RATIO
(X = .25°)

PHASE
ANGLE

10

5

AMP RATIO
(X = 1.25°)

PHASE
ANGLE

AIRPLANE NATURAL FREQUENCY

+10

+5

0

-5

-10

-15

-20

-25

**AMPLITUDE RATIO-DB**
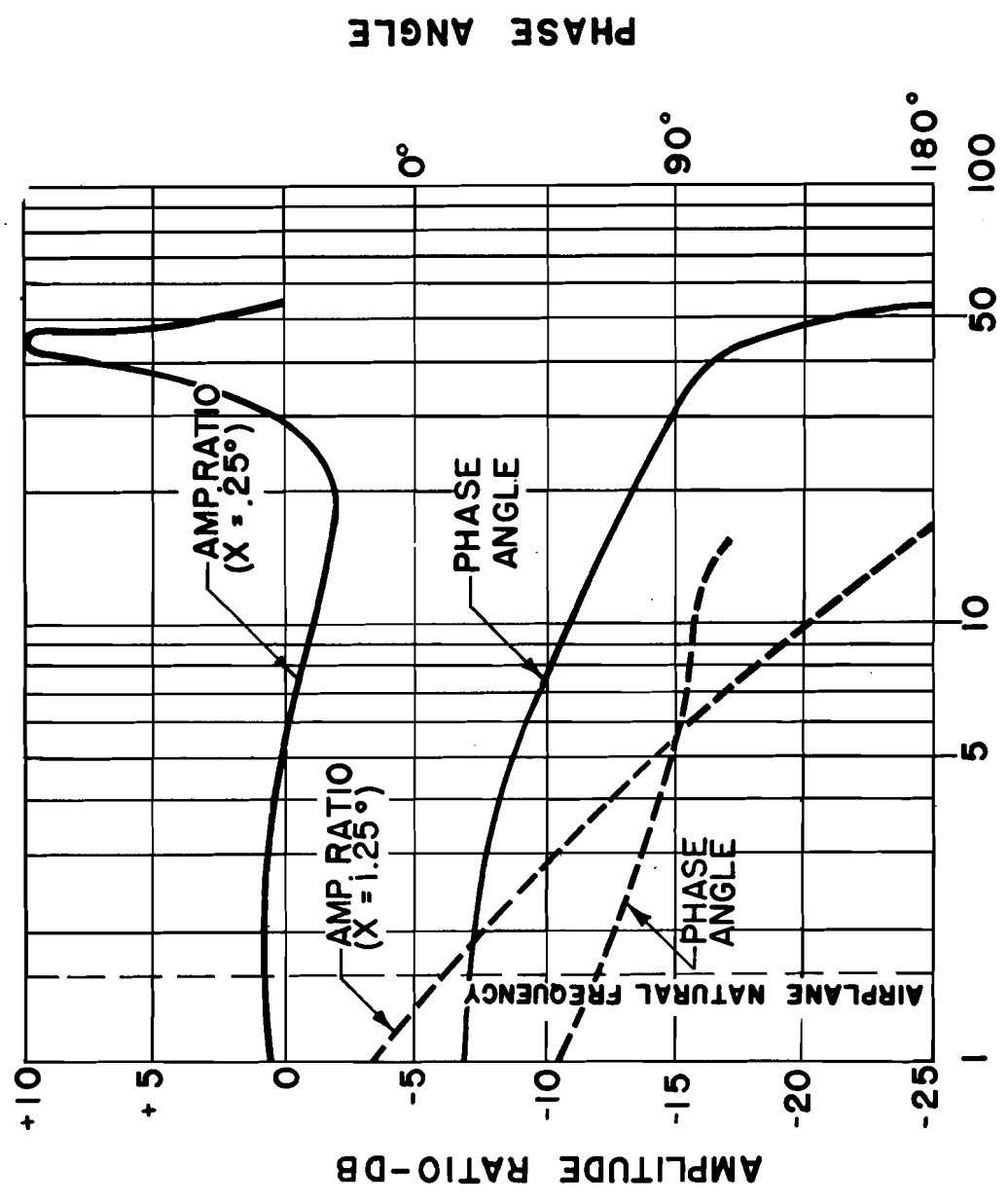
IMPRESSED FREQUENCY - RAD/SEC.

FIG 9 - FREQUENCY RESPONSE - WITH & WITHOUT COMPENSATION

In the range of airplane natural frequency, the phase lag of the powered surface control system has been reduced to 20°. Even though the airplane phase lag (rudder movement to yaw) is approximately 90° in this frequency range, the total lag is reduced to a value such that the necessary phase lead can be realized in an automatic pilot in order to attain satisfactory overall performance.

The final evaluation of the system, of course, depends on performance on a flight test airplane. The system which has been discussed here proved successful in eliminating steady state oscillations and improving maneuverability and performance for automatic pilot operation.

## CONCLUSIONS

1. The performance of a mechanical-hydraulic servo system is limited by the reaction spring rate.

2. This limitation can be overcome by utilizing structural deflection feedback.

3. The structural deflection feedback linkage can be designed to compensate for all deflections of the system.

4. Compensation results in a reversible system proportional to elasticity of reaction structure.

5. Higher response of the system can be realized with structural deflection feedback resulting in improved performance.

## SYMBOL DEFINITIONS

$X_0$ = displacement of output member

$X_i$ = displacement of pilot input

$X_s$ = displacement of structural portion of reaction system

$X_h$ = effective displacement of hydraulic portion of reaction system

$X_v$ = relative displacement of control valve slide with respect to valve sleeve

$K_s$ = effective spring rate of structural portion of reaction system

$K_h$ = effective spring rate of hydraulic portion of reaction system

$K_a$ = effective spring rate of aerodynamic forces acting on output member

$M_0$ = mass of output member

$K_v$ = flow coefficient of control valve (hydraulic flow/unit valve opening)

$A_0$ = area of operating cylinder (assume equal on both sides)

$a$ = compensating linkage length (reaction pivot to structural deflection input)

$b$ = compensating linkage length (reaction pivot to valve connection)

$e$ = differential linkage length (pilot input to follow-up)

$d$ = differential linkage length (pilot input to valve connection)

$C_a$ = aerodynamic dampening coefficient on output member

$\omega_r$ = undamped natural frequency of inertia - reaction system.

$\omega_a$ = undamped natural frequency of inertia - aerodynamic restoring force system.

$\omega_0$ = undamped natural frequency of the overall system.

$\gamma_a$ = damping ratio of the system

# A SURVEY OF SUGGESTED MATHEMATICAL METHODS

# FOR THE STUDY OF HUMAN PILOT'S RESPONSES

by EZRA S. KRENDEL
The Franklin Institute
Laboratories for Research and Development
Philadelphia, Pennsylvania

During the last decade considerable effort has been directed by several laboratories, both in this country and in England, toward the solution of the problem of rationally characterizing the human operator of various types of control equipment. The goal of this research has been the determination of what might be called human "transfer functions," where the term transfer function is used in a loose sense. In general, the work has dealt with problems arising in gun directing situations. Although relatively little effort has been concerned with the study of the guidance problems arising in the control of aircraft, the display and control problems for sighting systems and aircraft have sufficient similarity to make the suggested methods of study applicable to both problems. The purpose of this paper is to state some of the past suggestions for appropriate mathematical models to describe human operator performance, and to present some of the current thinking at The Franklin Institute on the problem.

The problem under discussion arises from the control situation wherein an operator is attempting to orient a device so that a visually perceived error may be minimized. Figure one represents this situation in a simple tracking task which was investigated at The Franklin Institute. The specification of the transfer functions in this figure is only for explanatory effect. The human element in this control system consists of the eye, which is the primary error sensing mechanism; the nerves, which are the data transmission system; and the arm muscles which are the motor system. It is, however, necessary to specify more about the situation. Since the operator is largely non-linear, the stimulus must be carefully specified. The visual signal can be characterized by the degree to which the operator is able to predict the stimulus. Close to perfect prediction can be achieved either by having the future behavior of the signal disclosed to the operator over a length of time greater than his reaction time plus movement time, or by conveying very little information in the visual stimulus by presenting the useful past history of a signal the future of which is determined simply from its past. Examples of the first type of easily anticipated signal arise in the driving of an automobile; whereas an example of the second type of predictable signal would be the tracking of a simple sine wave. The display which a gunner sees in his sights or which a pilot sees when getting on target differs from the foregoing in that the possible
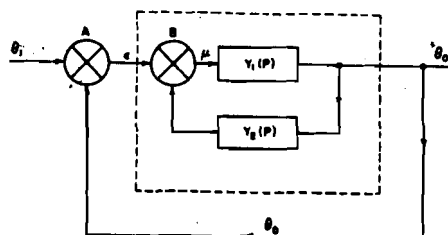
The Tracking Problem in Servomechanism Notation

$\theta_i$ is the input of step functions from the programmer.

$\theta_o$ is the position of the control stick.

A is a summing amplifier which generates the error signal, $\epsilon = \theta_i - \theta_o$, so as to produce the signal which is seen on the scope.

B is the human error detecting device which is sensitive to visual and kinaesthetic inputs.

$\mu$ is the signal determining the positioning of the operator's hand and is the difference between $\epsilon$ and $Y_2(P)\theta_o$.

$Y_1(P)$ is the transfer function describing the positioning of the control stick.

$Y_2(P)$ is the transfer function of the operator's internal filter which specifies the control limb's position by means of proprioceptive feedback.

Figure 1.

anticipation of the target's motion is limited by the narrow field of view as well as by the conditions generating the motion, such as evasive maneuvers and unforeseen random disturbances due to gusts. It can be seen from the foregoing examples that any study of human responses must carefully consider the nature of the visual input because of this anticipation characteristic of the operator.

Another well-known characteristic of the human operator is the ability to adjust to and compensate for specific tracking problems and specific equipment. For example the operator is able to adjust his response to take into account friction, different control ratios and other aspects of the equipment. Similarly the operator is able to adjust his response with regard to instructions such as "track accurately," "track rapidly" or in the case of aircraft flight to maintain a smooth course through a series of gusts instead of attempting to compensate for each one. In addition the operator's behavior is capable of changing as a function of experience and training in any particular tracking task.

The foregoing characteristics point up the difficulties in attempting to arrive at a linear, time invariant, description of human operator behavior. In addition this non-linear nature of the human operator makes any character-

isation of the human more or less particular to the circumstances under which the measurements were made. Thus, if a transfer or, more properly, descriptive function can be determined for the operator, it can only be specified for a given class of input signals, for a given piece of apparatus, and for given instructions and degree of practice. In addition, this function will exhibit variations arising from the individual differences in the sampled population of subjects. If a linear operator description is to be attempted, this linear operator expression will have validity only in discussing behavior with inputs roughly similar to the inputs used in the measuring experiments. Consequently, a statistical type of input function seems appropriate.

The following is of necessity a very brief introduction to some of the attempts to deal with the foregoing problem. Among the earliest attempts to characterize the human operator's operation were those by R. S. Phillips and A. Sobczyk;[1] and R. H. Randall, F. A. Russell and J. R. Ragazzini.[2] The Phillips equation for describing handwheel control which was developed for a study of aided tracking assumed that the operator generated a velocity proportional to the value of the error and to the rate of change of the error all delayed by a time lag, L. Thus the handwheel velocity pH(t) could be written in terms of the error signal input E(t) as follows:

$$p\,H(t) = \left[ (bp + c)e^{-pL} \right] E(t).$$

Both b and c are parameters, and p is the usual differential operator. Randall and his coworkers evolved an expression for describing human operator behavior which adds derivative control to the foregoing expression so that we have:

$$p\,H(t) = \left[ (ap^2 + bp + c)e^{-pL} \right] E(t).$$

The coefficient of the additional term is a parameter, a.

Tustin[3] studied the problem somewhat more elaborately by creating a signal composed of three harmonics and determining an approximate linear law by means of harmonic analysis of these three components. Tustin considered the handwheel displacement and error signal to be composed of components describable by this linear law and a remnant due to non-linearities and noise. Tustin arrived at an equation of the following form:

$$( \Bbbk + p ) \, H(t) = \left[ ( b + c p ) \, e^{-p^{L}} \right] E(t)$$

The constant k helped to improve the fit at low frequencies. Using two cam speeds Tustin studied eight frequencies from .018 to .204 cps.

L. Russell[4] in a recent MIT master's thesis conducted an extensive series of experiments in a study of linear approximations to human tracking behavior. He used a best linear model plus noise approach and employed a signal of four harmonics which could be presented at three speeds. He thus had a range of from .0442 to 1.43 cps in the input signal. Russell evolved an equation similar to the Phillips equation. Russell indicated that the human appears to adjust his response parameters in order to minimize the mean square error in tracking a signal of given power spectrum. In addition the human appears to set his gain at a value yielding a reasonable margin of stability. It is well to point out that the parameters found for the four preceding operational expressions were all different. The fact that a, b, and c differed indicates that the human's response is peculiar to given apparatus and display problems. The variation in L from .3 seconds to .5 seconds is probably a function of the training of the operators and the predictability of the signal.

North,[5] in a recent paper on the human transfer function, has developed a sophisticated framework for the study of human transfer functions. A mean linear operator of simple form is postulated and in addition the characteristics of a superimposed stochastic distribution are discussed. In simple position tracking North postulates a relation of the form

$$p \, H(t) = b \, e^{-p^{L}} \, E(t)$$

as the mean steady state operator; and, in addition, he posits a transient which is kept in a state of continuous excitation by the stochastic elements. This problem is studied by a system of finite difference equations as well as by differential equations in view of the evidence for discontinuity of human operator tracking responses. The discontinuity arises from the fact that there is a refractory period in tracking since the human appears to preset responses in accordance with his best estimate from available data, and that these responses, once initiated, can not be changed continuously. The stochastic process arises from two sources: one, is inaccurate estimations of the input signal, and two, is the inability of the operator to perform the appropriate response.

There has been some work done at.The Franklin Institute on the
problem of studying human frequency response with the view in mind of
obtaining "transfer functions," on a project sponsored by the United
States Air Force.[6,7,8] The method which this project has selected for
studying the human operator's frequency response is the comparison of
the output spectral density to the spectral density of the visual input
using a random signal as the input. Such a comparison yields useful
information whether or not the human operator behaves in a linear
fashion. Were a linear system under study, it can be shown that the
amplitude part of the system's frequency response is equal to the square
root of the ratio of the spectral density of the output to the spectral
density of the input. A complete description of the linear system would
require the cross spectral density of the output and input so that
phase as well as amplitude characteristics could be specified. Since
the computation of the cross spectral density would have required twice
as much work as the computation of spectral densities, it was decided
that only the amplitude response would be computed in the preliminary
experiments. The main purpose of the preliminary experiments, the
apparatus for which was a simple compensatory position tracking device,
was to determine whether the foregoing input-output analysis was a
suitable method for analyzing the data of more ambitious experiments using
a dynamic flight simulator for a high speed jet fighter built by The
Franklin Institute Laboratories. The random input function was obtained
by constraining a pip on an oscilloscope to take positions on a hori-
zontal axis alternatively to the left and to the right of a vertical
fiducial line so that the number of zero crossings were described by a
Poisson distribution. In order to make the display somewhat less
predictable the amplitudes to the left and to the right were randomly
selected from a Gaussian population of the same mean and standard
deviation for amplitudes to the left and to the right. One of the under-
lying reasons for selecting a random time series input was the belief
that the human operator is largely non-linear. This particular random
time series had a spectrum which was similar to the spectrum of atmos-
pheric turbulence.

In order. to add psychological interest to the investigation of the
applicability of the analytical procedures, three questions were examined.
Does the operator track the random input in a linear fashion? How does
his behavior change as a function of practice? How do different in-
structions affect his response patterns? The question of linearity was
examined by comparing the amplitude frequency response for two subjects
when tracking a distribution whose mean absolute amplitude was one
centimeter and when tracking a distribution of mean absolute amplitude
equal to two centimeters. The effect of practice, i.e., time variation
of the system, was examined by comparing the output of the two subjects
when naive and when highly trained in following a certain random input
signal. The effects of instructions to track for accuracy and of
instructions to track for speed were compared for two subjects in order
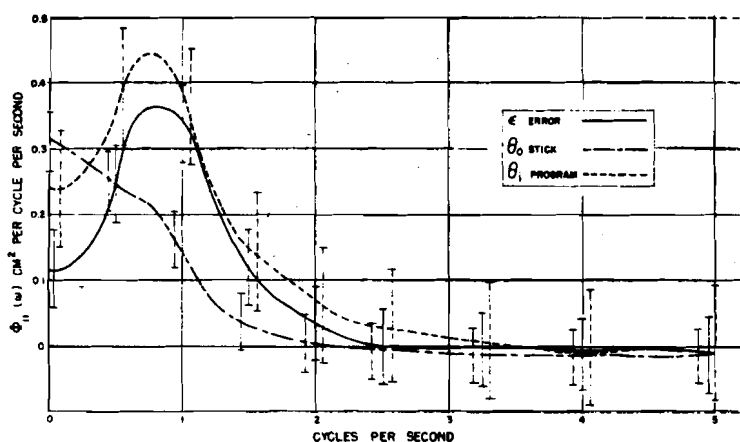
Figure 2. - Spectral densities of tracking time signals for
a trained subject instructed for accuracy.
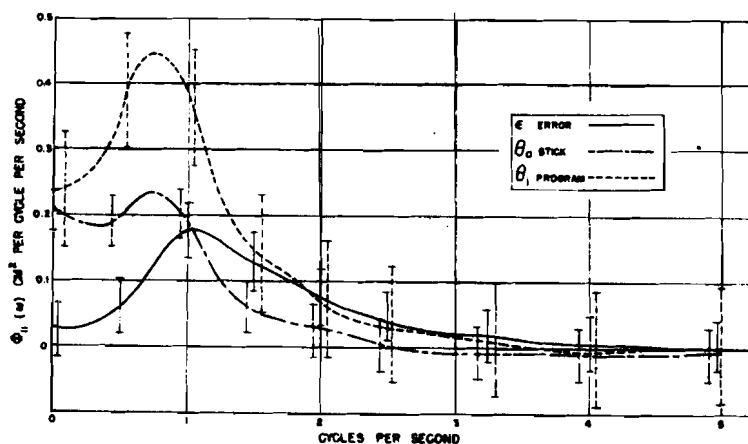


Figure 3. - Spectral densities of tracking time signals for
a trained subject instructed for speed.

to determine if there was behavioral evidence in the output spectra for two different sets to respond.

An example of the use of spectral densities for examining behavioral characteristics can be seen in figures 2 and 3 which illustrate a comparison of smoothed spectral densities for two different instructions for one highly trained subject. It will be noted that instructions for accuracy resulted in a considerably smoothed output. The fiducial lines represent 2 $\sigma$ confidence bands arising from instrument errors in the computations of the spectrum.

In general, the experiments were not of sufficient magnitude for an adequate test of the psychological questions raised. On the other hand, the form of the results indicates the fruitfulness of this method of analysis and its logical extension to the interpretation of tracking data from the dynamic simulator.

At present the dynamic simulator has been used for a small experiment utilizing three trained jet pilots. The data obtained, which is in the form of responses to gust inputs, will be used to obtain certain order of magnitude approximations to "human transfer functions" using The Franklin Institute Advanced Time Scale Analog Computer. The general research program for the study of the human operator envisions the use of special data reduction equipment to be constructed at The Franklin Institute for the determination of the pertinent spectral densities and cross spectral densities.

REFERENCES

1. James, Nichols, Phillips: Theory of Servomechanisms. Radiation Laboratory Series, Vol. 24, 1947, pp. 360-368.

2. Randall, R. H., Russell, F. A., and Ragazzini, J. R.: Engineering Aspects of the Human Being as a Servomechanism. Unpublished mimeographed notes, 1947.

3. Tustin, A.: The Nature of the Operator's Response in Manual Control and its Implications for Controller Design. Journal Institution of Electrical Engineers, Part 11 A, No. 2, May 1947.

4. Russell, L.: Characteristics of the Human as a Linear Servo-Element. Sc.M. Thesis, Mass. Inst. Tech., Cambridge, Mass., May 1951.

5. North, J. D.: The Human Transfer Function in Servo Systems. Ministry of Supply, Report No. WRD/6/50, November 1950.

6. Krendel, E. S.: A Preliminary Study of the Power Spectrum Approach to the Analysis of Perceptual Motor Performance. USAF, Wright-Patterson Air Force Base, Dayton, Ohio, AFTR 6723, Oct. 1951.

7. Krendel, E. S.: A Spectral Density Study of Tracking Performance, The Effect of Instructions. USAF, Wright-Patterson Air Force Base, Dayton, Ohio, WADC TR 52-11 Part 1, Jan. 1952.

8. Krendel, E. S.: A Spectral Density Study of Tracking Performance, The Effects of Input Amplitude and Practice. USAF, Wright-Patterson Air Force Base, Dayton, Ohio, WADC TR 52-11 Part 2, Jan. 1952.

# SYNTHESIS OF FLIGHT CONTROL SYSTEMS

by  DR. JOHN G. TRUXAL
of
Purdue University
Lafayette, Indiana

During the past year Purdue University has been privileged to have a contract from the Office of Naval Research to investigate design techniques for power boost systems for aircraft control. We at Purdue feel that the university research groups can not, and should not, be in direct or indirect competition with industrial research. Rather we feel that the primary job of university research should be the development of basic synthesis techniques.

In line with these aims, our primary interest has been in the investigation of the basic general problem of the stabilization and design of power boost systems. We have attempted to clarify and delineate the problems involved in this design and to develop and determine those design techniques which will be generally applicable in this problem. We have not worried particularly about specialized methods of stabilization which might be applicable to one aircraft, not to another. Rather, our main concern has been with methods which we hope will be generally applicable; in the absence of any one specific problem, we leave the more specialized techniques to the industrial research groups.

What is the fundamental problem? As we see it, the problem arises from a basic conflict between speed of response and stability. On the one hand, we have the speed of response of our control system; on the other, the stability of the overall aircraft. The relative location of these two conflicting requirements depends on a number of factors--e.g., the aircraft speed. As long as we are dealing with low-speed aircraft, there is essentially no problem. At low-speeds, a relatively sluggish aircraft response is permissible. In addition, the aerodynamical characteristics of the plane itself may be relatively stable. However, as the required aircraft speed increases, two things start to happen: the speed of response must be increased; the relative stability of the aircraft decreases. Inevitably, as we demand better and better performance from our aircraft, the problems involved in realizing a system which is sufficiently stable and at the same time responds with adequate speed becomes more difficult. We feel that we are now at the point where design has become difficult, particularly in those cases in which we deal with the aircraft as a gun platform. Essentially, the situation here is no different than that in many fields of engineering. This is a universal phenomena--this development of tauter and tauter specifications, as the years go by; this demand, as these specifications become more taut, for a more complete understanding of the basic system--and in particular a fuller understanding of what factors influence the system performance.

Our first concern then has been with a determination of those factors which do determine the stability and the speed of response of the aircrafts

with a control system actuated by a power boost system. The system we have considered is shown in Fig. 1. Our system consists basically of five parts. Working from the stick to the control surface, from left to right on the diagram, we have first a mechanical coupling system between the stick and the hydraulic power system. k here represents the compliance of the push rod or control cable from the stick to the input to the hydraulic system. The damper $f_p$ and mass $m_p$ represent the impedance seen looking into the input to the hydraulic system from the output end of the control cable. In our initial study of the system, we have assumed that these parameters are independent of the gain of the hydraulic system. I will have more to say concerning these simplifying assumptions later.

The input to the hydraulic system is the displacement $x_p$. We consider a single-stage hydraulic system, with an output displacement $x_c$ actuating the bell crank to give a deflection of the control surface $\delta$. The normal, or vertical acceleration of the airplane, n, is determined by this deflection through the aerodynamical characteristics of the aircraft. The artificial feel system we consider is the simplest possible, consisting only of the bobweight of mass small m. We do not imply that this is at all typical of general artificial feel systems. Certainly our system probably should include at least a spring. However, we feel very strongly, as I shall try to point out later, that the design of a suitable artificial feel system depends on considerations of dynamic stability (and when I speak of stability, I refer to dynamic stability) and the nature and characteristics of the pilot in the closed loop system. We feel, and perhaps you will agree as we continue, that this simple bobweight system suffices as an example of the general procedures and ideas I hope to present to you. The introduction of a spring does not, for example, materially change our development.

Figures 2, 3, and 4 show the basic components of our system in more detail. Figure 2 shows the aerodynamic axes and basic equations, Fig. 3 the stick dynamics and Fig. 4 the hydraulic system. The pertinent equations accompany the figures. A considerable portion of the effort of the Purdue group over the past year has been spent in the analysis of the hydraulic system, the development of measuring techniques and the correlation of valve configuration with static and dynamic characteristics. However, today I would like to consider the hydraulic valve as described simply by the flow-proportional-to-displacement equation, which is an adequate description over the frequency range of interest to us, and omit any detailed discussion of other possible linear and nonlinear analytical descriptions of the system.

Referring again to figure 1, we see that there are basically two feedback systems to be designed—the hydraulic system, which is a closed-loop, positional feedback system, and the overall airplane control system which contains the hydraulic loop as one component. Our initial interest at Purdue was concentrated on the hydraulic system, but it rapidly became apparent that this one component could not be intelligently designed or analysed without consideration of the overall system. I would like to speak briefly about the stabilization of the hydraulic system and then consider in more detail the design of the overall loop.

Block Diagram

n = vertical acceleration
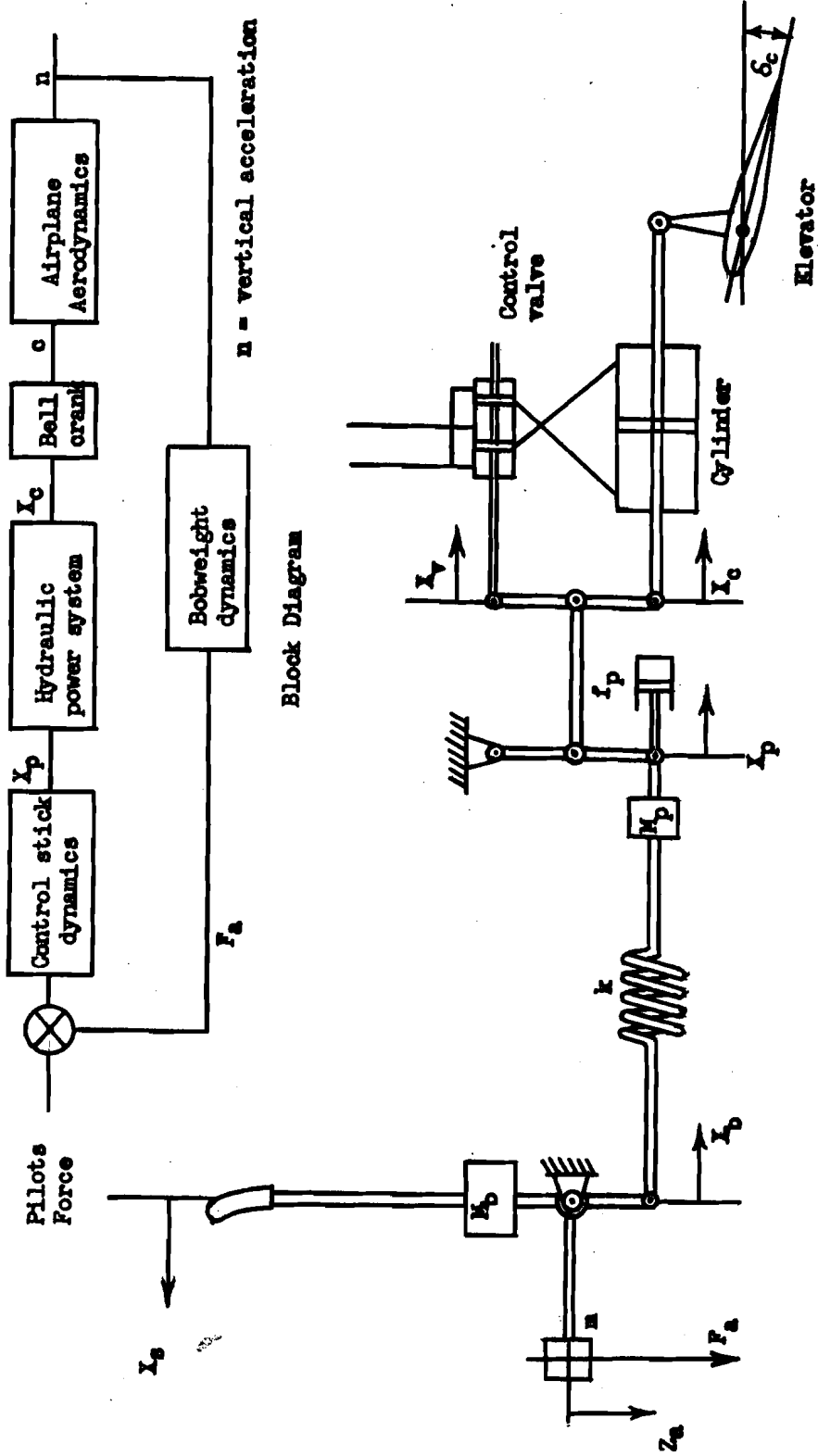
Schematic of Airplane Control System
Fig. 1

AERODYNAMIC DERIVATIVES FROM NACA TN. 2275

$$\frac{\partial C_M}{\partial u'} = 0.15$$

$$\tau = \frac{M}{\rho s V} = 0.97$$

$$\frac{\partial C_M}{\partial \delta} = -0.63$$

$$\left(C_{T_o} + \frac{\partial C_L}{\partial \alpha}\right) = 5.3 \qquad \frac{\partial C_M}{\partial \theta} = -0.034 \qquad \left(2C_{D_o} - 2C_{T_o} + \frac{\partial C_D}{\partial u'}\right) = 0.55$$

$$\left(2C_{L_o} + \frac{\partial C_L}{\partial u'}\right) = 0.3 \qquad \left(\frac{\partial C_D}{\partial \alpha} - C_{L_o}\right) = 0.16 \qquad \frac{\partial C_M}{\partial \alpha} = -0.64$$

$$C_{L_o} = .069 \qquad \left(\frac{1}{\tau^2}\frac{\partial C_M}{\partial \theta} - 2x'\right) = -0.12$$

$$\frac{\partial C_M}{\partial \alpha} = -0.016$$

$$\left(C_{T_o} + \frac{\partial C_L}{\partial \alpha}\right)\alpha + 2\tau s(\alpha - \theta) + \left(2C_{L_o} + \frac{\partial C_L}{\partial u'}\right)u' = 0$$

$$\left(\frac{\partial C_D}{\partial \alpha} - C_{L_o}\right)\alpha + C_{L_o}\theta + \left(2C_{D_o} - 2C_{T_o} + \frac{\partial C_D}{\partial u'}\right)u' + 2\tau s u' = 0$$

$$\frac{\partial C_M}{\partial \alpha}\alpha + \frac{\partial C_M}{\partial \alpha}s\alpha + \frac{\partial C_M}{\partial \theta}s\theta + \left(\frac{1}{\tau^2}\frac{\partial C_M}{\partial \theta} - 2x'\right)\tau^2 s^2\theta + \frac{\partial C_M}{\partial u'}u' = \frac{\partial C_M}{\partial \delta}\delta$$

$$\frac{u'}{\delta} = \frac{U s(\alpha - \theta)}{\delta} = \frac{150 U s(s + .28)}{(s^2 + .31s + .025)(s^2 + 7.1s + 63)}$$

$$\frac{150 U}{s^2 + 7.1s + 63}$$

Horizontal

U = avg forward velocity
u = perturbation forward velocity
u' = u/U
α = w/U

Mach No. = .85
at 10000' altitude

Reference Axes for Airplane Aerodynamics
Fig. 2

## Dynamics of Pilot's Stick System

$$ng = \left\{ \frac{k}{2m} - \left[ \left( \frac{M_b}{2m} + 2 \right) s^2 + \frac{k}{2m} \right] \left[ \frac{M_p}{k} s^2 + \frac{f_p}{k} s + 1 \right] \right\} x_p$$

$M_b = 4$ slugs $\quad m = 2$ slugs $\quad M_p = 0.2$ slugs

$k = 10^4$ lbs/ft $\quad f_p = 100 \frac{lb\ sec}{ft}$

$$\frac{x_p}{ng} = -\frac{16100}{s(s^3 + 500s^2 + 1.9 \times 10^4 s + 4 \times 10^5)} \longrightarrow \frac{-0.33}{s(s + 8.2)}$$
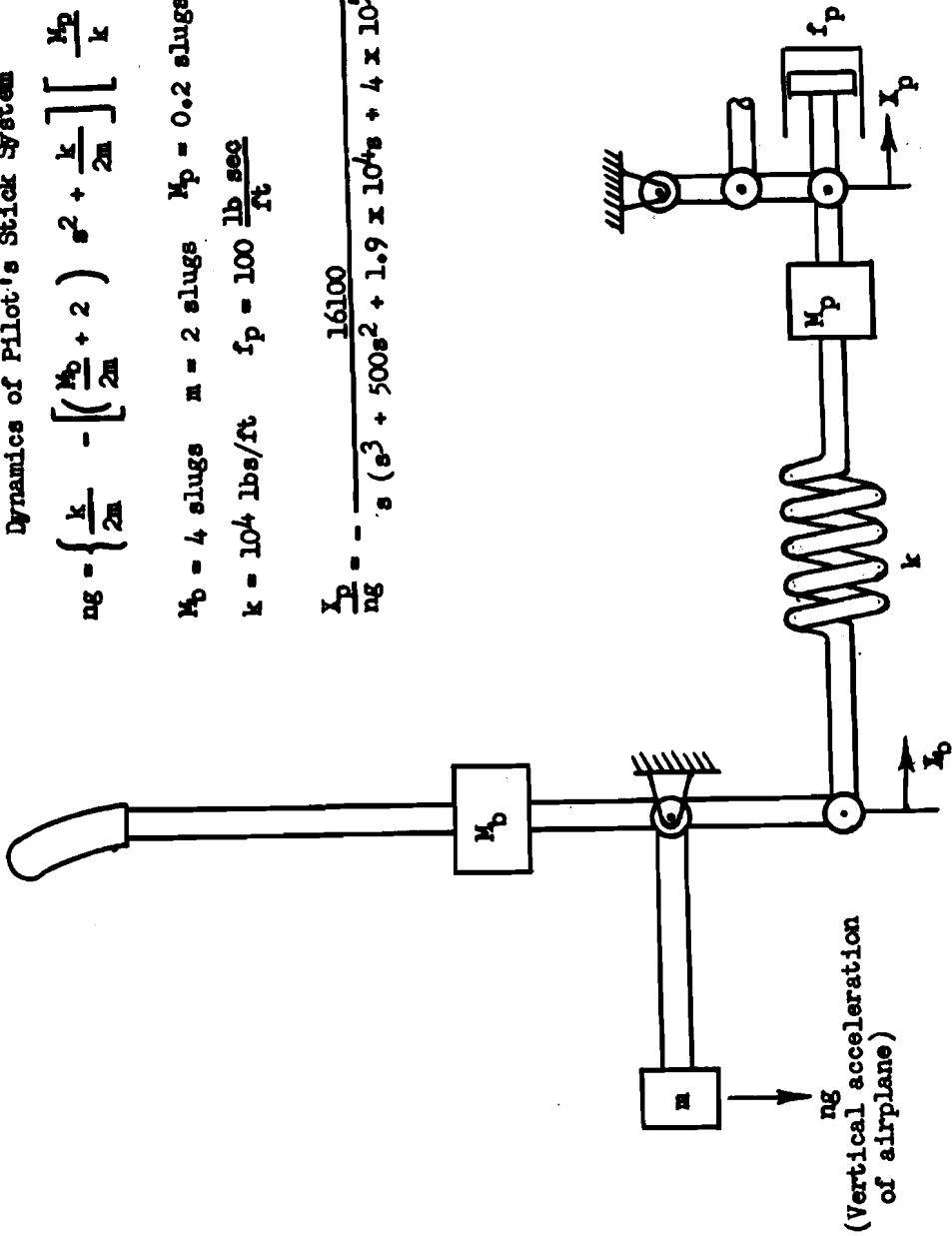


Mechanical Part of Control System
Fig. 3

ng
(Vertical acceleration of airplane)

$$(M_c s^2 + f_c s + k_c) X_c = PA \qquad X_v = K_Q Q$$

$$\frac{Q}{A} = \frac{PA}{k_B} s + X_c s \qquad X_c = \delta_c$$

$$\frac{X_c}{X_v} = \frac{2.4 \times 10^6}{s(s^2 + 30s + 30000)}$$

Q = oil flow

To pressure

To reservoir
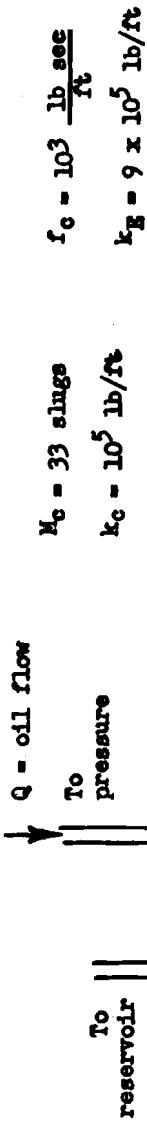
$M_c = 33$ slugs

$k_c = 10^5$ lb/ft

$f_c = 10^3 \dfrac{lb \ sec}{ft}$

$k_B = 9 \times 10^5$ lb/ft

$M_c$ = effective mass of elevators

$K_c$ = Aerodynamic force spring rate

$f_c$ = friction factor

Control valve

Piston area - A

$X_v$

$X_c$

Schematic of Hydraulic System
Fig. 4

The hydraulic system itself is a high-gain feedback system. The load parameters of the hydraulic system are the effective mass of the elevators, the aerodynamic spring rate and the damping, both the aerodynamical damping and that associated with the main power piston. In addition, the compressibility of the oil acts essentially in shunt with the main load, since the flow of oil can go either into compression of the oil or into motion of the main piston and control surface. Up to reasonably high frequencies, typically in the order of magnitude of 15 cps or above, the open-loop hydraulic system integrates, or, if we look at it from the frequency-response standpoint, the gain drops off inversely proportional to frequency. As we reach the frequency at which resonance occurs between the oil compressibility and the load, the output tends to increase. In other words, in this band of frequencies the compressibility effect is such that it tends to increase the motion of the main piston. When the main piston is moving to the right, for example, the oil in the left cylinder is expanding, tending to give the piston motion an extra push. This resonance phenomena is very lightly damped due to the low frictional losses in the system. When the hydraulic loop is closed, through the input linkage, the system will ordinarily oscillate with an amplitude driving the system into the nonlinear region of oscillation. In certain cases, these nonlinearities, inherently present in the system, or the frictional losses which we have neglected tend to stabilize the system, but the relative stability is poor.

This resonance phenomena, and the consequent instability or poor relative stability occurs at such a high frequency compared to the significant frequencies of the remainder of the overall aerodynamical system, it does not appear troublesome on the surface. The main difficulties arise because these frequencies are, however, of the same order of magnitude as the flutter frequencies of the aircraft. The coupling between the flutter system and the hydraulic and control system may cause undesirable amplification of the flutter amplitudes.

This coupling between the unstable hydraulic system and the flutter system and the resulting tendency to increase flutter troubles can be circumvented in either of two ways. First, we might simply cut off the hydraulic system at a frequency much lower than the band of frequencies of significance in flutter phenomena. Secondly, we might try to increase the relative stability of the hydraulic system while maintaining the high low-frequency gain. The first solution is certainly the simpler. The principal disadvantage of this method of cutting off the hydraulic system at low frequencies is the resultant sluggish response of the overall aircraft system, or even of the system from the stick to the control surface. This relationship between the bandwidth and the time delay or time of the transient response is nothing quantitative, but in general it can be said that, if the system is suitably damped so that there is not undesirable overshoot in the transient response, the time required for the system to respond to a step function input and essentially reach the steady state is inversely proportional to the bandwidth. In particular, if the bandwidth is one cps, as an example, the system will respond to a transient input in something like one-half to one

second, at least to the proper order of magnitude. Thus, if we attempt
to rid ourselves of the trouble with the relative or absolute instability
of the hydraulic system by cutting down the bandwidth, we soon reach a
point where the time of response of this part of the overall system becomes
undesirably long. In one sense, this is indeed an unfortunate circumstance,
since the bandwidth of this part of the system can simply be reduced by
cutting down the gain, the bandwidth being roughly proportional to the gain
over the range of frequencies of interest to us.

The second alternative for eliminating the undesirable effects of
coupling between two highly underdamped systems--the flutter system and
the hydraulic system--involves stabilization of the hydraulic system while
maintaining the high gain essential for fast response. The diagram of
figure 5 indicates the difficulties involved here. As it now stands, the
hydraulic system is characteristied by a transfer function--the Laplace
transform of the ratio of the output over the input--with three poles--
one at the origin, and the other two a conjugate complex pair very close
to the $j\omega$-axis. If we use the root-locus method of analysis we can see
at once the effect of closing the loop with varying amounts of gain. In
particular, we study what happens to the poles of the closed-loop transfer
function of the hydraulic system as the gain is increased. For very low
values of gain, the poles of the closed-loop system function are identical
with those of the open-loop transfer function. As the gain is increased,
the poles of the closed-loop system function move toward infinity, the
location of all the zeros of the open-loop function. The particular paths
taken by these poles as the gain is varied are shown in Fig. 6: one moves
out from the origin along the negative-real axis, the other two move away
from the conjugate complex pair of poles over into the right-half plane.
For a relatively low value of gain, these poles have crossed into the right-
half plane, indicating that the closed-loop system is unstable.

How can such a system be stabilized? There are a variety of ways, in
terms of the pole-zero loci, and then a number of ways in which these desired
changes may be instrumented. We consider only one general method in any
detail. The fundamental difficulty is the proximity of the conjugate poles
to the $j\omega$ axis. This arises because of the very sharp resonance between
the compressibility of the oil and the mechanical and aerodynamical load.
This resonance can be made less sharp, and also incidentally moved to a lower
frequency, if the compressibility of the oil can be effectively isolated from
the load--in other words, if at the same time the expanding oil is giving the
piston an extra push, there exists an alternate network which is absorbing
this extra effective flow. One possible system for doing this is shown in
Fig. 7.

Here in Fig. 7 both the hydraulic-mechanical system and the equivalent
electrical network are shown. In the equivalent circuit, the load corresponds
to the series resonant circuit made up of $L_c$, $R_c$, and $C_c$, representing
respectively the mass, damping, and compliance of the aerodynamical and
mechanical load. The oil compressibility is represented by the parallelling
condenser C. The resonance phenomena, speaking in electrical terms, is
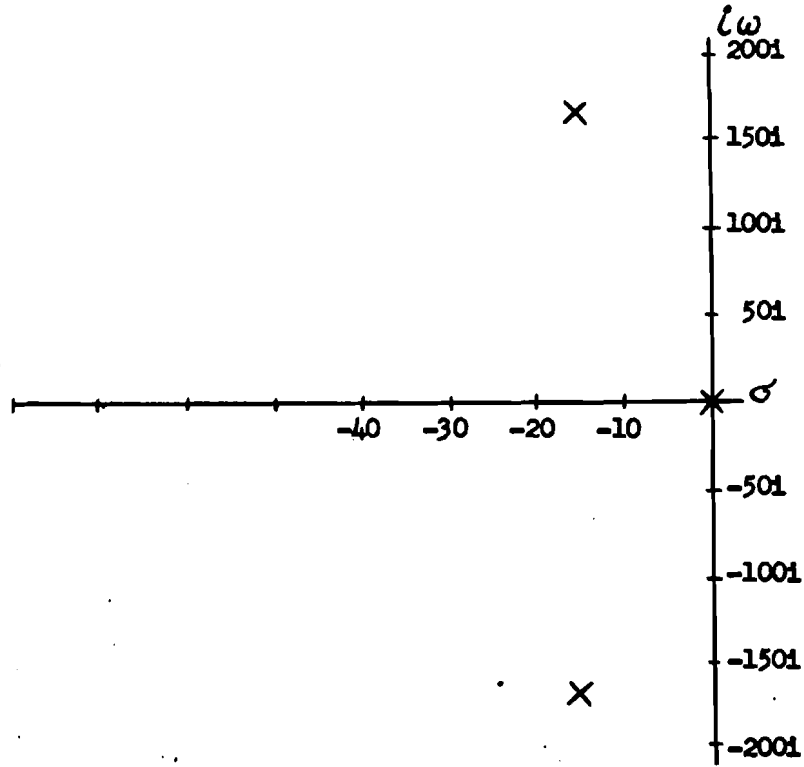
Poles of Open-Loop Transfer Function
of Uncompensated Hydraulic System
Fig. 5
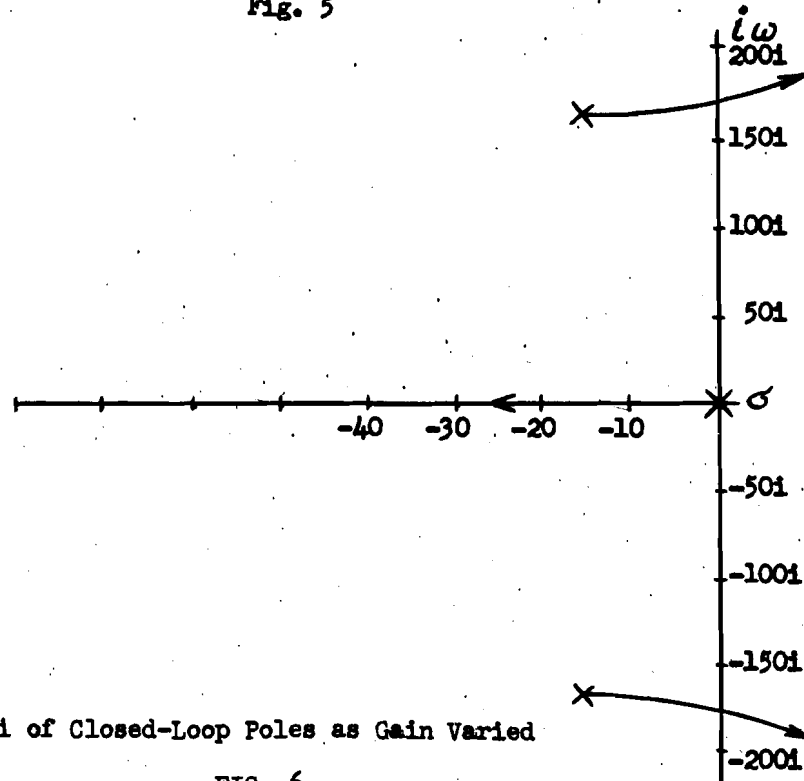


Loci of Closed-Loop Poles as Gain Varied

FIG. 6

Main Power Cylinder

$$L_n = \frac{M_n}{A}$$
$$C_n = \frac{A^2}{K_n} \qquad C = \frac{A^2}{K_E}$$
$$R_n = \frac{f_n}{A^2} \qquad \text{(oil compress.)}$$

$$L_C = \frac{M_C}{A^2}$$
$$C_C = \frac{A^2}{K_C}$$
$$R_C = \frac{f_C}{A^2}$$

Cylinder output impedance parameters

Equivalent Electric Circuit

Damper - $f_n$

Compensating System

Spring Rate - $K_n$    Mass - $M_n$
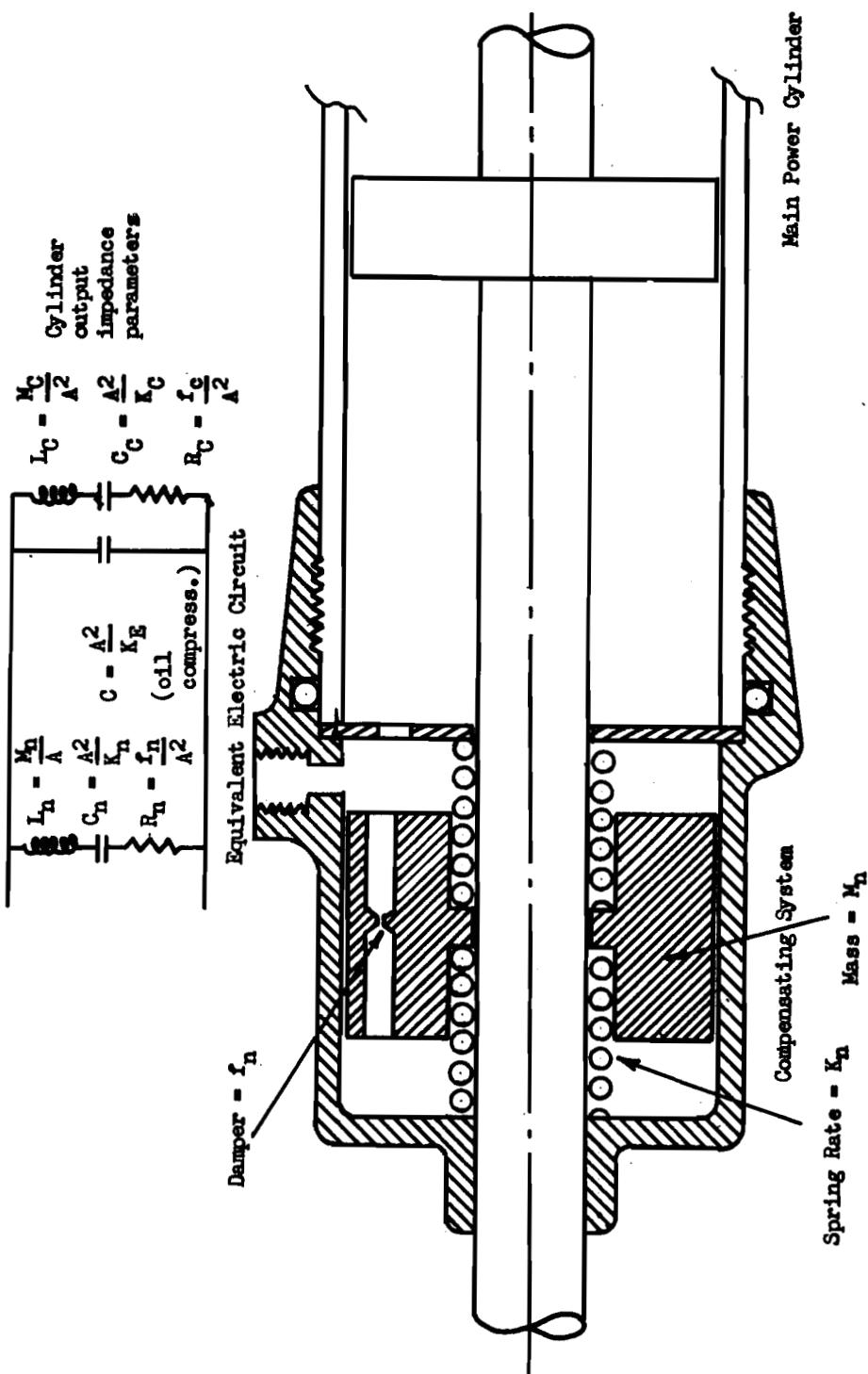
Suitable Element Values From Our Example

$$\frac{k_n}{M_n} = 3000 \qquad k_n = 1000 \text{ #/ft}$$

$$\frac{f_n}{M_n} = 110 \qquad \text{or} \quad f_n = 330 \text{ #sec/ft}$$

$$M_n = 1/3 \text{ slug}$$

Cross Section of Hydraulic Compensating System
Fig. 7

essentially a parallel resonance of the compressibility condenser and
the load circuit. At resonance there is a large circulating current between
the two branches—corresponding in the actual system to a large output-
shaft velocity due to the alternate expansion and compression of the oil,
a shaft velocity which may be many times that due to the actual quantity
of oil flowing through the control valve. One possible method of compensa-
tion involves addition of a system such as that shown in Fig. 7. In the end
of the main cylinder is inserted a mechanical-hydraulic resonant circuit,
similar to that of the load. This circuit is essentially tuned to the same
frequency as the parallel resonance of the oil compressibility and the actual
hydraulic system load. At this frequency, the motion of this auxiliary system
absorbs the equivalent flow due to the compression and expansion of the oil.
The parameters of this compensation system are chosen such that the overall
circuit, including, for example, in the electrical circuit, all three parallel
arms, resonates at a frequency much higher than the original resonance of the
oil compressibility and the load.

More explicity, the effects of this compensation scheme on the significant
poles and zeros of the open-loop and closed-loop transfer functions is shown
on the diagram of Fig. 8. The poles and zeros of the open-loop transfer
function of the hydraulic system with compensation are determined as shown
in this figure and using the root-locus method. These poles are located at
points in the complex frequency plane determined by plotting the poles due
to the actual load and the zeros determined by the impedance of the compen-
sating network. In other words, the zeros at $-50$ and $-60$ are the points at
which the impedance of the compensation network goes to zero. The poles at
$-15 \pm 50i$ are the points at which the impedance of the load goes to zero.
It can be readily shown that the poles of the open-loop transfer function
of the overall hydraulic system with this compensation added occur on the
loci for this configuration. The particular points on the loci are determined
by the ratio of the spring constant of the compensation network, $k_n$, and the
aerodynamical spring constant, $k_c$. Since ordinarily $k_n$ is much less than $k_c$,
these poles will lie very close to $-15 \pm 50i$, the poles of the load alone.
Consequently, the open-loop transfer function of the system with the compen-
sation added has zeros at $-50$ and $-60$, poles at about $-15 \pm 50i$ and at the origin,
and a pair of poles at a very high frequency. The poles of the closed-loop
system function are then found at once. The loci are shown in Fig. 9, with
the actual closed-loop pole positions shown for a velocity constant of 80.

With the hydraulic system stabilized by any logical scheme—possibly
merely by the addition of friction either intentional or unintentional, we
proceed to the primary design problem, the design of the overall loop. We
continue to consider the general block diagram shown in Fig. 1, consisting
of the control stick dynamics, hydraulic power system, bell crank, aero-
dynamics and bobweight dynamics. We are now dealing with a hydraulic system
which has been made stable, and an airplane with known aerodynamical charac-
teristics. Our problem is to select suitable systems for the control stick
dynamics and the feedback system, and to modify the hydraulic system in such
a way that we realize a system with satisfactory stability and control.

Zeros introduced by resonance
of the stabilization system
Poles introduced by the load characteristics
Poles (at over 1000 rad/sec) representing
resonance of stabilization system with
compressibility and load not shown

O Zeros
X Poles
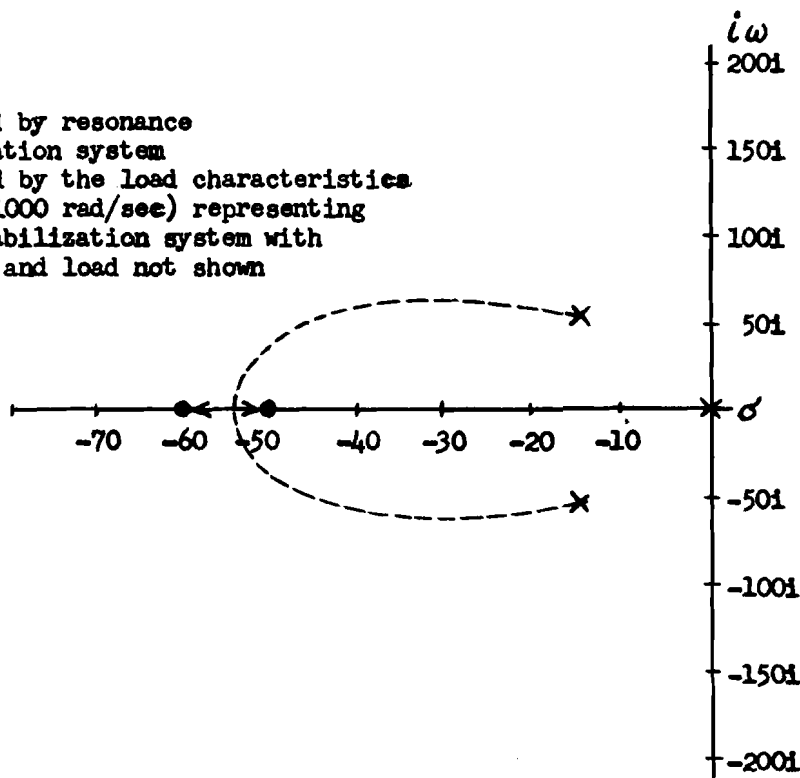
Determination of Open-Loop Poles with Compensation
Fig. 8

● Closed-loop pole
positions for $K_V = 80$

54.9
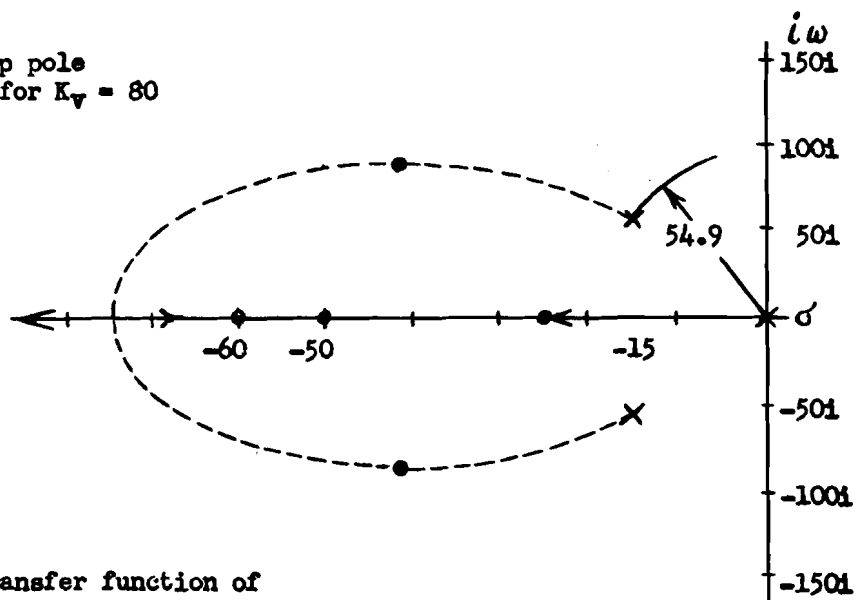
Open-loop transfer function of
the stabilized system

$$\frac{X_O}{X_V} \approx \frac{80\ (s + 50\ )\ (s + 60\ )}{s\ (s^2 + 30s + 3000\ )}$$

Closed-Loop Poles for Compensated System
Fig. 9

By way of introduction to this problem, I would like to revert for
a moment to some of the ideas expressed in the excellent paper we heard
on Tuesday morning by Mr. Andrews of Hughes Aircraft and presented by
Mr. Turner. In this paper it was rather forcibly pointed out that we
are rapidly reaching the point where we must design our power boost
control system to meet quantitative specifications concerning both
stability and control. I like to think of the situation in something
like the following light, with a very simple analogy. I picture the
control system designer in a position somewhat analogous to a sixteen-
year old boy in a baseball game. As the game starts, the other boys are
all under ten years old; the mere presence of our sixteen-year old is enough
to throw fear into the opposition, just as in the early years of power boost
systems, the mere presence of the control system designer and a little
imagination on his part solved the problems. As the game progresses, however,
older boys arrive. Our sixteen-year-old has to work to get his base hits.
He begins to look around for a better bat and tools; he starts to consider
using a little strategy instead of the previous brute-force tactics. In an
analogous manner, the control systems engineer starts to adopt some of the
servomechanism theory--the use of Nyquist diagrams that have been mentioned
several times here during the past few days, for example. But unfortunately,
the game has not yet stabilized. For, approaching our ballfield are a half
dozen professional ball players, eager to get into the game. Our sixteen-
year old is going to have to call on all his ability if he is to hold his
own. In our immediate problem, we see these professional ball players as
the problems associated with our planes flying at a Mach number of 1.5.
If we are to design successful power-boost systems and tactically-capable
aircraft operating at these high speeds, it seems imperative to us at Purdue
that all available knowledge be brought to bear on the problem. We feel
that in a few years, when we are confronted with the design of the power
boost systems for these high-speed aircraft, there will be no excuse for
us not having a understanding of the problem and a general idea of a suitable
approach to the solutions.

What specifically are the problems associated with the design of a high-
performance power-boost system? They are many in number. We wish to mention
only a few of them today in any detail. The problem we have heard most about
at this meeting is the design of an appropriate artificial feel system. I
feel, however, that this is only one of the basic problems. It has received
considerable attention here during the past few days principally because it
is a problem which is already confronting the engineer. Of a perhaps more
basic nature, however, are the twin problems of stability and control. Indeed,
the satisfactory solution of the artificial feel problem can only be arrived
at in conjunction with at least partial solutions to the stability and control
problems, for the artificial feel system is an integral part of the overall
loop which does determine both the relative stability and the control character-
istics.

What essentially are the problems associated with control and stability?
The most pressing problem, it seems to me, is the development of a more

explicit set of specifications—or a more quantitative description of the behavior we desire from our system. Some of you may say that quantitative specifications can not be written—instead we must be satisfied with such specifications as the statement—The airplane must fly satisfactorily. This field of engineering is not alone in this difficulty of writing a quantitative set of specifications. The servomechanisms field in general is plagued by the same difficulties. I have heard many times the statement— We want a real fast servo that has practically no error—or something equally vague. If there is to be any logic to the system design, the first step involves making this specification quantitative. Indeed, when this is done, the problem is half solved.

In particular, what specifications are appropriate to the aircraft control problem? We consider still, for the sake of explicitness, only the longitudinal control system. In addition, we consider only the performance specifications, taking the word performance in its common, narrow meaning, and excluding such factors as the maximum allowable acceleration, etc. We consider only specifications governing the stability and dynamic performance in general of the aircraft under small deflections of the control surface.

The specifications, it seems to me, should include at least the following quantities: the relative damping of the overall aircraft system, the damped (or undamped) natural frequencies of oscillation, the low-frequency gain of the system, and the time lags in the various parts of the system. The first two quantities, relative damping and oscillation frequency, determine the relative stability. The third quantity, the low-frequency gain, determines, essentially, the effectiveness of the feedback, the ability of the system to continuously calibrate itself, reduce the effect of nonlinearities, and control the effect of corrupting signals entering the system (for example, wind gusts). The last quantity, the time lag in the various system components, measures the speed of response of our aircraft.

Other quantities will of course have to be specified eventually, in the complete problem. For example, we are interested not only in the low-frequency response of the system to wind gusts, but also the overshoot and settling time associated with the response to a gust of wind. However, the above four parameters will give us a basis for the remainder of this paper.

On the basis of specifications of this sort, at least the preliminary design of the system can be carried out on a logical basis. The discussion here is somewhat difficult, because the two aspects of control and stability can not be divorced, but I shall try to indicate the general trend of a method which we think is reasonable for design. First, let us consider the stability problem. Why does the system basically tend toward instability? And why does the stability problem become more difficult as the speed of the aircraft increases. In the very simple system we are considering here (shown in Fig. 1) significant phase lags in the system are introduced from two

150

sections, the aerodynamics and the control stick dynamics. If the phugoid
motion and very low frequency behavior is neglected, the aerodynamics
behaves essentially as a second-order system, with a transfer function
of the form shown in Fig. 1. The relative damping ratio associated with
the conjugate poles here is in our example about 0.4. At high speeds,
this relative damping ratio could be expected to go as low as 0.1 or less.
Additional phase lag is introduced in the control stick dynamics, the
mechanical system from the control stick to the input to the hydraulic
system. The system we are considering here is shown in Fig. 3 and has
an approximate transfer function of the form:

$$-\frac{0.35}{S(S+8.2)}$$

The overall open-loop system then has a transfer function proportional
to the product of these two individual functions.

$$\frac{K}{S(S+8.2)(S^2+7.15+63)}$$

The corresponding pole configuration for the open-loop system is of the
form shown in Fig. 10.

We now consider what happens as we close the loop and bring up the loop
gain from a very low value. The poles of the closed-loop transfer function
move in the manner shown in Fig. 11. For relatively low values of loop gain,
the closed-loop system is unstable. How can this system be stabilized? In
particular, how can the system be stabilized at a value of loop gain which
is sufficiently high to insure that we have adequate control characteristics?
The first and most obvious method is to introduce a device to cut the system
off, at least part way, at very low frequencies—a device which the electronic
engineer would term integral control. Such a device necessarily tends, as
we saw earlier, however, to decrease the speed of response of the system. We
have felt that the primary job of any stabilization that is introduced should
be to force the airplane to respond more rapidly than the aerodynamical
coefficients would ordinarily allow. Certainly, at least, the stabilization
system should not make the system more sluggish.

Considering this pole configuration, one possibility is immediately
evident. We might attempt to move the pole due to the stick dynamics, now
at-8.2, so far out into the left-half plane that the system essentially
reduces to a third-order rather than a fourth-order system. This can be
readily accomplished as shown in Fig. 11 simply by an increase in the value
of the damping coefficient $f_p$. There are two difficulties that arise at
once however, with such a scheme of partial stabilization. First, the force
required of the pilot to move the stick at a constant velocity, when he is
moving essentially against this damper, increases intolerably. Secondly,
the time lag between the stick and the output of the hydraulic system
increases proportional to this damping coefficient. In particular, this
time lag, assuming the hydraulic system acts instantaneously, is given by
the ratio of the damping coefficient, $f_p$, to the spring constant of the
push-rod, k, as is shown in appendix A. Thus, about the best we can do
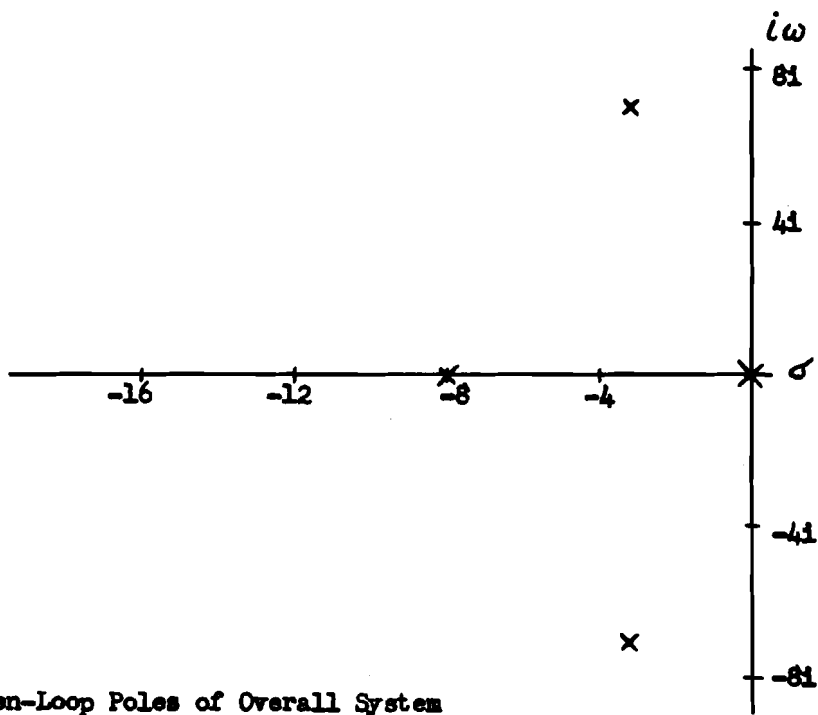
Open-Loop Poles of Overall System
Fig. 10
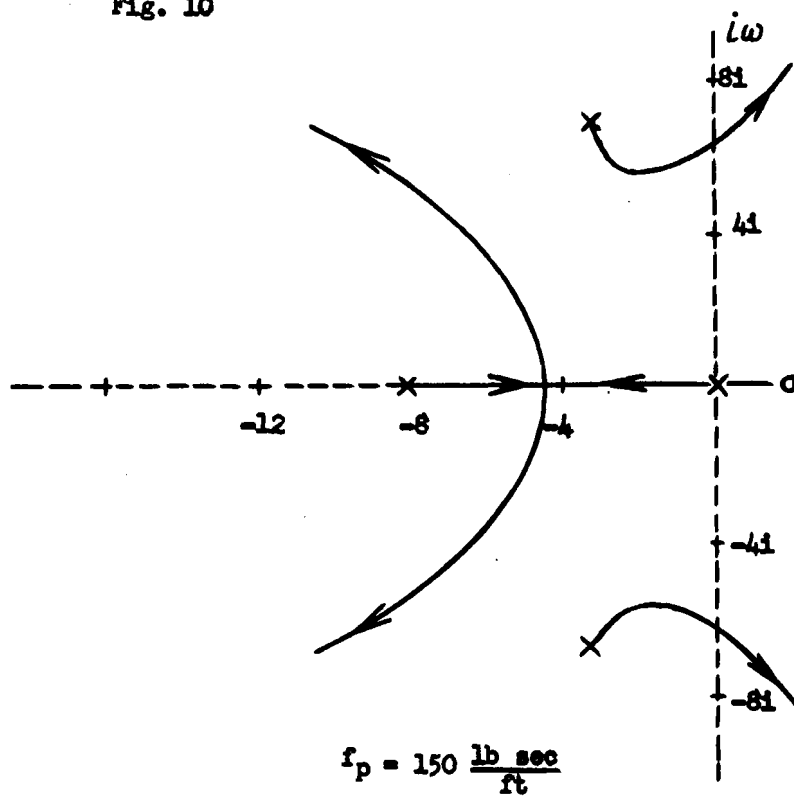


$f_p = 150 \frac{lb \cdot sec}{ft}$

Loci for Uncompensated Overall System
Fig. 11

152

here is to make the push-rod as stiff as possible, and increase the damping $f_p$ as much as permissible and then live with these components.

It appears then that in the absence of the ability to effect any remarkable improvements in system components, the stabilization of our system with the simultaneous realization of high performance characteristics demands the introduction of additional components. We ask ourselves what distortion of the pole configuration we now have for the open-loop system would result in desirable characteristics. One particularly simple configuration is shown in Fig. 13. We leave the two poles due to the stick dynamics at the origin and -8.2, but move the conjugate complex poles due to the aerodynamics either onto the negative-real axis or at least well out into the left-half plane. Now what happens as we close the loop and increase the gain? The poles way out to the left are of little interest to us. The important loci are those stemming from the two poles on the negative-real axis and close to the origin. At low frequencies, these poles move as a function of gain in the manner shown in Fig. 14. By the addition of a zero at -10 and the moving of all other poles way out into the left-half plane we have kidded these two poles into thinking we have a configuration of the form shown in Fig. 15. It is not until we reach reasonably large values of loop gain and fairly high frequencies, that these two poles realize the deception and bend over toward the right-half plane. Then if we keep the gain at a value corresponding to these poles located at the points A and A', we have a closed-loop system, an overall aerodynamical system, which behaves essentially as though it had this pole-zero configuration. The response is characteristized by one pair of conjugate complex poles at a reasonable damping ratio and a dipole on the negative real axis. The transient response will be roughly of the shown in Fig. 16.

Essentially the same results can be achieved by a slightly different, and basically more logical approach. Suppose we simply start off by saying that we want a transient response of the form shown in Fig. 16. Let us write the overall system function, the Laplace transform of this transient response. We denote this desired closed-loop transfer function as $H(s)$. From this $H(s)$ we determine the required open-loop transfer function, which we might call $p/q$, the ratio of two polynomials in s. This open-loop transfer function, $p/q$, is related to $H(s)$ as shown at the bottom of Fig. 17. p and q, the numerator and denominator polynomials of the open-loop transfer function are readily determined from this relationship. p is simply the numerator of $H(s)$. q is simply the denominator of $H(s)$ minus the numerator, and can be determined in factored form by a simple graphical subtraction, plotting the polynomials for negative-real values of the variable s. A plot of this form is shown above the equations in Fig. 17.

Let us review for a moment. We have said that our fundamental philosophy in the design of the power boost system should be something like the following: We first decide on suitable specifications for our
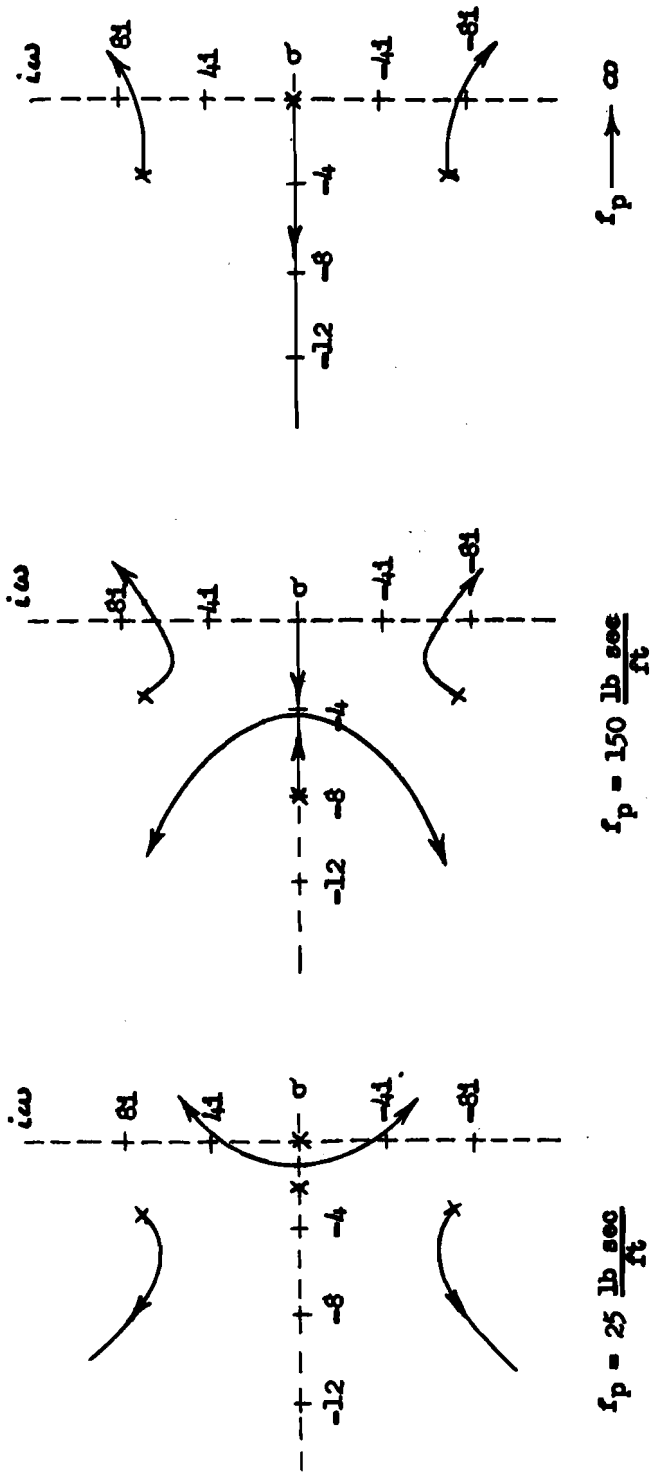
Effect of Variation of Damper $f_p$ on Poles and Zero
of Closed-Loop Transfer Function
Fig. 12

154
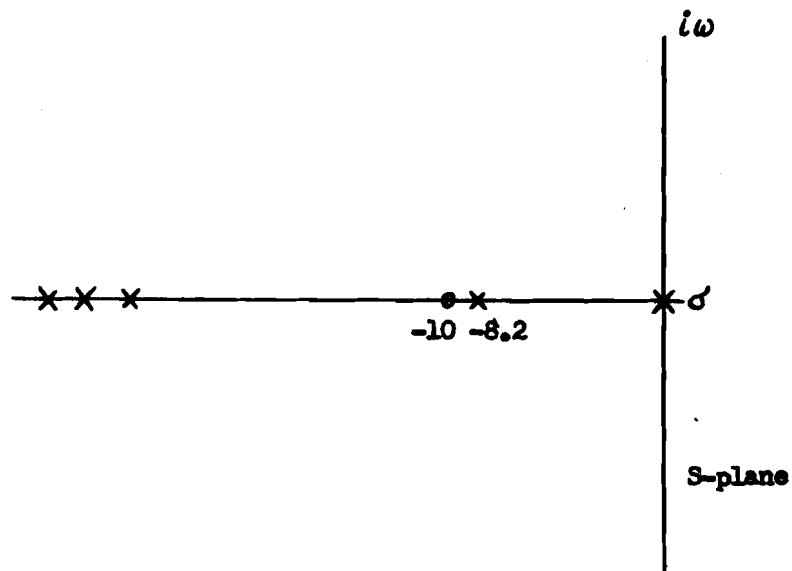


Desirable Open-Loop Pole-Zero Position
Fig. 13
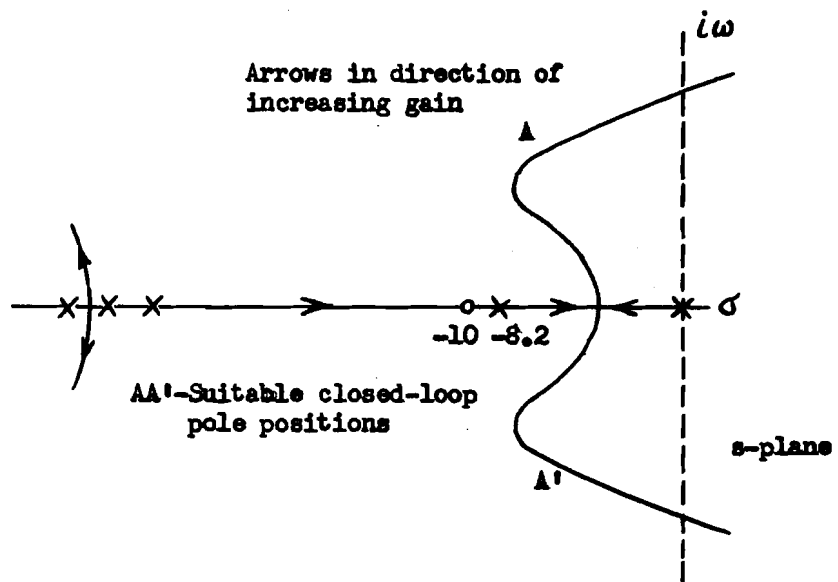


Desirable Open-Loop Pole-Zero Position
and the Effect of Closing the Loop
Fig. 14
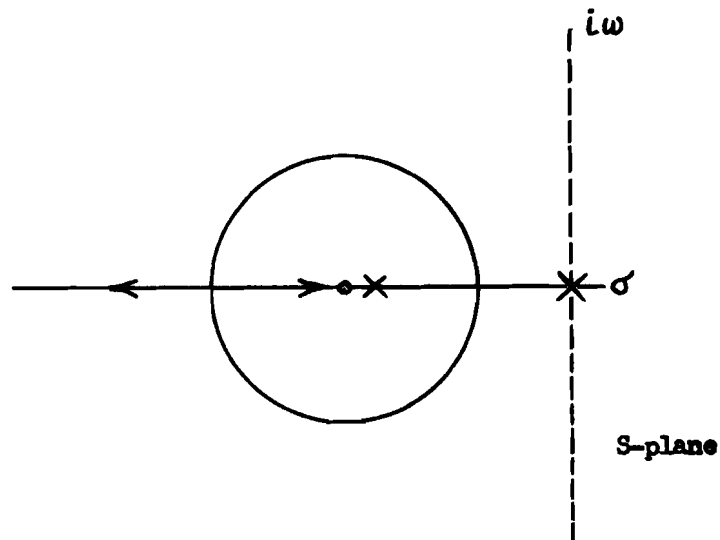
Simplified Configuration Representing
that of Fig. 14 Near the Origin
Fig. 15



$$H(s) = \frac{90.1\ (s+7.1)}{(s^2 + 8s + 64)(s + 10)}$$

$$h(t) = -3.1e^{-10t} + 10.8e^{-4t}\sin (6.9t + 16.9°)$$
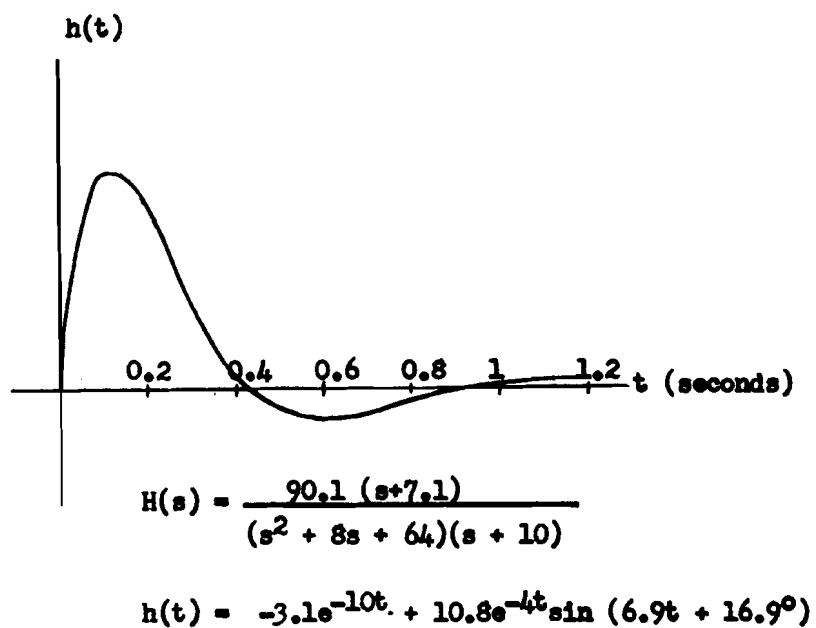
System Response to Impulse
of Pilot Force
Fig. 16
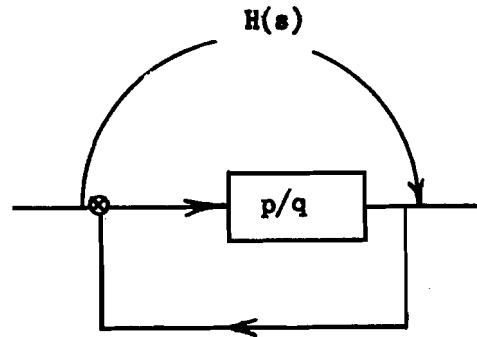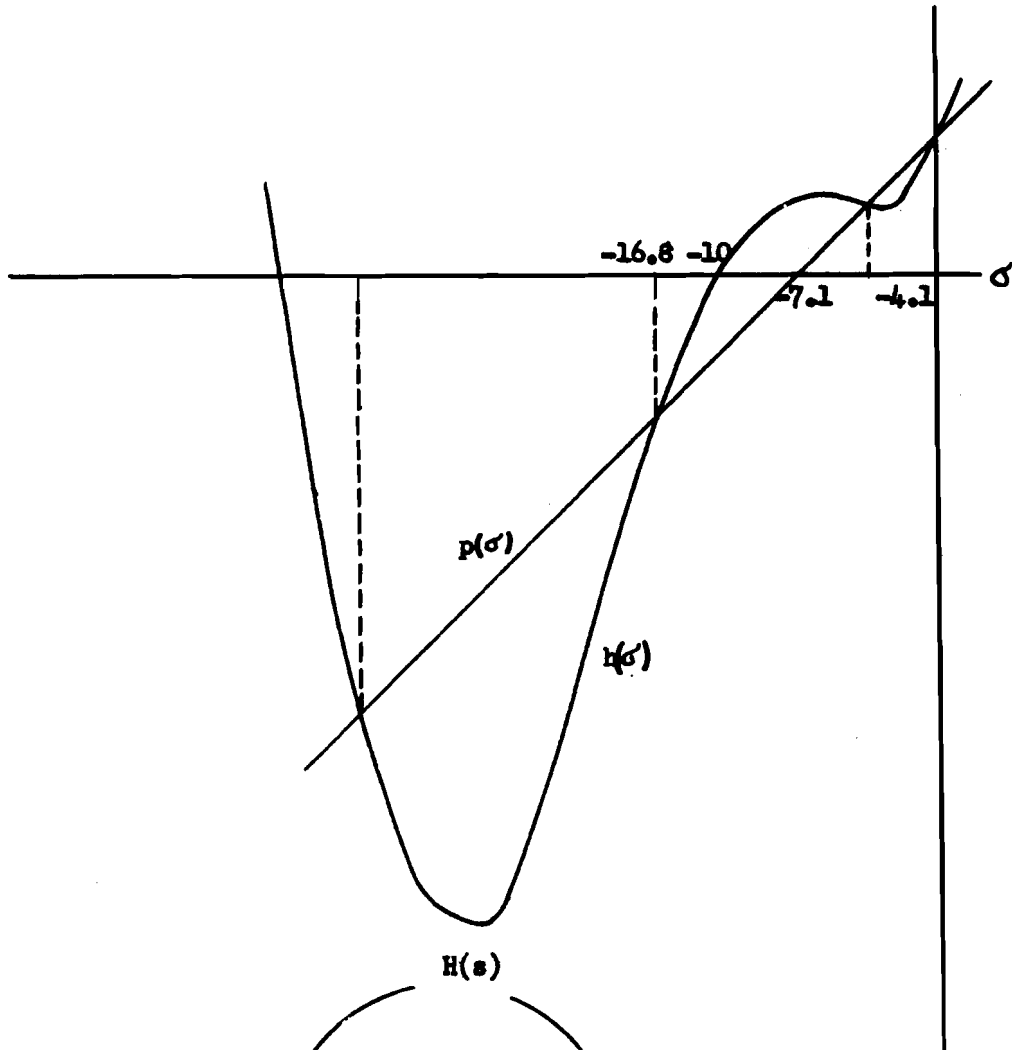
$$H(s) = \frac{p/q}{1 + p/q} = \frac{p}{p + q} = \frac{p(s)}{h(s)}$$

$$q = h - p$$

Determination of Suitable Poles for
Open-Loop Transfer Function
Fig. 17

particular problem. We then choose a transfer function which yields
these specified characteristics. The last step in the design involves
the instrumentation of a system which will yield our desired transfer
function. Several of you will undoubtedly object to this general approach
which we are postulating. The principal objection possibly will be that
we can not in general force our aerodynamical system to behave in any way
we want. We know, for example, that we can not demand an overall system
function of unity in practise. That is, we can not expect to realize a
power-boost control stick motion, with absolutely no time lag. However,
we are obviously being ridiculous in asking for performance of this quality.
Clearly, we are limited in attainable performance by the saturation of the
control surface effectiveness. What our stabilization and equalization
system is doing is anticipating the lags and instability inherent in the
aerodynamics and stick dynamics and attempting to compensate.

Up to this point the design of the system is straightforward, following
lines well established in the servomechanism field. (I of course do not
mean to imply simplicity by the word straightforward). If the control system
is electrical in nature, or at least contains certain electronic components,
the compensation can be conveniently and readily introduced. However, if
the control system is mechanical-hydraulic system, the design of suitable
compensation networks is not as straightforward. The Purdue University group
is now investigating a number of mechanical and hydraulic circuits which look
promising for the accomplishment of this compensation. The design of
compensation networks is made difficult by several factors which can not
readily be expressed analytically, but which are of paramount importance
if the networks are to be of practical value. First, we have felt that any
compensation must be accomplished simply. We do not feel that we can introduce,
for example, a large number of nonlinear circuits or complicated circuits.
Secondly, the synthesis of suitable mechanical-hydraulic networks is complicated
by the requirements on the allowable forces against which the pilot will have
to work. In other words, networks introduced in that section of the system
which we have called the stick dynamics must not lead to undesirable forces
referred back to the stick handle. Thirdly, it is very difficult, if not
impossible, to anticipate difficulties with distributed friction, etc. In
the last analysis, the propriety of any system must depend upon experimental
tests. At this time, we have not yet reached the point where we are able to
present experimental data.

The basic type of compensation which seems to be most effective theoret-
ically is a lead form of network. A generalized form of transfer function
for the desired compensation network would be of the form:

$$\frac{s^2 + 2\zeta\omega_n s + \omega_n^2}{s^2 + as + b^2} \qquad \omega_n < b$$

We have spent some time investigating the possibility of instrumenting
mechanically and hydraulically a transfer function of this type and feel
that a twin-T system of the form shown on Fig. 18 holds considerable promise.
The mechanical schematic is shown at the top of the page and a sketch of
the system at the bottom. Referring to the sketch, the top half of the
twin-T is realized by the center two springs and the orifice, the bottom
half of the twin-T by the two end orifices and springs and the hydraulic

158
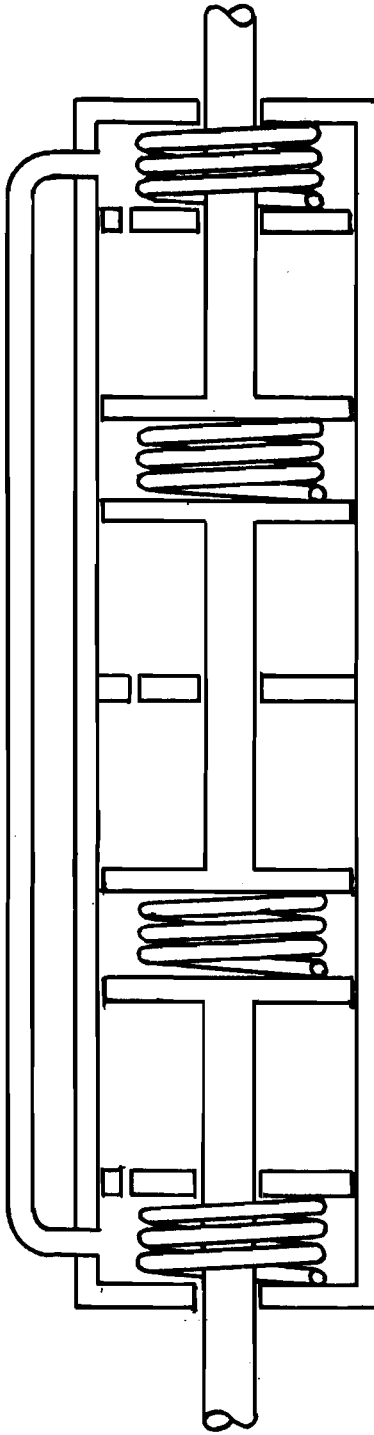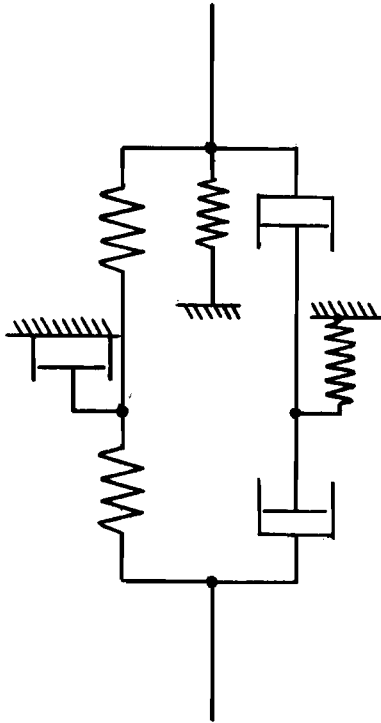


Schematic of Twin Tee Compensating System
Fig. 18

coupling between the two ends and through the line shown above the main part of the figure. The output spring, shown in the schematic is not shown on the figure at the bottom of the page.

There are a number of other systems which accomplish essentially the same results, but the difficulty of realizing a decent range of element values has led us to consider a scheme of this sort in some detail. For the stabilization of the control system with the numerical parameter values used as an example during this paper, the spring and damper values for the twin-T shown here come out to be of order of magnitude yielding time constants of about 1/10 second. Specific values depend on the location in the system. The element values can be readily determined using the methods of network synthesis well known in electrical engineering.

Clearly a fundamental question is the proper location of this twin-T or any other form of compensation network in the overall loop. The answer to this question depends on a number of theoretical factors (e.g., the effect of loading at either end of the network on its characteristics, the effect of the loading on the rest of the system produced by the network, etc.) as well as such practical factors as space availability, effect of failure, etc. One possible scheme is shown in Figure 19, where the compensation network is inserted at the input to the hydraulic system.

Two comments are appropriate at this time concerning the stabilization and compensation concepts discussed in the past few minutes. First, it is clear now, I hope, why we feel that the entire question of artificial feel is one which can not be divorced from the stability and control questions. In the airplanes which have been discussed during the past few days, the performance characteristics have been sufficiently low, in many cases, so that the artificial feel system presented a more or less isolated problem. However, as the satisfaction of performance specifications becomes more difficult (and we do not envision this as being too far in the future) the artificial feel system and the characteristics of the pilot (or at least some generalized description of these characteristics) must be of basic importance in determining system stability and controllability.

If the stability and controllability problems are to be resolved without unnecessary difficulties, the feel system must be designed as part of the overall loop.

The second comment I would like to make at this time concerns the effect of nonlinearities in the various system components on the stabilization procedures we have discussed. These nonlinearities are, as I see it, of two general types--the nonlinearities of specific hardware, as the hydraulic system. We feel that nonlinearities of this type can be controlled and kept small enough to make a linear analysis and synthesis at least a good first order approximation. In the last analysis, final adjustment must of course be done experimentally. The second type of nonlinearity is perhaps more troublesome. I refer to the changing aerodynamical coefficients with

System with Compensation
Fig. 19

changing flight conditions. Ideally, one would design dynamic compensation networks, as suggested in some of the earlier talks--compensation networks which would be automatically compensated for changing longitudinal velocity, etc. If the compensation is effected entirely electrically, this dynamic compensation can be approximated fairly well, although the complexity of the instrumentation necessarily is greater than with a linear system. If as we have tried to suggest in the past few moments, the compensation is effected hydraulically and mechanically, dynamic compensation is a more difficult problem. As yet we have done nothing along this line.

I would like to summarize briefly. We feel that the time is rapidly approaching when the stability and controllability problems of design will be of paramount importance. We feel that it is essential that logical design procedures be established in anticipation of these difficulties. Any logical design procedure must proceed from quantitative specifications. It must lead to suitable general networks for accomplishing the compensation. We feel that compensation systems can be determined which will essentially force the airplane to meet the selected performance specifications. The realization of these compensation systems can be accomplished electronically. We also feel that compensation can be effected hydraulically and mechanically. We believe that there is a great deal of work yet to be done in evaluating various hydraulic-mechanical systems for compensation, in studying the effects of various locations of these networks in the overall system, in considering the possibility of using parallel compensation, and in the related problems.

The system I have used throughout this paper as an example of some of these ideas is about as simple a system as one can devise to accomplish even theoretically the desired control. We feel that it is essential that more complex (and realistic) systems be considered from this standpoint of stabilization devices. Any appreciable complication of the system will necessitate going to computer and simulator studies, as the introduction of additional degrees of freedom rapidly places the complexity of the system beyond the bounds of human comprehension. Thus far, we have not done anything appreciable with analog computer studies, as we have felt that intelligent use of computer data required a solid understanding and background in the behavior of simpler systems.

## APPENDIX A

### Interpretation of Specifications in Terms of System Parameters

Specification on low-frequency loop gain:

At low frequencies, open-loop transfer function behaves as $K_v/s$

$K_v$ is directly related to the poles and zeros of the closed-loop transfer function:

If $H(s) = \dfrac{K\,(s+z_1)\,(s+z_2)}{(s+p_1)\,(s+p_2)\,(s^2+2\zeta_1\omega_{n1}s+\omega_{n1}^2)\,(s^2+2\zeta_2\omega_{n2}s+\omega_{n2}^2)}$

$$\frac{1}{K_v} = \frac{1}{p_1} + \frac{1}{p_2} + \frac{2\zeta_1}{\omega_{n1}} + \frac{2\zeta_2}{\omega_{n2}} - \left(\frac{1}{z_1} + \frac{1}{z_2}\right)$$

$$\frac{1}{K_v} = \sum_m \frac{1}{p_m} - \sum_n \frac{1}{z_n}$$

Specification on time lag between stick motion and motion of control surface:

Denote transfer function from stick motion to control surface as:

$$\frac{\delta(s)}{X_s(s)} = J(s)$$

Then with constant velocity input, time lag (steady-state) is:

$$T_{lag} = \frac{J'(0)}{J(0)}$$

If $J(s) = K\dfrac{(s+z_1)\ \cdots\ (s+z_n)}{(s+p_1)\ \cdots\ (s+p_m)}$

$$T_{lag} = \sum_m \frac{1}{p_m} - \sum_n \frac{1}{z_n}$$

with our unstabilized system

$$T_{lag} = \frac{f_p}{k}$$

Specification on stability:

A specification that the short period dynamic oscillation of normal acceleration shall be damped to 0.1 amplitude in one cycle* means that if the response is primarily controlled by one pair of conjugate complex poles, the associated relative damping ratio should be greater than about 0.37.

* U.S. Air Force Specification No. 1815-B

## List of Symbols

| | |
|---|---|
| $A$ | Area of hydraulic jack piston. |
| $C$, $C_c$, $C_n$, $L_c$, $L_n$, $R_c$, $R_n$ | |
| | Parameters in electrical system analogous to hydraulic system with compensation. |
| $f_p$ | Damping coefficient of mechanical linkages. |
| $f_n$ | Damping coefficient of hydraulic system compensator. |
| $f_c$ | Damping factor in hydraulic system load. |
| $F_a$ | Bob weight acceleration force. |
| $g$ | Acceleration of gravity. |
| $H(s)$ | Overall system function |
| $h(s)$ | Denominator polynomial for $H(s)$ |
| $J(s)$ | System function from stick to control surface. |
| $K$ | Gain constant. |
| $k$ | Spring constant of push rod from stick to hydraulic system. |
| $k_c$ | Aerodynamic force spring rate. |
| $k_e$ | Oil compressibility spring rate. |
| $K_Q$ | Hydraulic system control valve gain. |
| $k_n$ | Spring constant of hydraulic system compensation network. |
| $K_v$ | Velocity constant. |
| $m$ | Bob weight mass. |
| $M_p$ | Mechanical linkage mass. |
| $M_b$ | Control column mass. |
| $M_c$ | Effective mass of elevator. |
| $M_n$ | Mass of hydraulic system compensation network. |
| $n$ | Load factor. |
| $P$ | Pressure across hydraulic jack. |
| $P_1$, $P_2$,.. | Negative of poles of transfer functions. |
| $p(s)$ | Numerator polynomial for $H(s)$. |
| $q(s)$ | Denominator polynomial for open loop transfer function. |
| $Q$ | Net rate of flow through hydraulic system control valve. |
| $s$ | Laplace transform variable |
| $t$ | Time |
| $T_{lag}$ | Time lag from stick to control surface. |
| $U$ | Average forward airplane velocity. |
| $X_p$ | Input to hydraulic system |
| $X_c$ | Output displacement of hydraulic system. |
| $X_v$ | Valve displacement |
| $X_s$ | Control column displacement |
| $X_b$ | Mechanical linkage displacement. |

$z_1$, $z_2$, ..Negative of zeros of transfer function.

$Z_a$         Displacement of bob weight.

$\alpha$         Perturbation angle of attack.

$\delta_c$         Angular motion of elevator.

$\zeta$         Relative damping ratio.

$\theta$         Angle of pitch.

$\sigma$         Real part of complex frequency, s.

$\omega$         Imaginary part of complex frequency, s.

$\omega_n$         Undamped natural resonant frequency.